The Pound-Drever-Hall Frequency Control

Tutorials of the 2015 EFTF / IFCS
Denver, CO, USA, April 12–16, 2015

Enrico Rubiola
CNRS FEMTO-ST Institute, Besancon, France

- Overview
- Basic mechanism
- Key ideas
- Control loop
- Resonators stability
- Optimization
- Applications
- Alternate schemes

home page http://rubiola.org

Overview

- Frequency stabilization to a passive resonator
- Relevant cases:
  - The Resonator is unsuitable to an oscillator
  - Cryogenics, vacuum, etc.

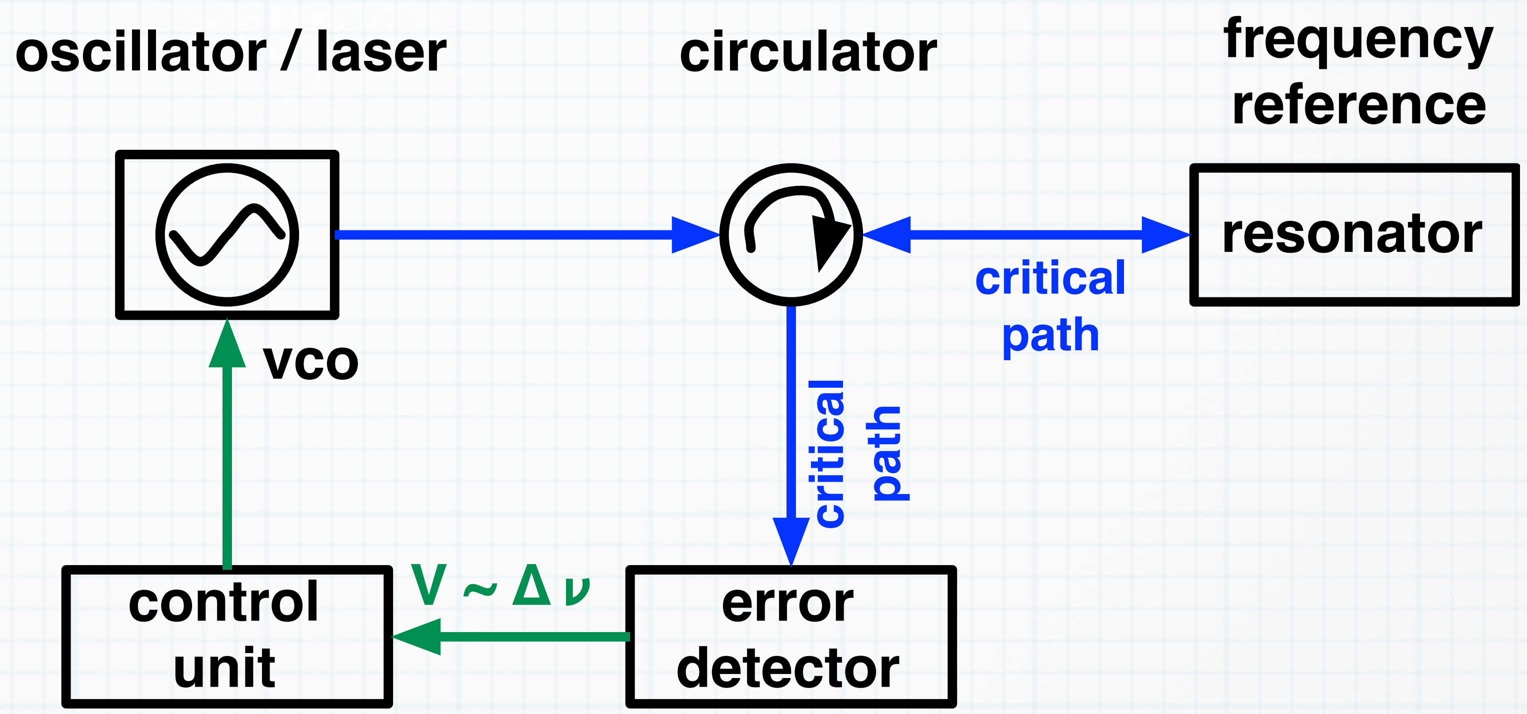

Points of interest

- Power (intensity) detector – available from RF to optics
- Compensation of the critical path
- Null measurement of the frequency error
- Use frequency modulation to get out of the flicker region
- One-port resonator –> lowest dissipation –> narrowest linewidth

Basic mechanism

Featured article

Black E. D., An introduction to Pound–Drever–Hall laser frequency stabilization, Am J Phys 69(1) January 2001

Also Technical Note LIGO-T980045-00-D 4/16/98

The full scheme

ω_n = natural (resonant) frequency
ω_0 = oscillation frequency

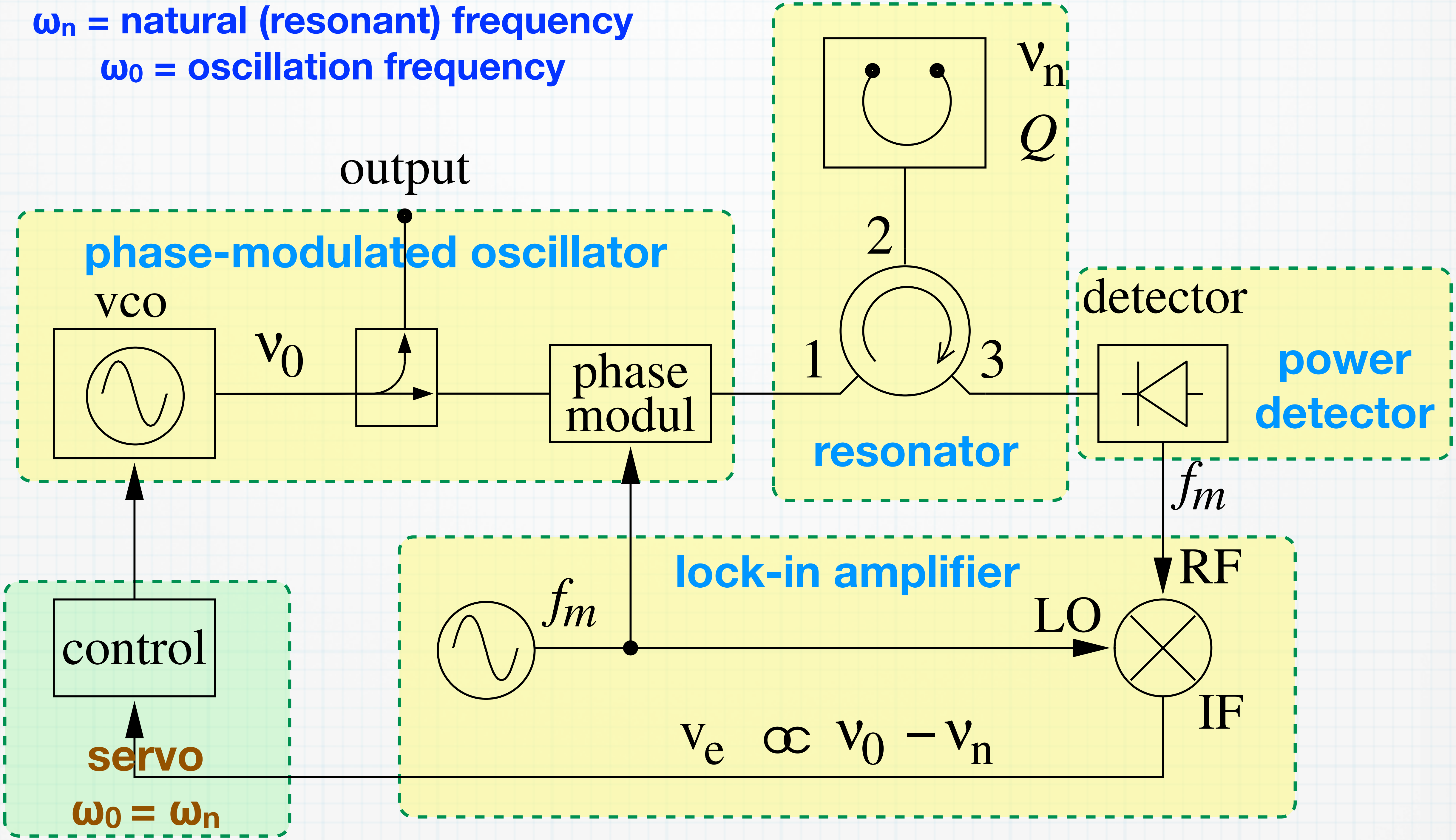

The error signal is proportional to the frequency error

$$v_e = D(\omega_0 - \omega_n)$$

Phase modulation – Physics

$$V(t) = V_p \cos[\omega t + m \cos(\Omega t)]$$

Phasor diagram

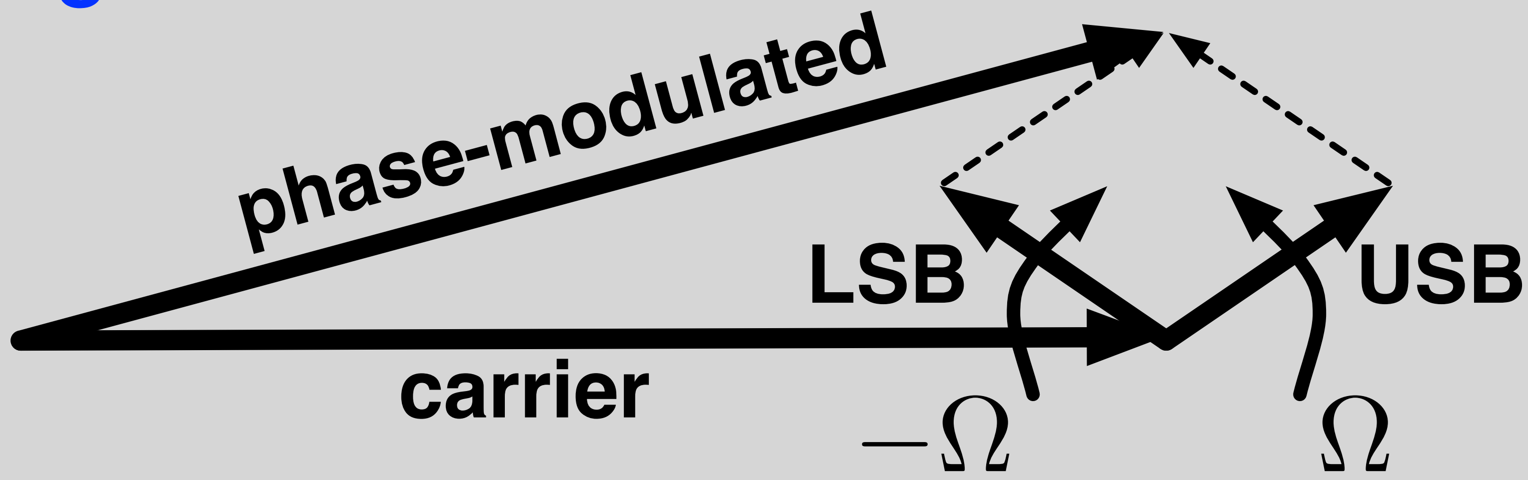

Frequency domain

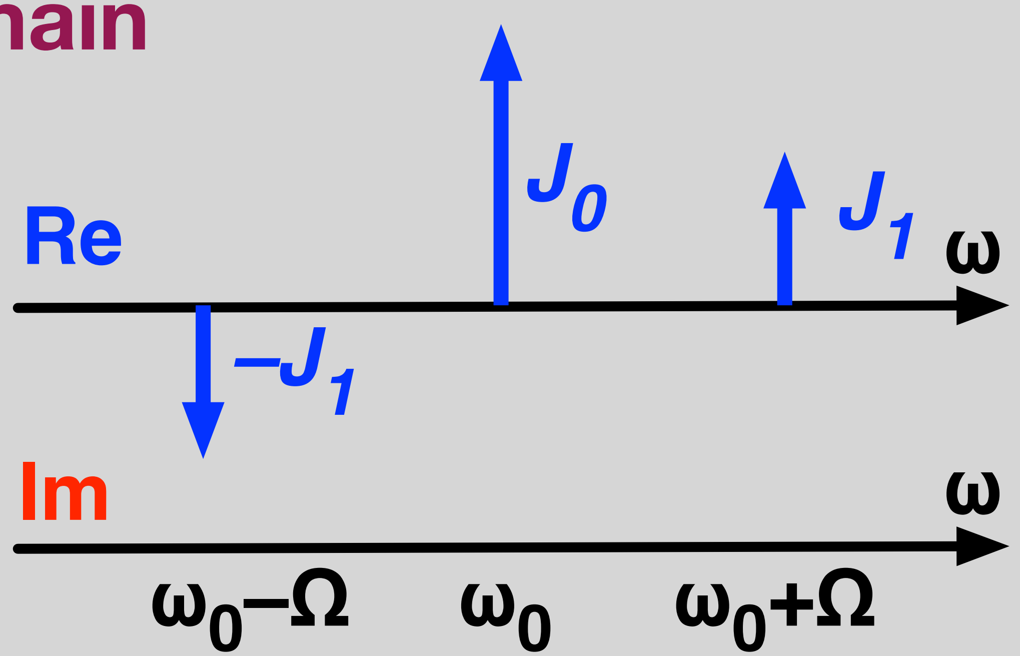

Bessel functions $J_n(m)$

Phase modulation – Math

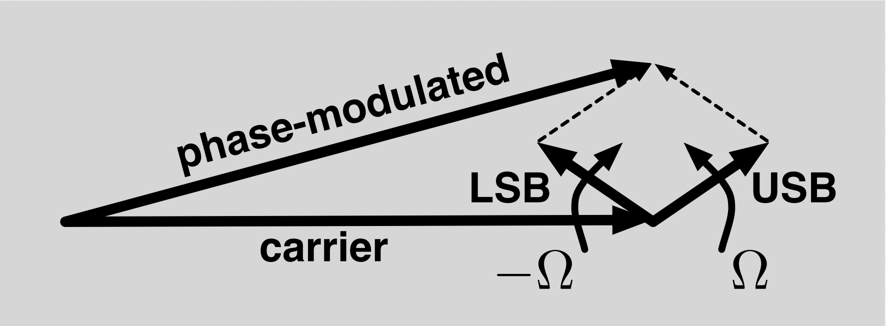

$$V = V_0\, e^{i\omega t}\, e^{im\sin\Omega t}$$

$$= V_0\, e^{i\omega t} \sum_{n=-\infty}^{\infty} J_n(m) e^{in\Omega t}$$

(not too) small m

$$\simeq V_0\, e^{i\omega t} \left[J_0(m) + J_{-1}(m)e^{-i\Omega t} - J_1(m)e^{i\Omega t}\right]$$

$$= V_0 \left[J_0(m)e^{i\omega t} - J_1(m)e^{i(\omega-\Omega)t} + J_1(m)e^{i(\omega+\Omega)t}\right]$$

small m

$$\simeq V_0 \left[1 + \frac{m}{2}\left(-e^{-i\Omega t} + e^{i\Omega t}\right)\right] e^{i\omega t}$$

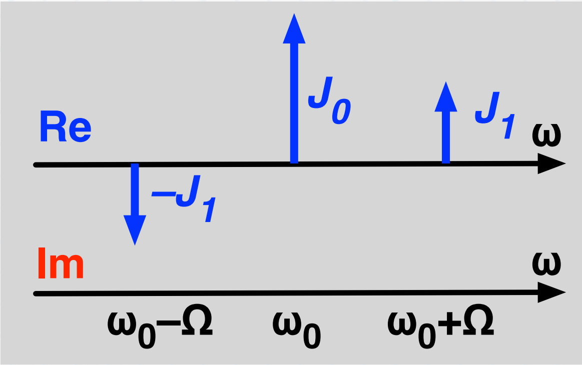

Carrier power

$$P_c = J_0^2(m)\, P_0 \simeq P_0$$

Sideband power

$$P_s = J_1^2(m)\, P_0 \simeq \frac{m^2}{4} P_0$$

Jacobi-Angers expansion

$$e^{iz\cos(\phi)} = \sum_{n=-\infty}^{\infty} i^n J_n(z) e^{in\phi},$$

$$e^{iz\sin(\phi)} = \sum_{n=-\infty}^{\infty} J_n(z) e^{in\phi},$$

Symmetry (real z)

$$J_{-n}(z) = \begin{cases} -J_n(z) & \text{odd } n \\ J_n(z) & \text{even } n \end{cases}$$

For moderate m

$$J_0(m) \simeq 1 - m^2/4$$

$$J_1(m) \simeq m/2$$

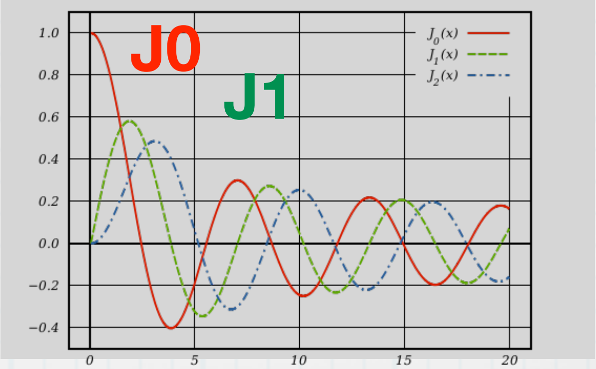

The reflection-mode resonator

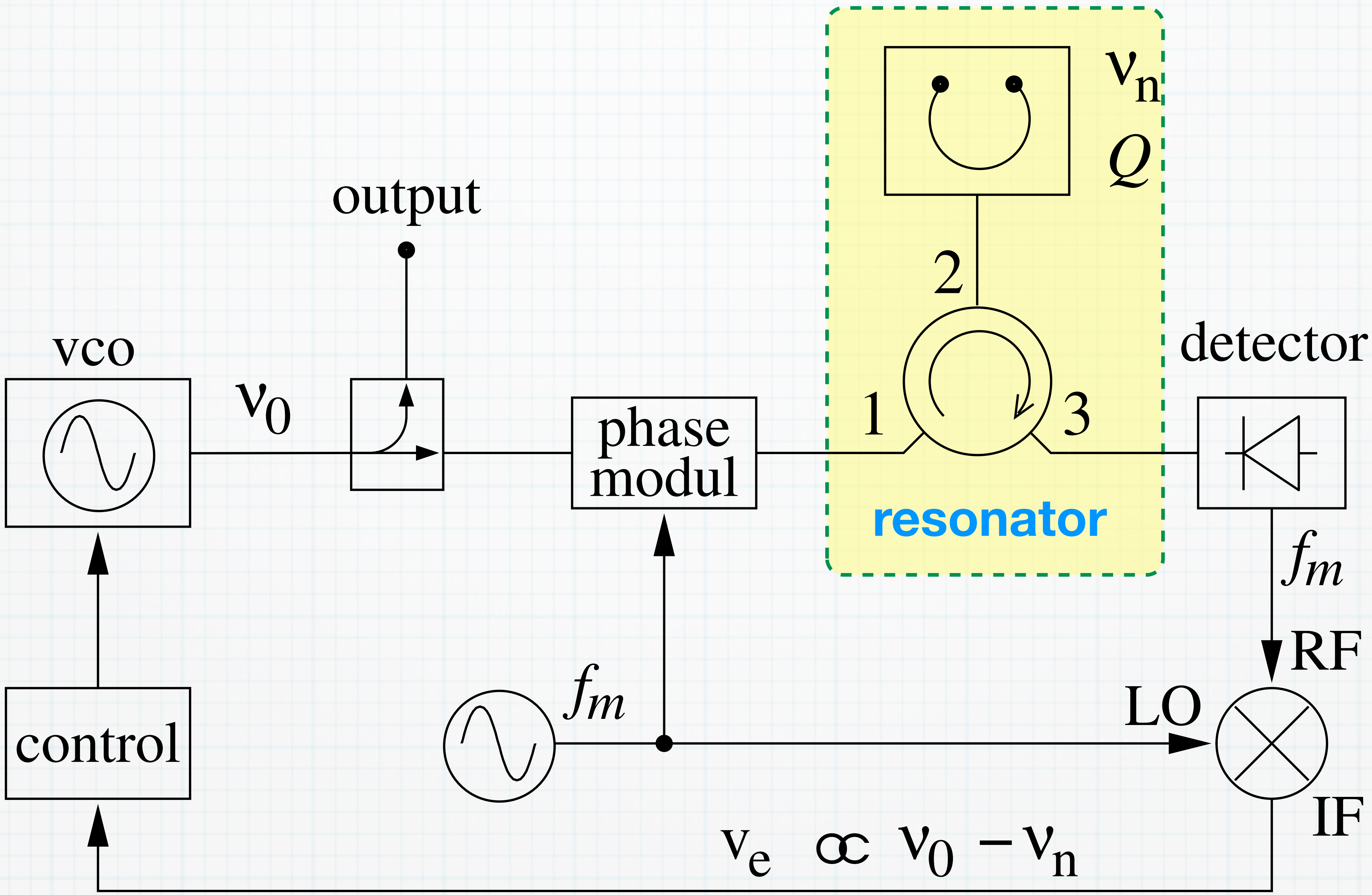

Figure from E. Rubiola, Phase noise and frequency stability in oscillators, © Cambridge University Press

Featured textbook

D. M. Pozar, Microwave engineering 4th ed, Wiley 2011, ISBN 978-0-470-63155-3

Chapter 6 – Microwave Resonators

Notice that the formalism is suitable to optics

Reflection coefficient Γ

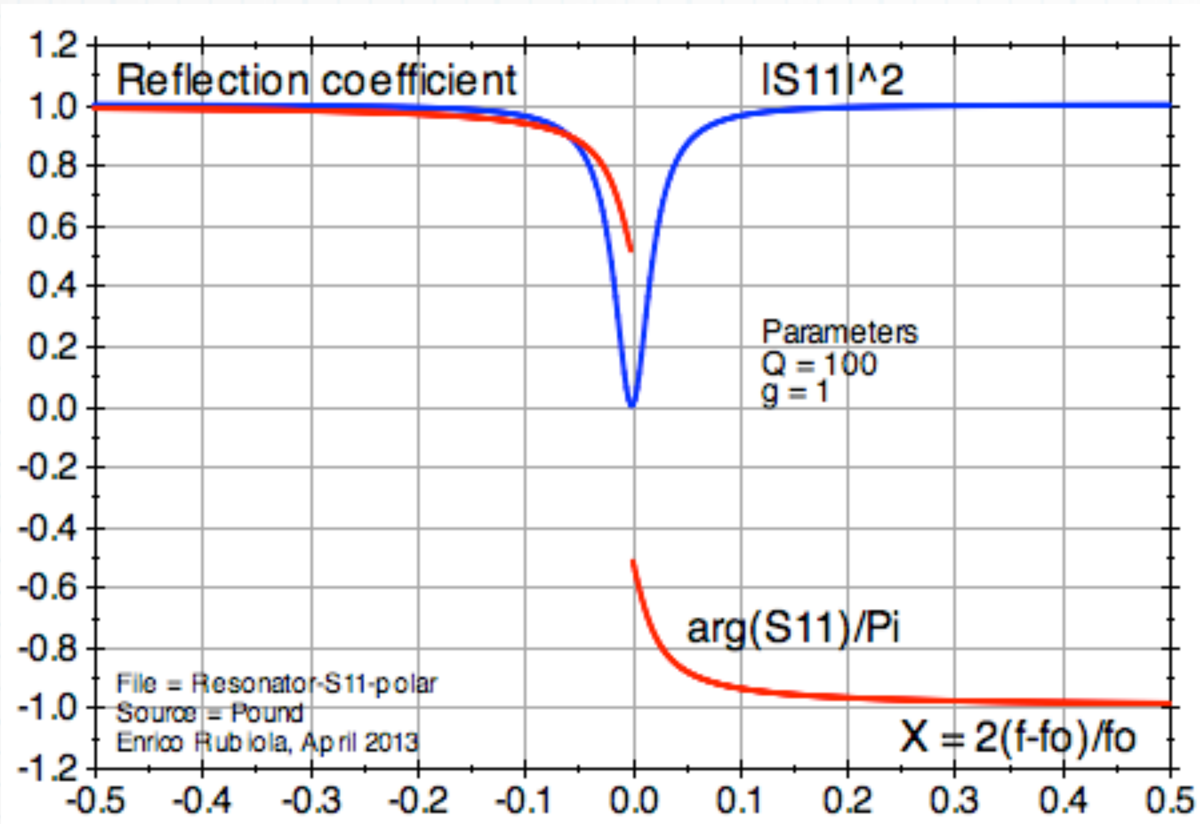

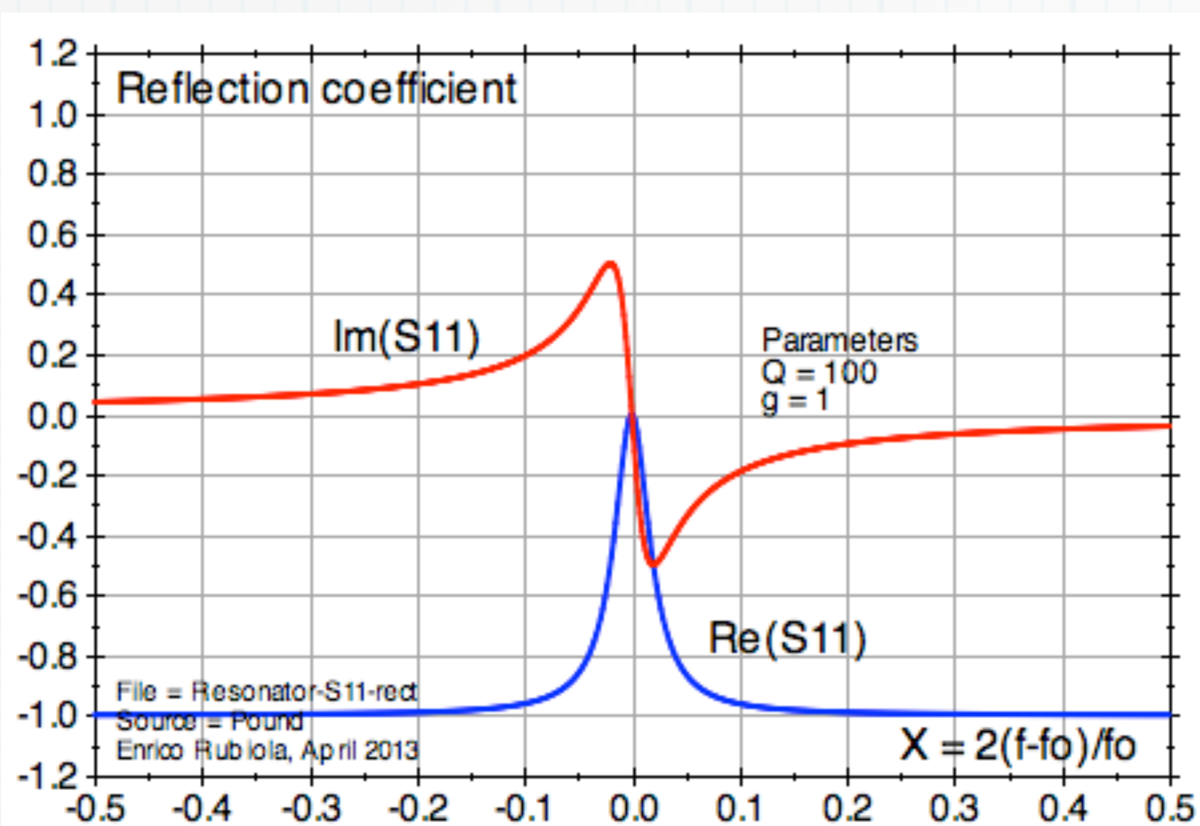

reflection coefficient

$$\Gamma = V^{-} / V^{+}$$

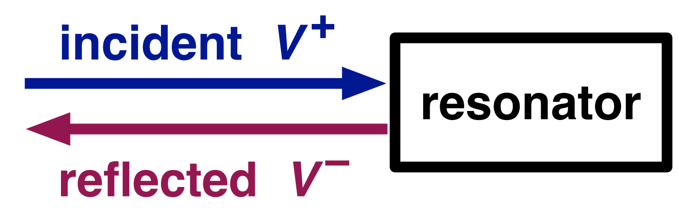

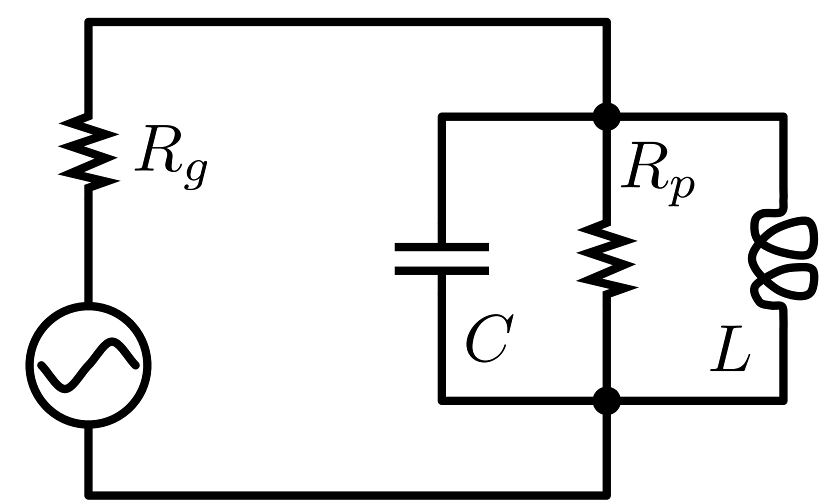

$$\Gamma = \frac{g - 1 - iQ_0\chi}{g + 1 + iQ_0\chi}$$

$Q_0 =$ unloaded 'Q'

$g = R_p / R_g$ coupling

$\chi = \dfrac{\omega}{\omega_n} - \dfrac{\omega_n}{\omega}$ detuning

Approximations for Γ

Off-resonance

$$\Gamma \simeq -1$$

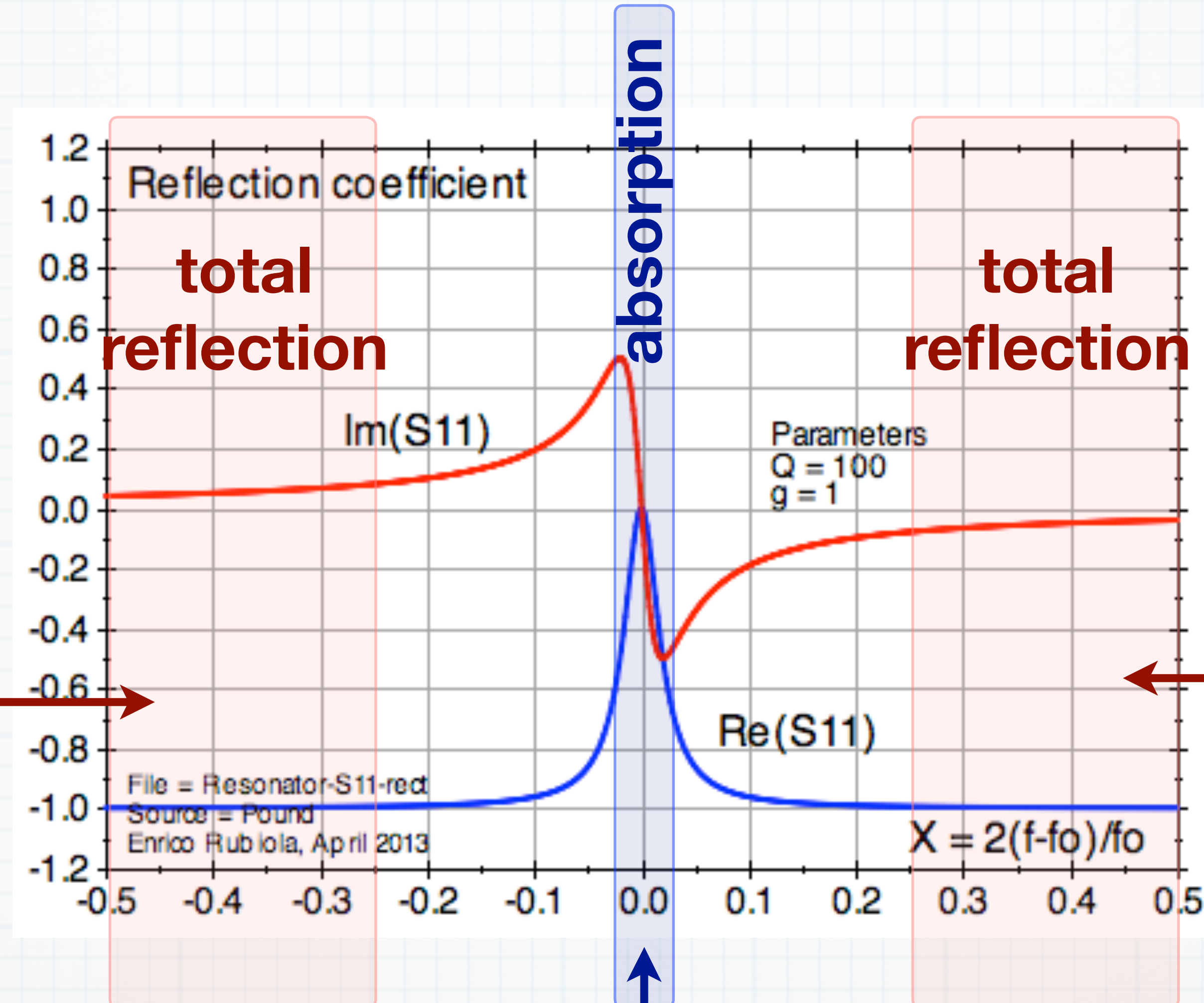

Off-resonance

$$\Gamma \simeq -1$$

Recall

$$\Gamma = \frac{g-1-iQ_0\chi}{g+1+iQ_0\chi}$$

$Q_0 = \text{unloaded '}Q\text{'}$

$g = R_p/R_g$ coupling

$\chi = \dfrac{\omega}{\omega_n} - \dfrac{\omega_n}{\omega}$ detuning

$\chi \simeq 2\dfrac{\Delta\omega}{\omega_n}$ close to ω_n

Resonance, close to ω_n

$$\Gamma \simeq \frac{g-1}{g+1} - i\frac{4Q_0 g}{(g+1)^2}\,\frac{\Delta\omega}{\omega_n}$$

even function → **resistance mismatch**

odd function → **frequency error**

Resonator reflected signal – Physics

phase-modulated incident signal

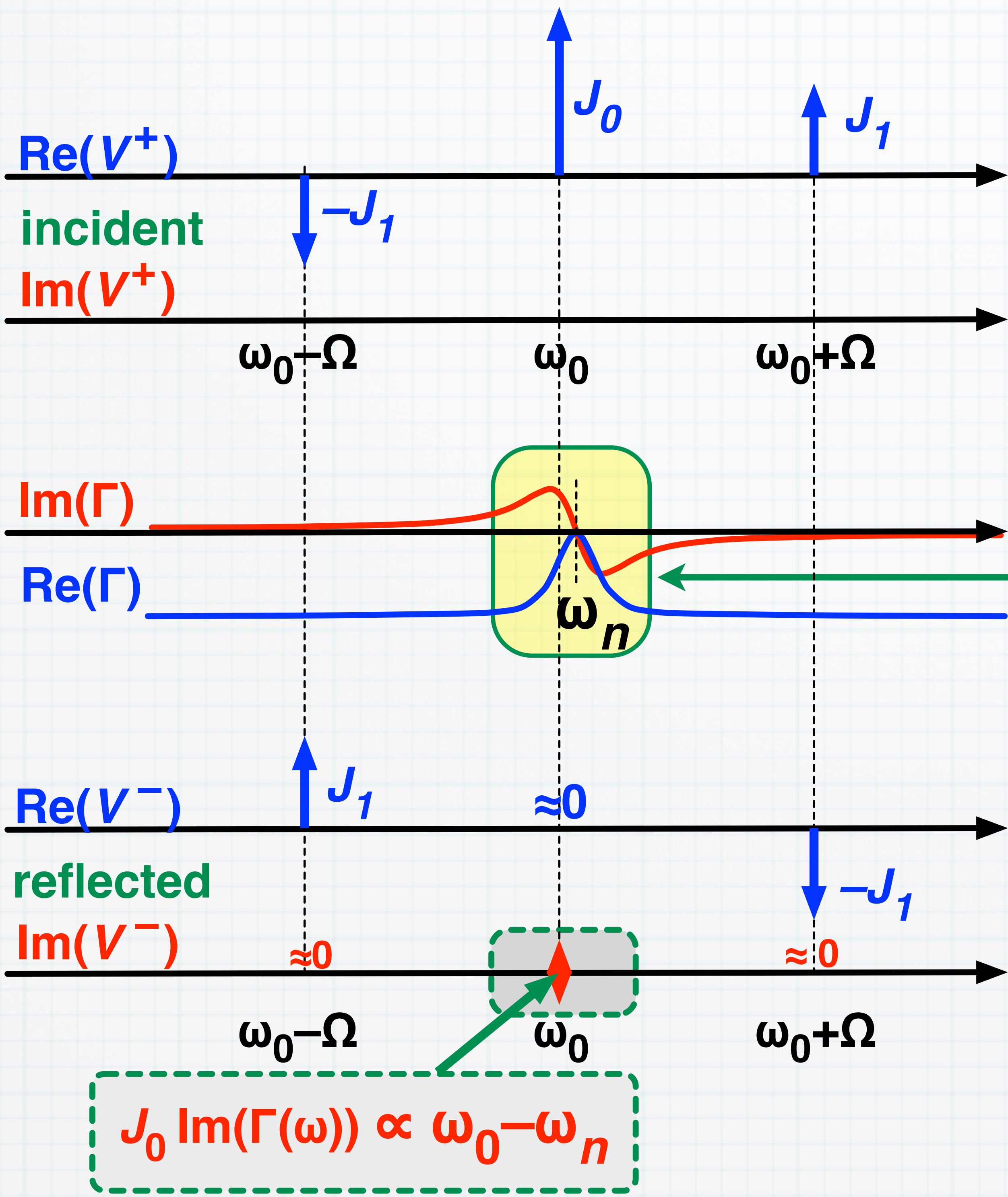

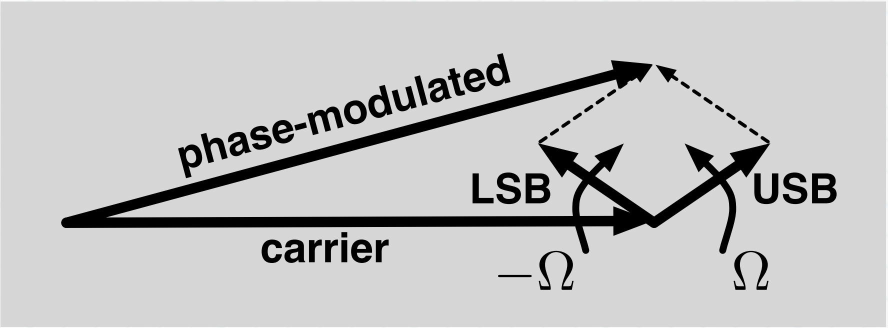

$$\Gamma \simeq \frac{g-1}{g+1} - i\frac{4Q_0 g}{(g+1)^2}\frac{\Delta\omega}{\omega_n}$$

reflection coefficient

$\Gamma = V^- / V^+$

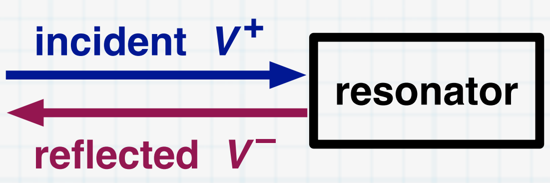

Resonator reflected signal – Math

phase-modulated incident signal

Incident wave

$$V^+ = V_0 \Big[\underbrace{-J_1(m)e^{i(\omega-\Omega)t}}_{\text{LSB}} + \underbrace{J_0(m)e^{i\omega t}}_{\text{carrier}} + \underbrace{J_1(m)e^{i(\omega+\Omega)t}}_{\text{USB}} \Big]$$

use $\quad \Gamma(\omega \pm \Omega) \simeq -1 \quad$ and $\quad \Gamma(\omega) \simeq \dfrac{g-1}{g+1} - i\dfrac{4Q_0}{g+1}\dfrac{\Delta\omega}{\omega_n}$

Reflected wave

$$V^- = V_0 \left\{ \underbrace{J_1(m)e^{i(\omega-\Omega)t}}_{\text{LSB}} + \underbrace{J_0(m)\left[\frac{g-1}{g+1} - i\frac{4Q_0}{g+1}\frac{\Delta\omega}{\omega_n}\right]e^{i\omega t}}_{\text{carrier}} - \underbrace{J_1(m)e^{i(\omega+\Omega)t}}_{\text{USB}} \right\}$$

proportional to $\omega-\omega_n$

Power (quadratic) detector

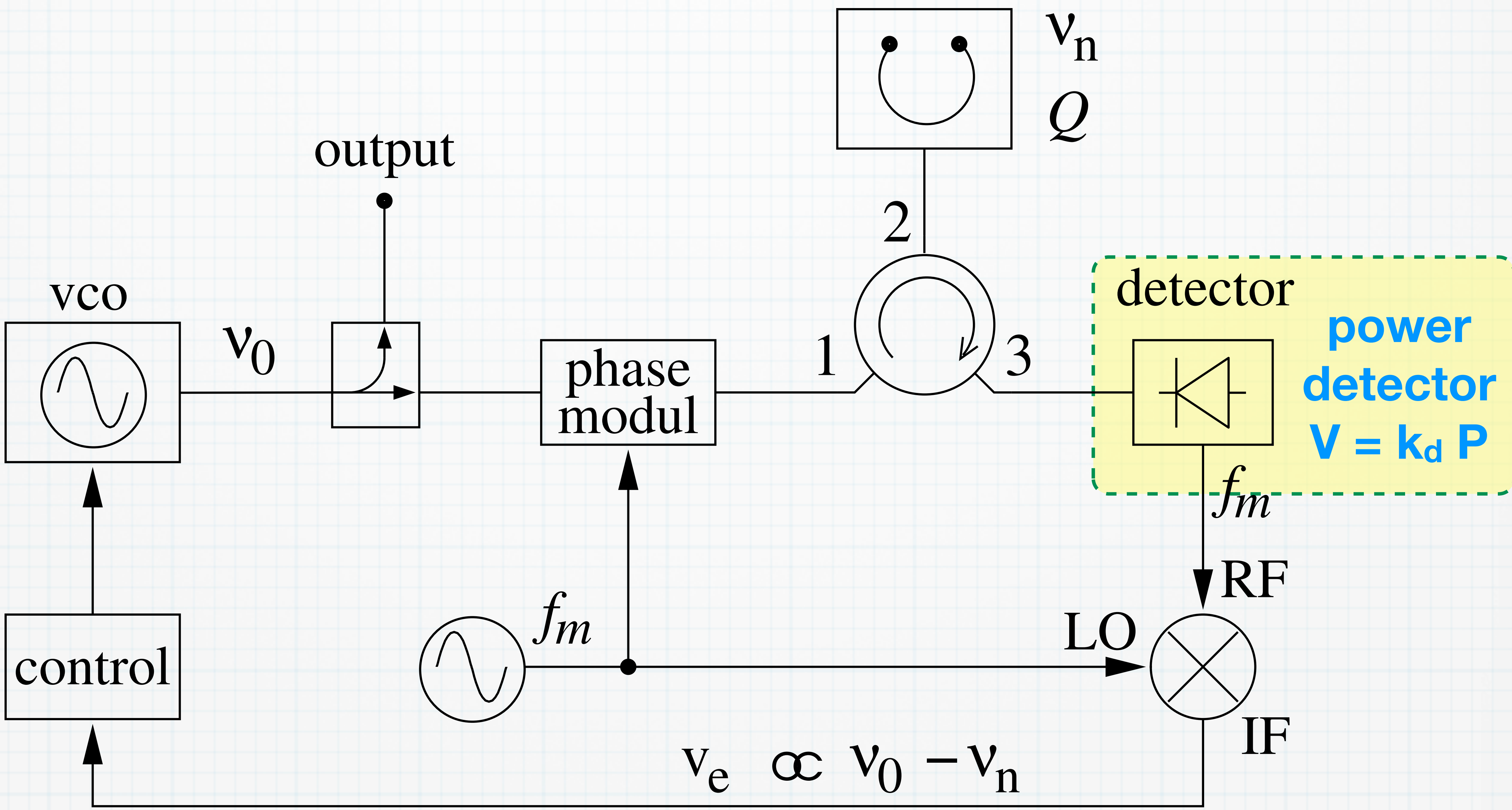

Figure from E. Rubiola, Phase noise and frequency stability in oscillators, © Cambridge University Press

$$\text{Power } P = \frac{1}{2}\Re\{VI^*\} = P\frac{1}{2R_0}\Re\{VV^*\}$$

V and I are peak values

Power (quadratic) detector

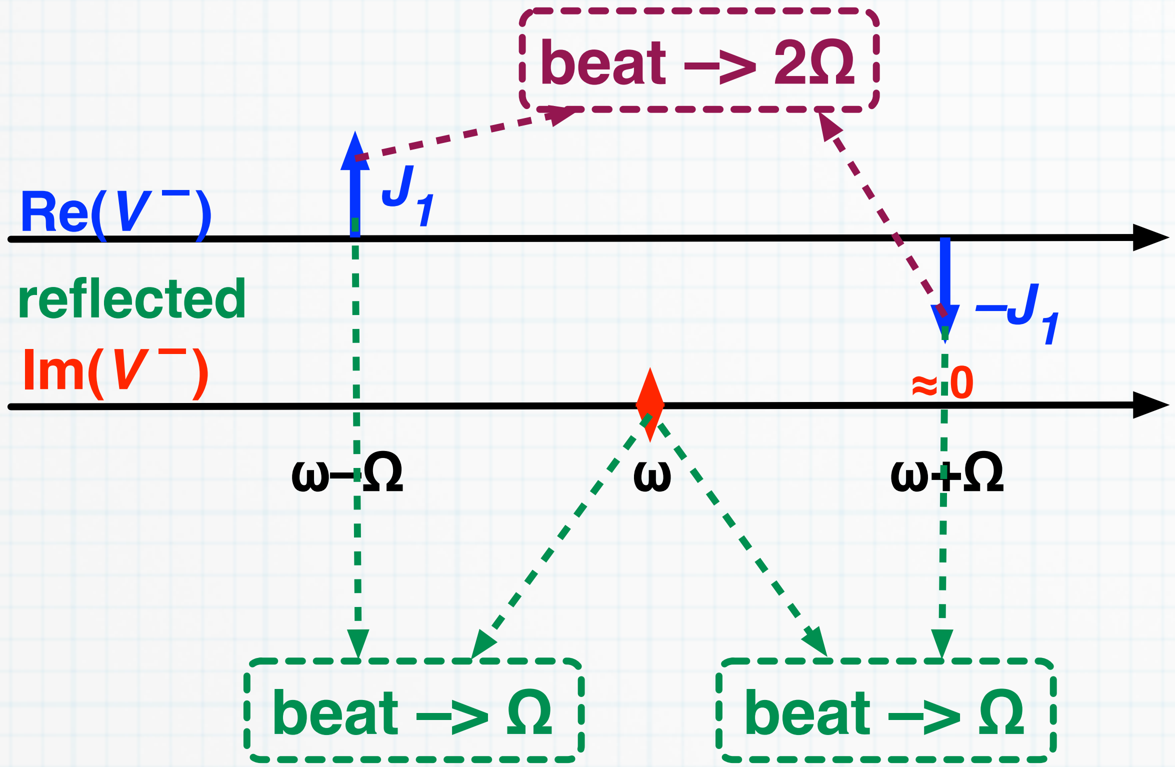

$$P = \frac{1}{2R_0}\Re\{VV^*\}$$

$(a+b+c)^2 =$

$$\underbrace{a^2 + b^2 + c^2}_{\text{dc terms}} + \underbrace{2ab + 2ac + 2bc}_{\text{beat terms}}$$

dc terms

$$P = \frac{|V_0|^2}{2R_0}\left\{J_1^2(m) + \frac{1}{2}J_0^2(m)\left[\frac{g-1}{g+1}\right]^2 + \frac{1}{2}J_0^2(m)\left[\frac{4Q_0}{g+1}\frac{\Delta\omega}{\omega_n}\right]^2\right\} +$$

$$-\frac{|V_0|^2}{2R_0}J_1^2(m)\cos(2\Omega t) + \frac{|V_0|^2}{2R_0}2J_0(m)J_1(m)\frac{4Q_0}{g+1}\frac{\Delta\omega}{\omega_n}\sin(\Omega t)$$

diagnostic

error signal

The lock-in amplifier

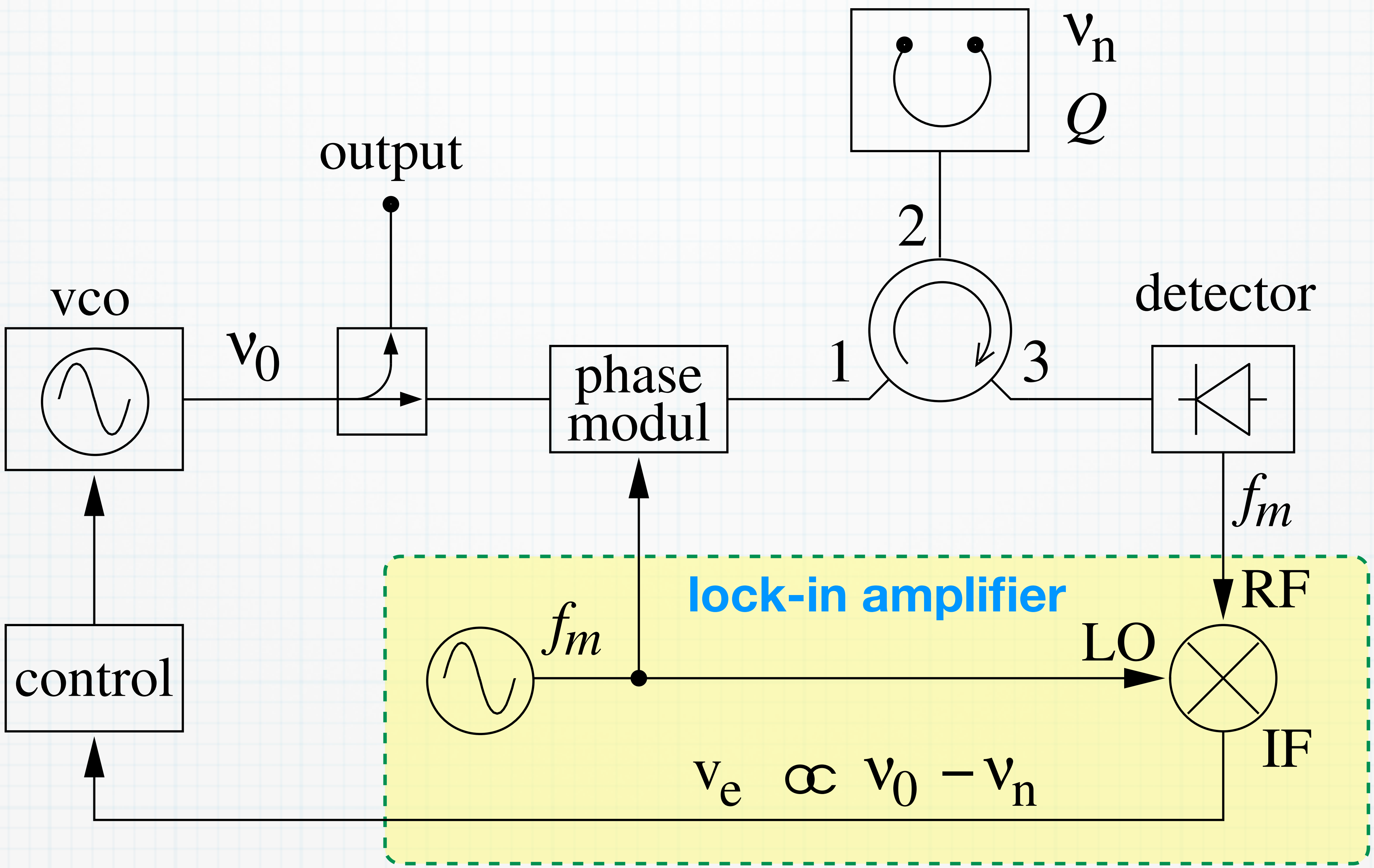

Two-channel lock-in amplifier

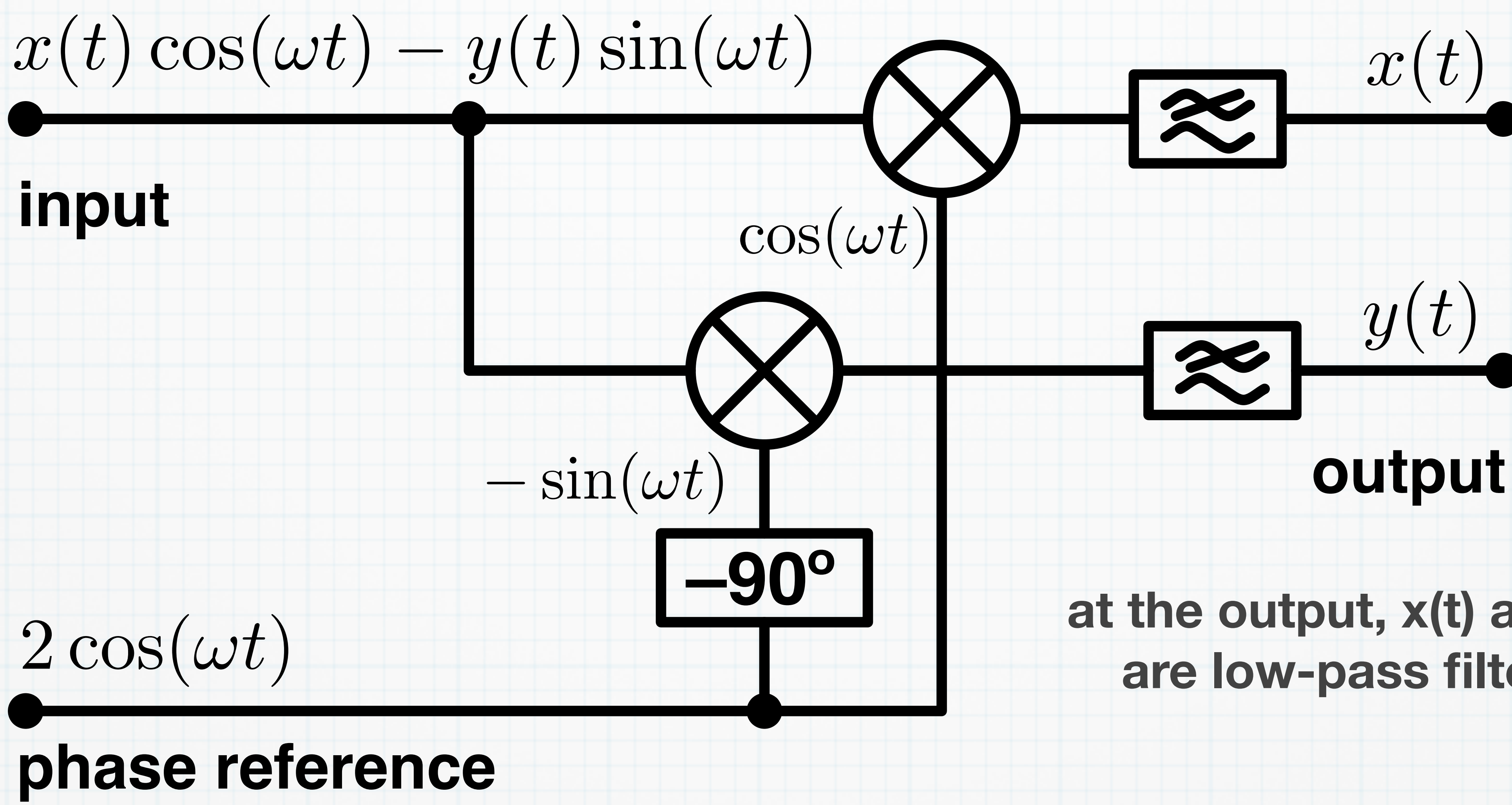

at the output, x(t) and y(t) are low-pass filtered

error $\longrightarrow$ $$v_e = \frac{|V_0|^2}{2R_0} 2J_0(m)J_1(m)\frac{4Q_0}{g+1}\frac{\Delta\omega}{\omega_n}$$

diagnostic $\longrightarrow$ $$v_d = -\frac{|V_0|^2}{2R_0} J_1^2(m)$$

In synthesis

The frequency discriminant D is proportional to

- **Oscillator power P_0**
- **Modulation index m**
- **Resonator's Q_0/ω_n**
- **Power-detector gain k_d [V/W]**
- **RF gain at the detector output (not shown)**
- **Gain of the lock-in amplifier (not accounted for in equations)**

…And affected by the coupling coefficient g

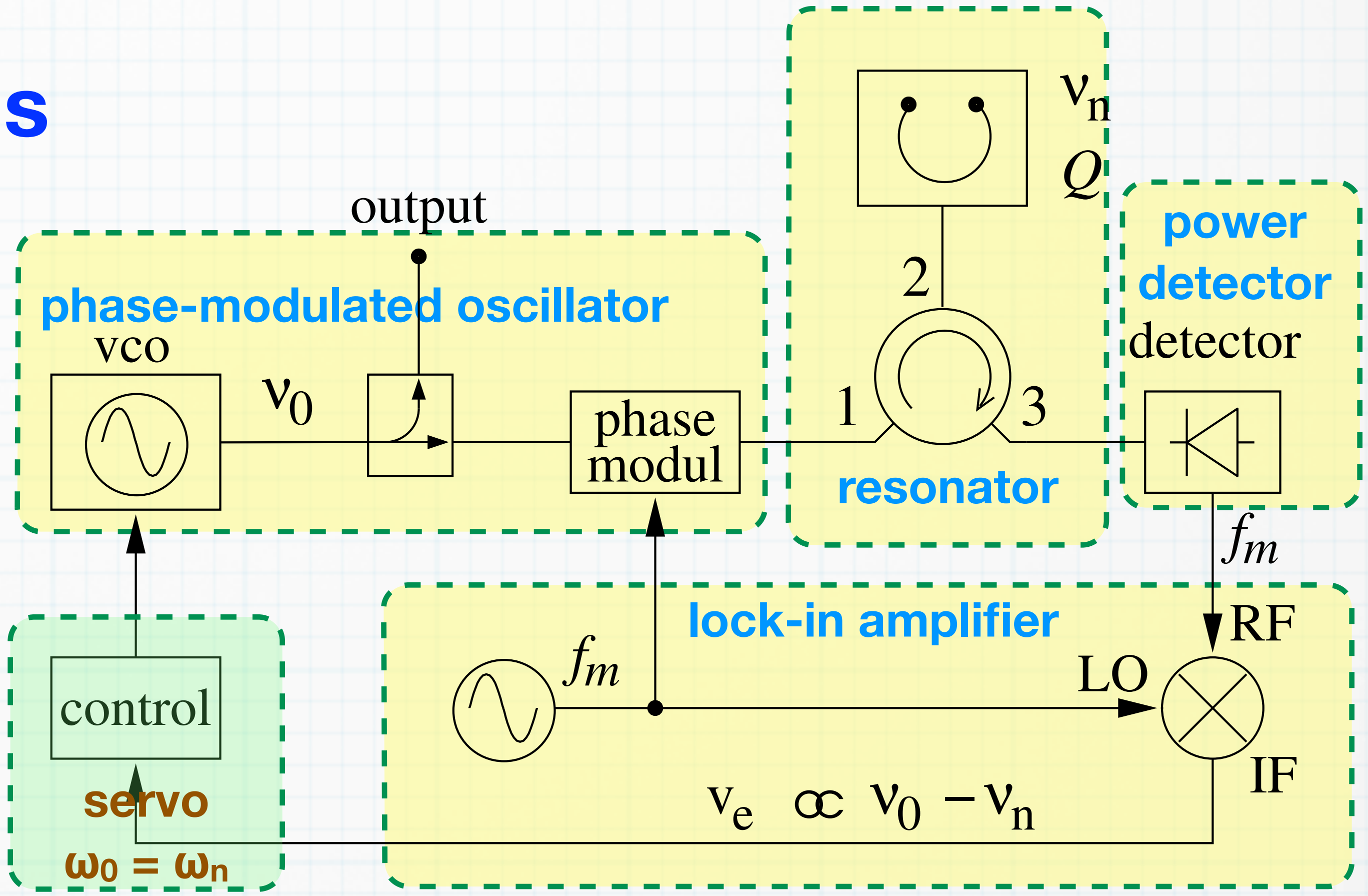

error signal

$$v_e = D(\omega_0 - \omega_n)$$

Key ideas

Use a power (intensity) detector

- Power detectors are available in the widest frequency range
  - Sub-audio to UV, and more
  - Including the THz band
- The power detector has quadratic response to voltage – or to electric field

Even function vs odd function

- **The detector provides a signal proportional to the power (intensity)**
  - **Even function at ω_0**
  - **Unmodulated signal not suitable to feedback control**

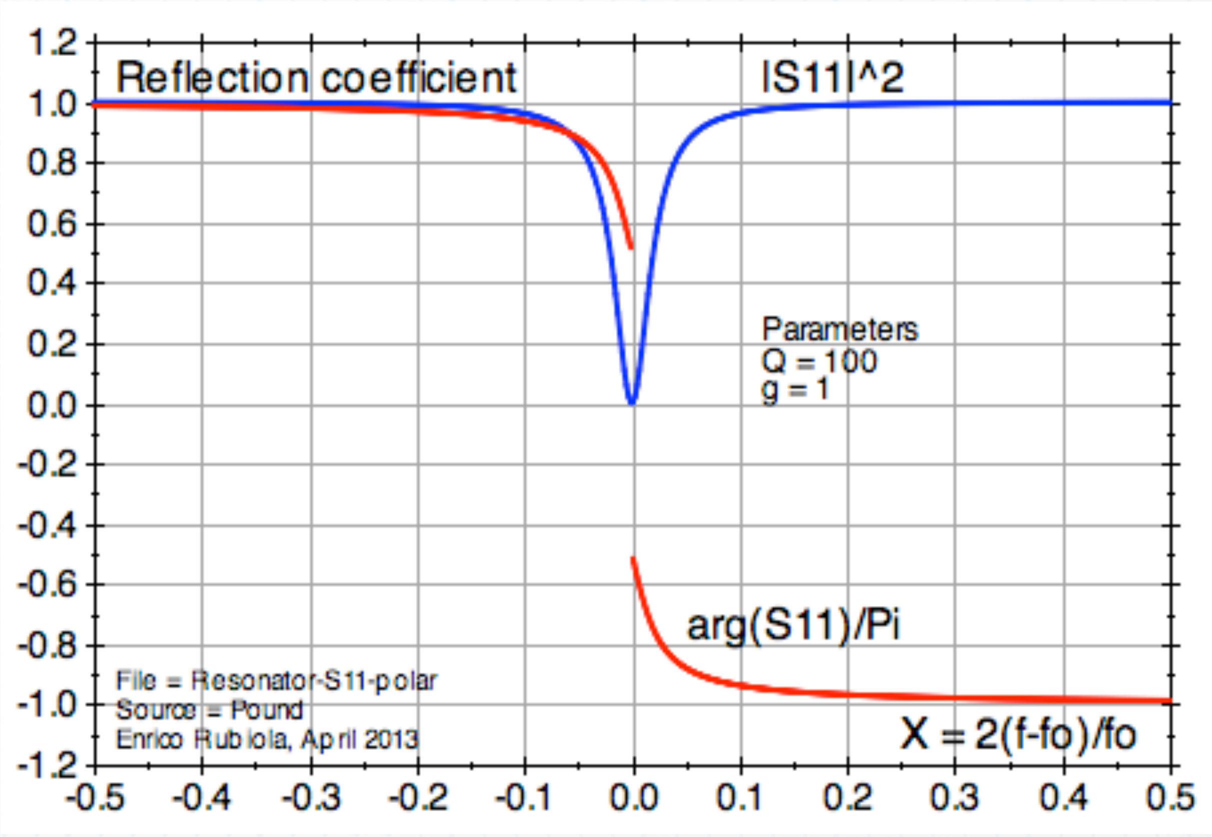

- **The modulation mechanism provides a signal proportional to the imaginary part**
  - **Odd function at ω_0**
  - **Great for feedback control**

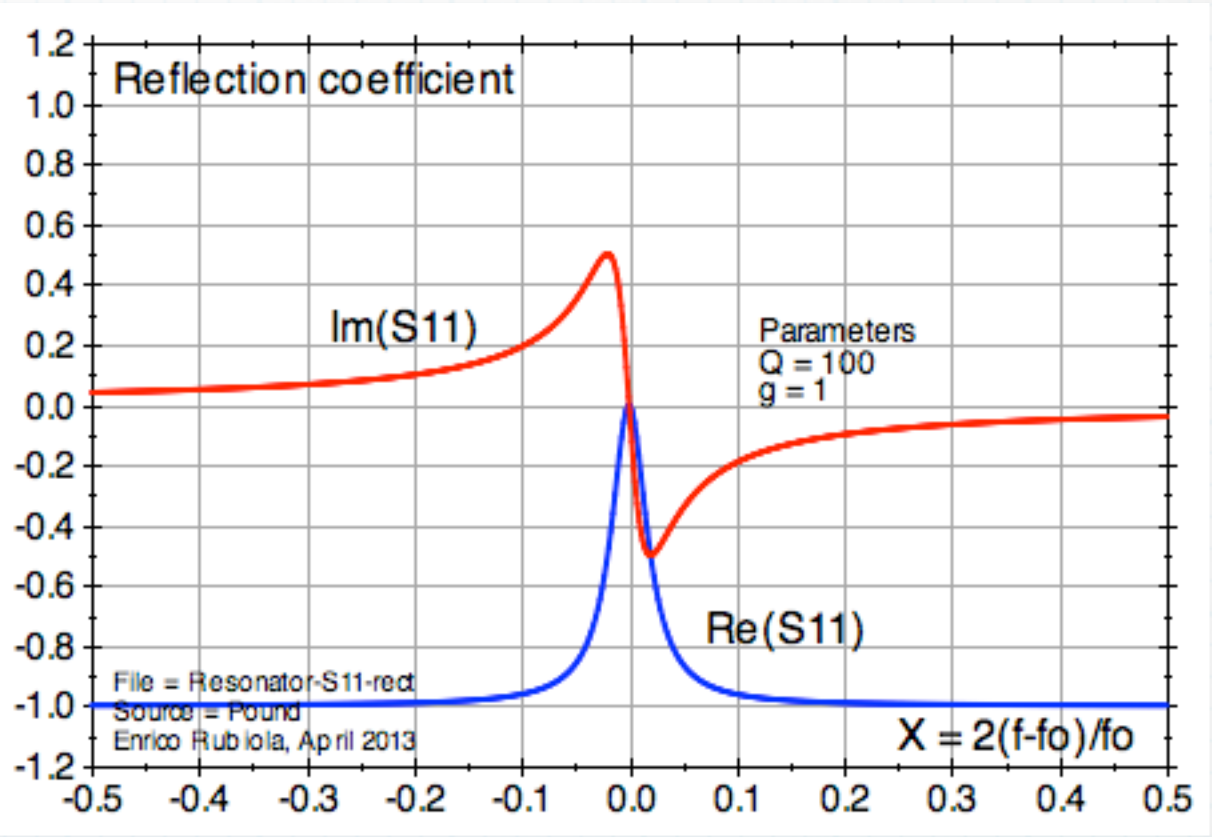

Modulation and flicker

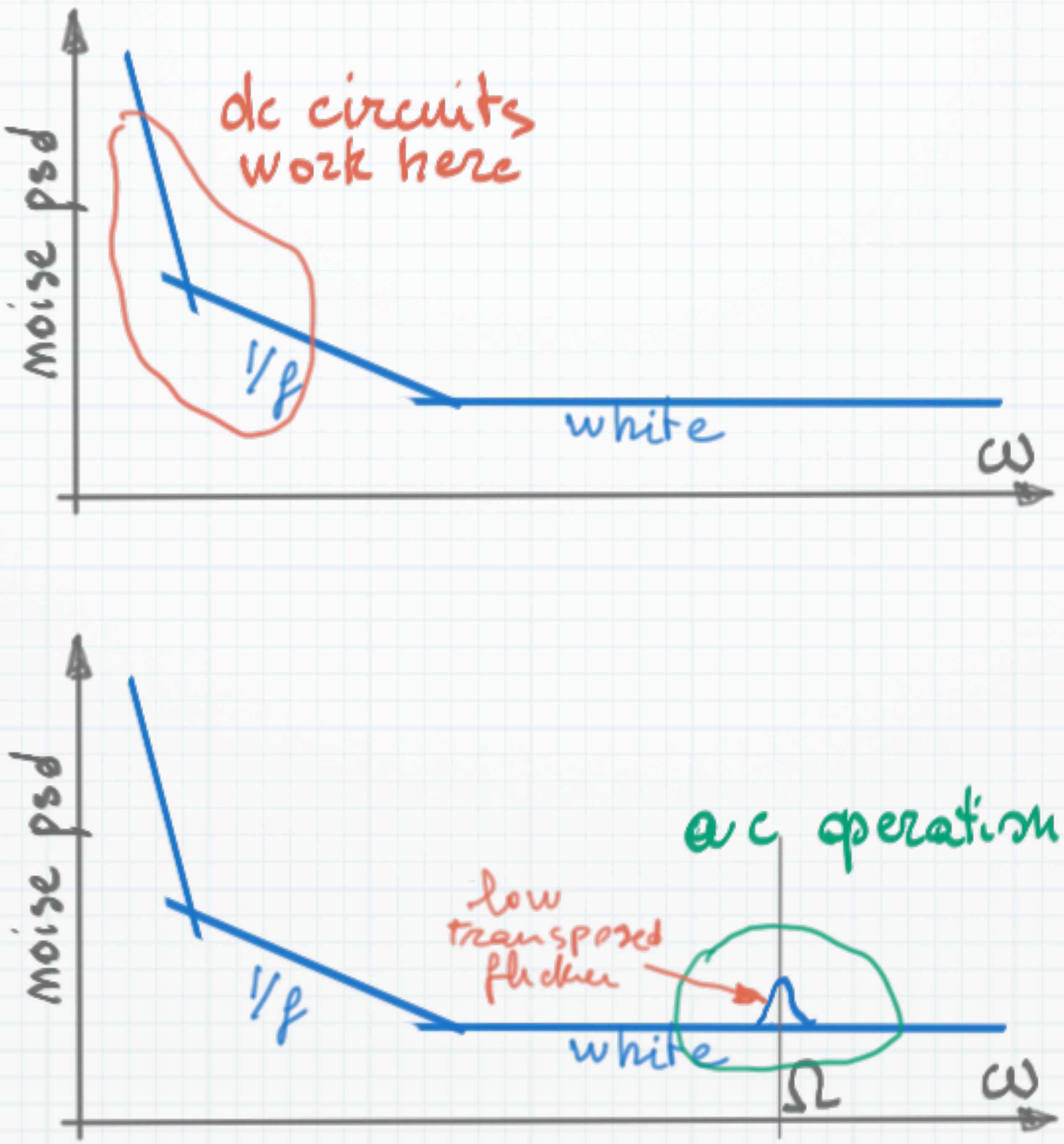

Get out of the flicker & drift region

Null measurement

- **Absolute measurements** rely on the “brute force” of instrument accuracy
- **Differential measurements** rely on the difference of two nearly equal quantities, something like $q_2–q_1$. However similar, this is not our case!
- **Null measurements** rely on the measurement of a quantity as close as possible to zero – ideally zero.
- **The Pound scheme detects**
  - Null of Im(Γ(ω))
  - AC regime, after down-converting to Ω

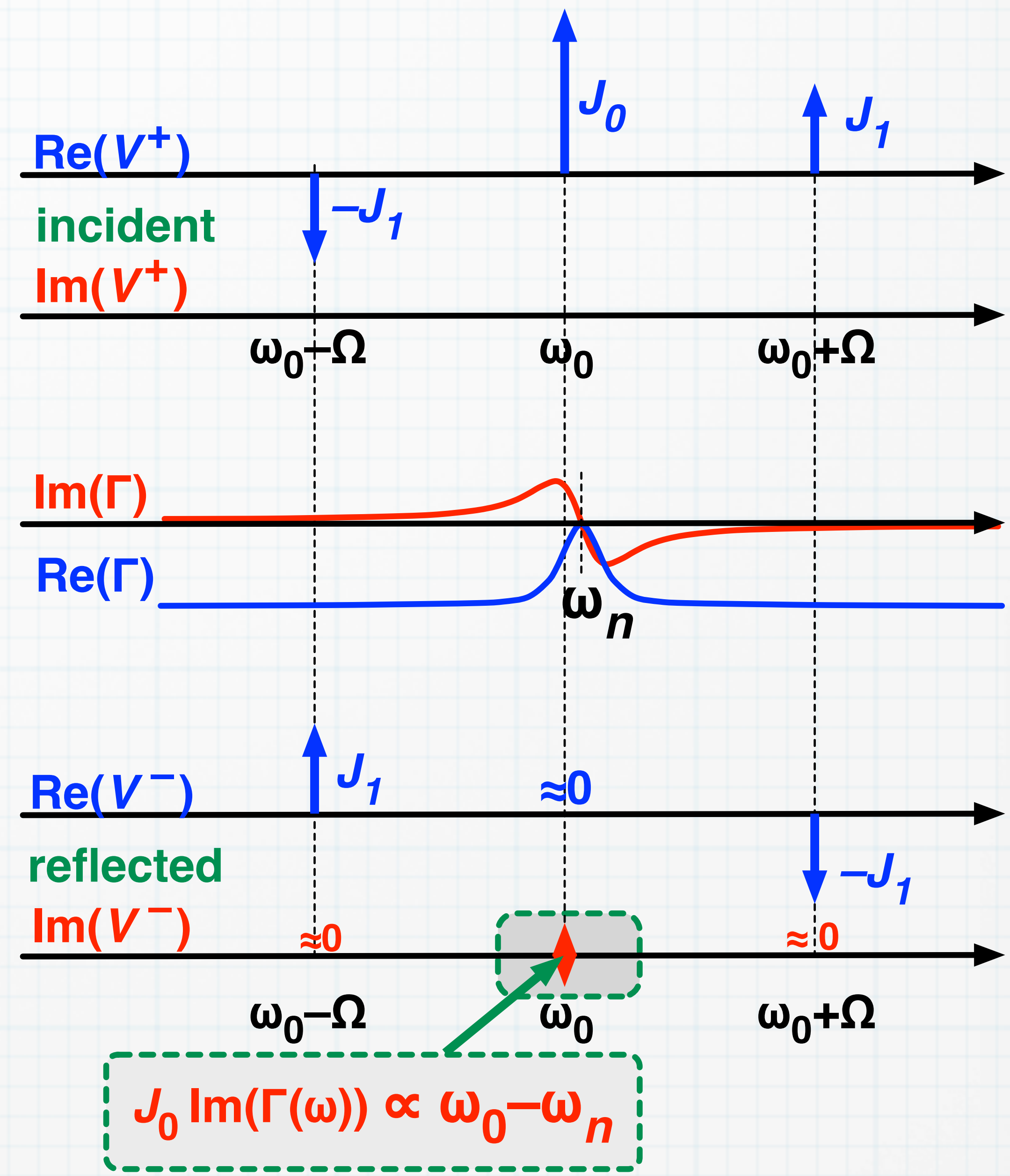

Insensitive to the critical path

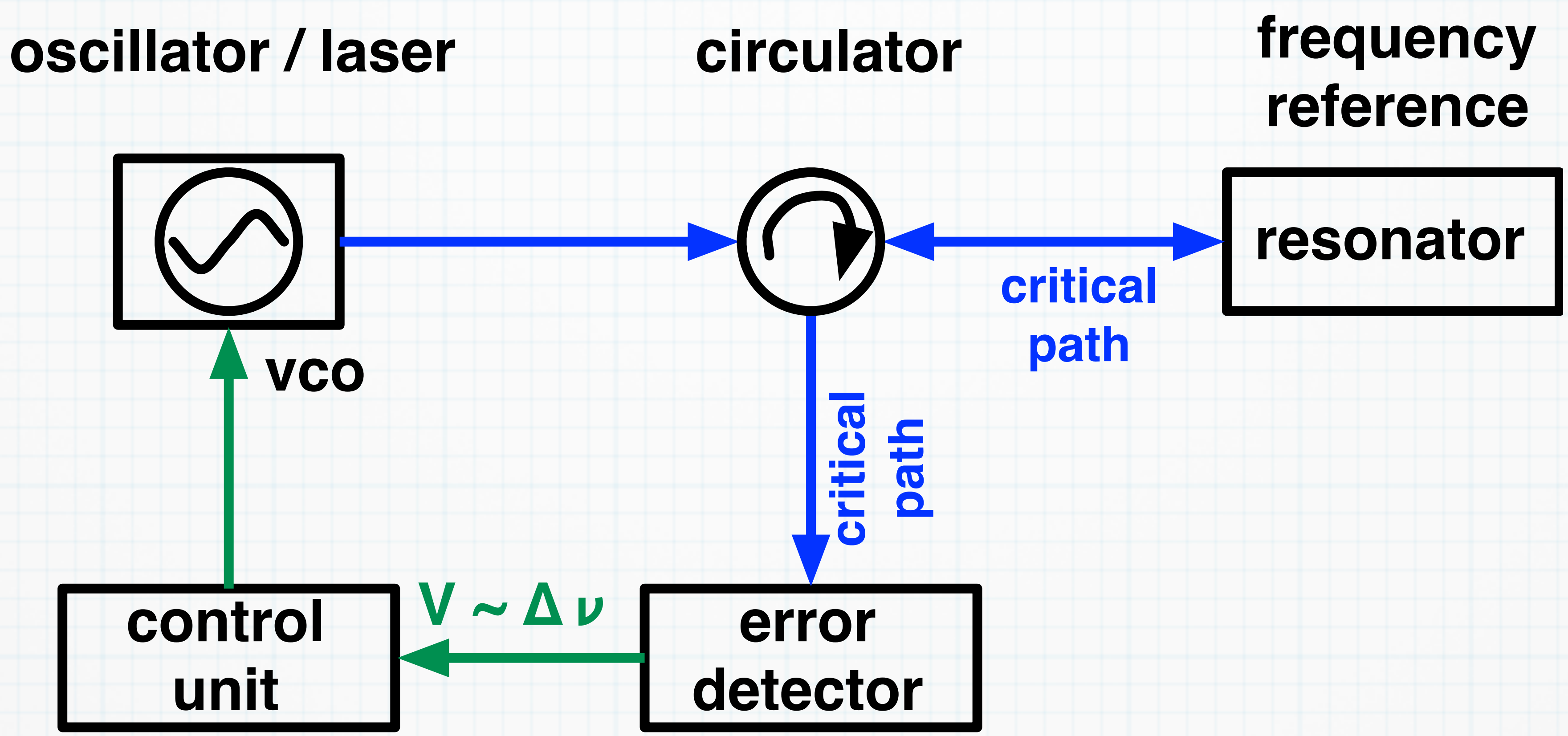

A length fluctuation does not affect

- The phase and amplitude relations between carrier and sidebands
- In turn, the measurement of $\Delta\omega$

(No longer true in the presence of dispersion)

The mechanism is the same of radio emission

One-port vs two-port resonator

— one port is better than two —

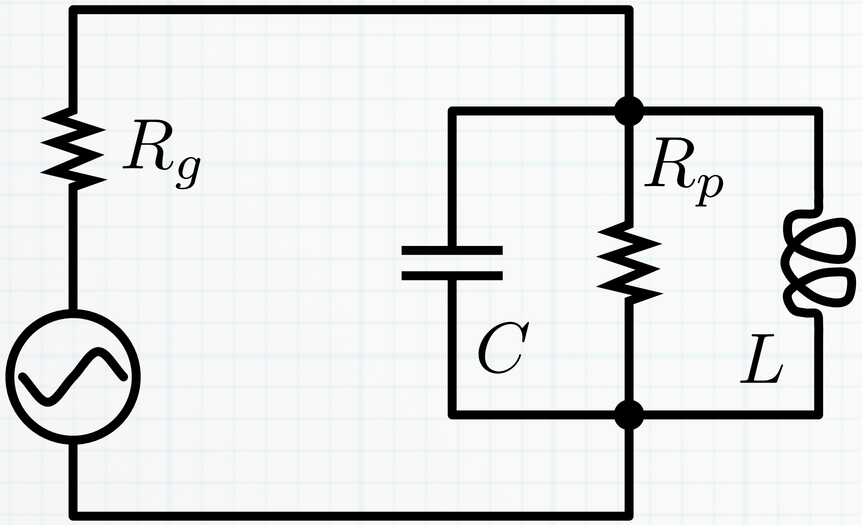

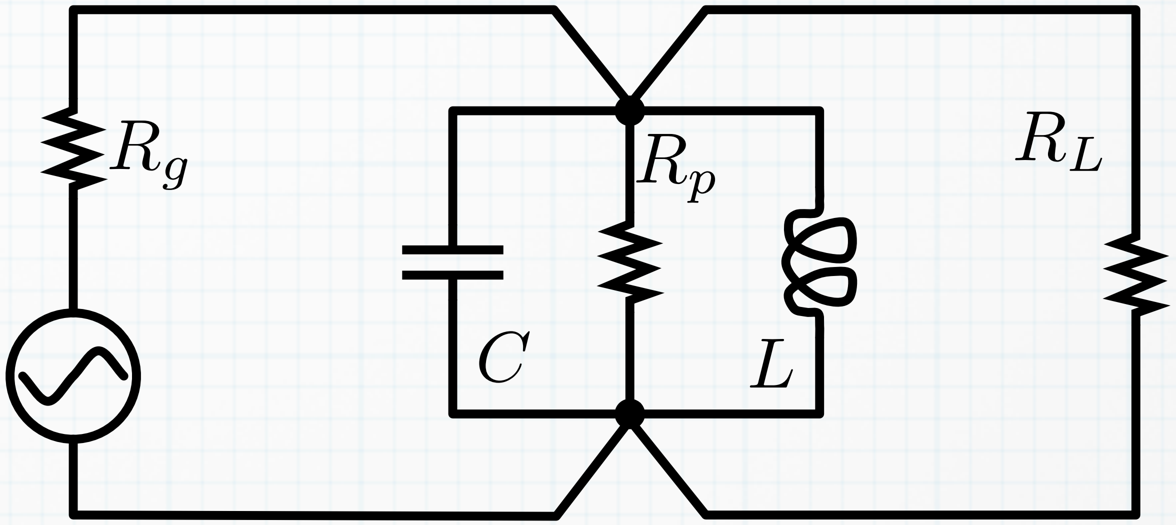

- Electrical
  - Smaller dissipation than the two-port resonator
  - Hence higher Q
- Physical / System level – Simpler
  - Vacuum
  - Cryogenic environment
  - Resonator far from the oscillator

Control loop

Featured book

K.J. Åström, R.M. Murray, Feedback Systems, Princeton 2008

– Caveat: however outstanding, does not focus on TF applications –

The 10^{-6} golden rule

- It is generally agreed that a microwave frequency control loop can lock within 10^{-6} of the bandwidth
  - Cs standard: $10^{-6} \times$ (100Hz/9.2GHz) $\approx 10^{-14}$ stability
  - Cryogenic sapphire: $10^{-6} \times$ (10Hz/10GHz) $\approx 10^{-15}$ stability
- In optics, the 10^{-6} rule yields still unachieved stability
  - Optical FP: $10^{-6} \times$ (10kHz/200THz) $\approx 5{\times}10^{-19}$ stability
- The resonator fluctuation is not a part of the control, and accounted for separately

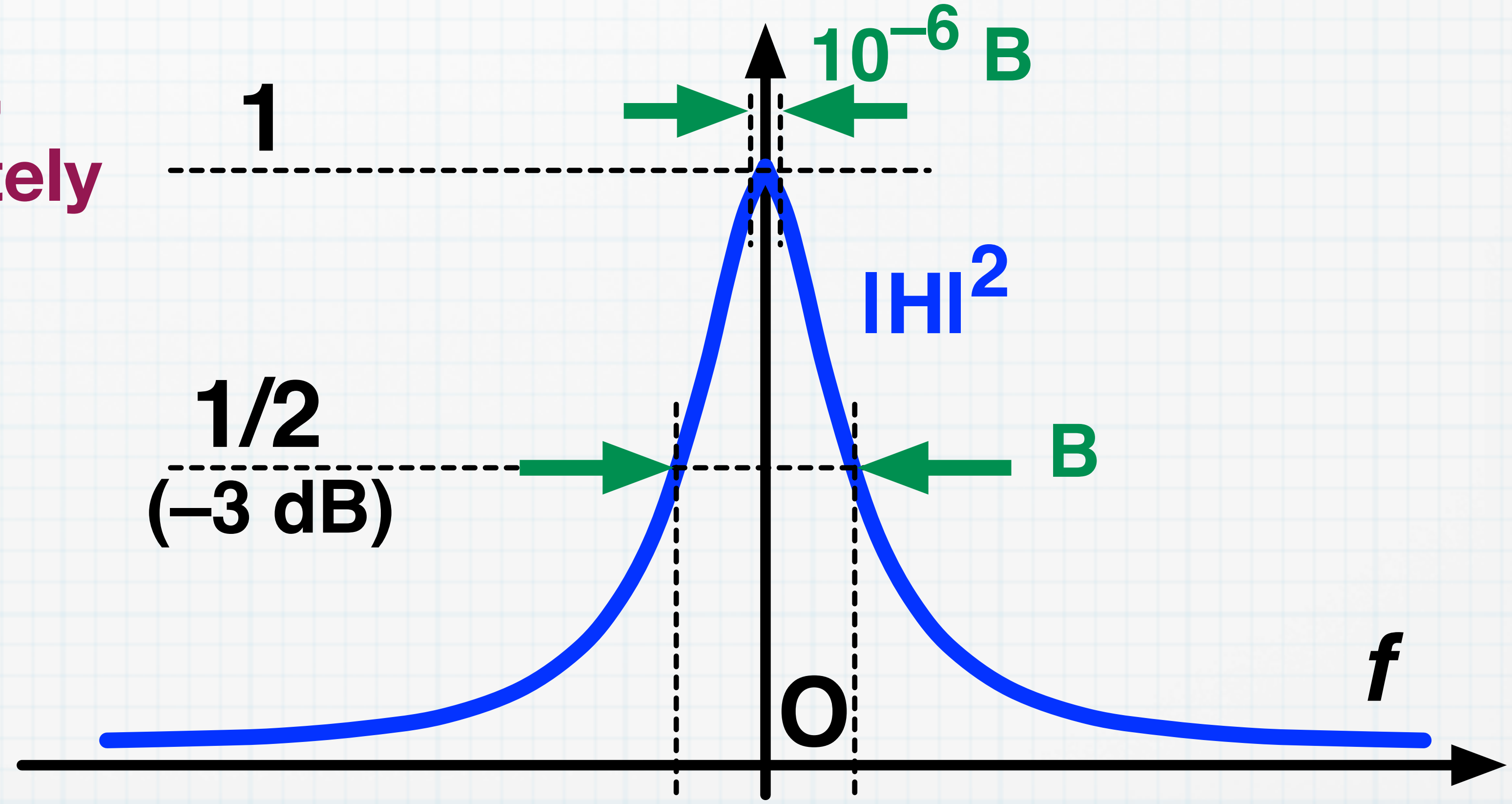

Sweep the oscillator frequency

– High modulation frequency –

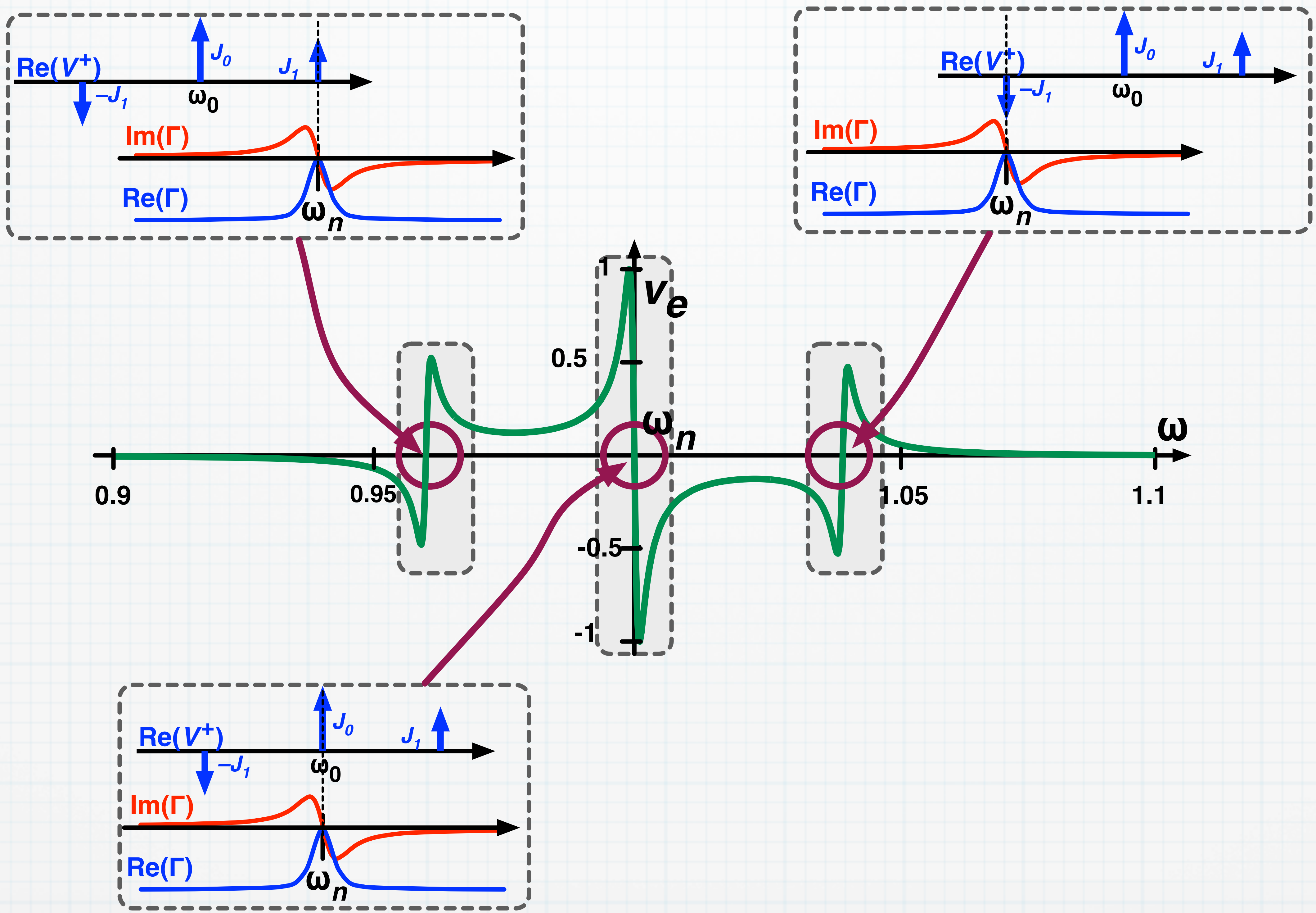

Sweep the oscillator frequency
– High modulation frequency –

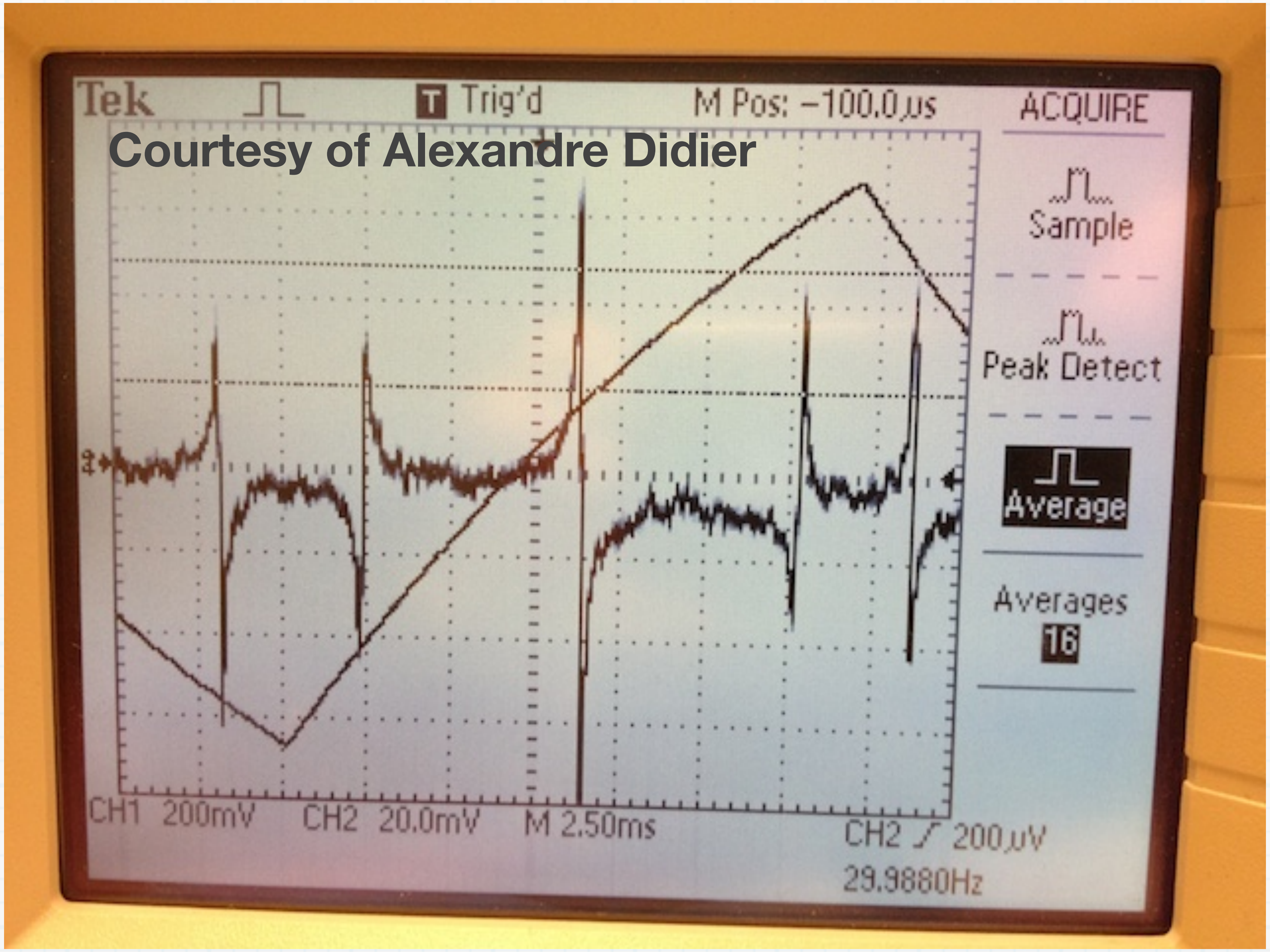

Low modulation frequency

Featured article – Black ED, An introduction to Pound–Drever–Hall laser frequency stabilization, Am J Phys 69(1) January 2001 – Fig.6

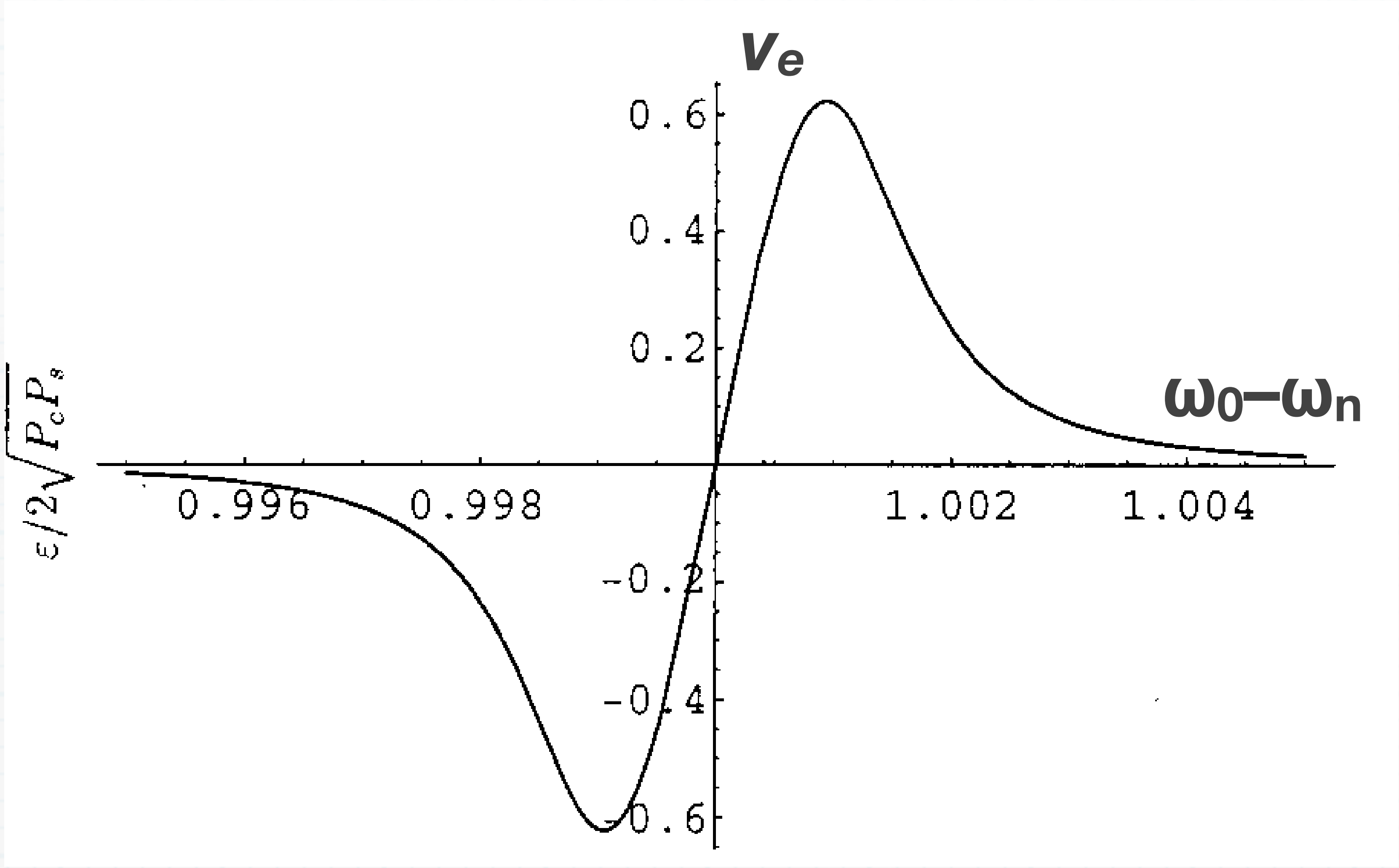

Carrier and PM sidebands are in the resonance bandwidth

Control loop

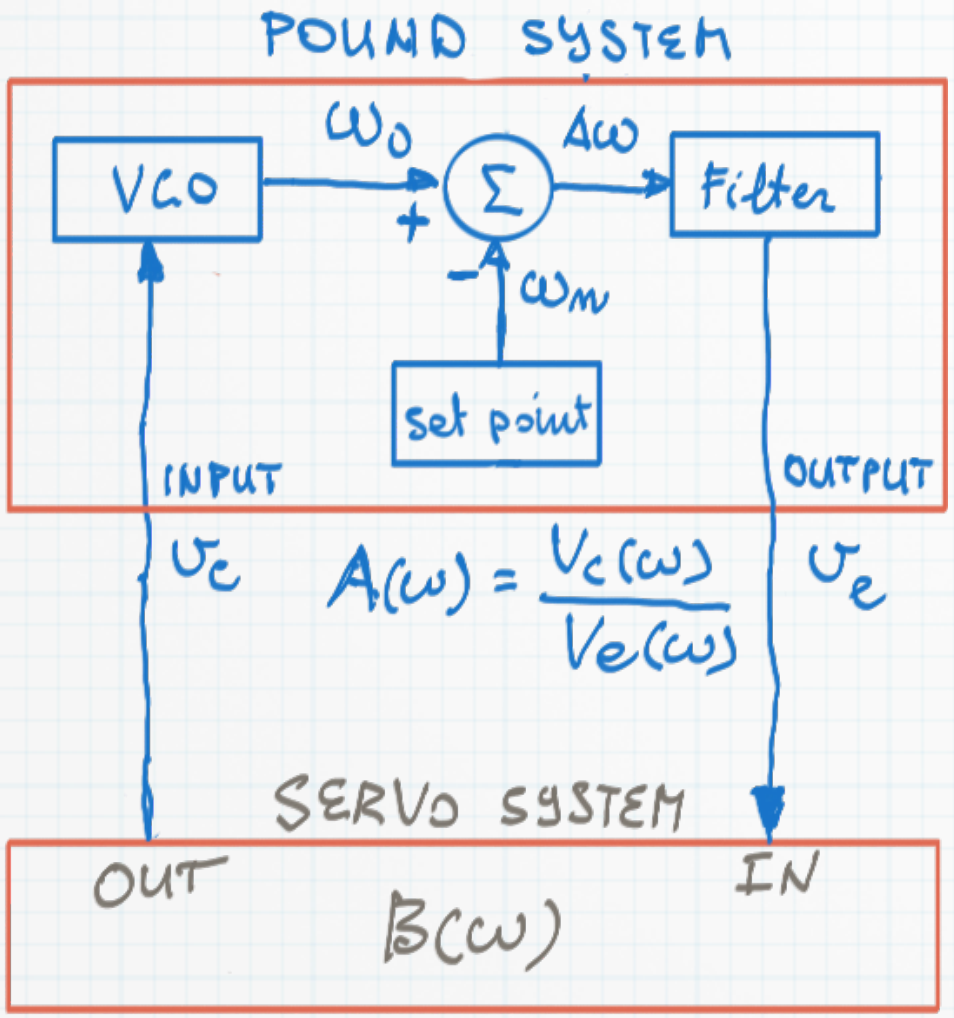

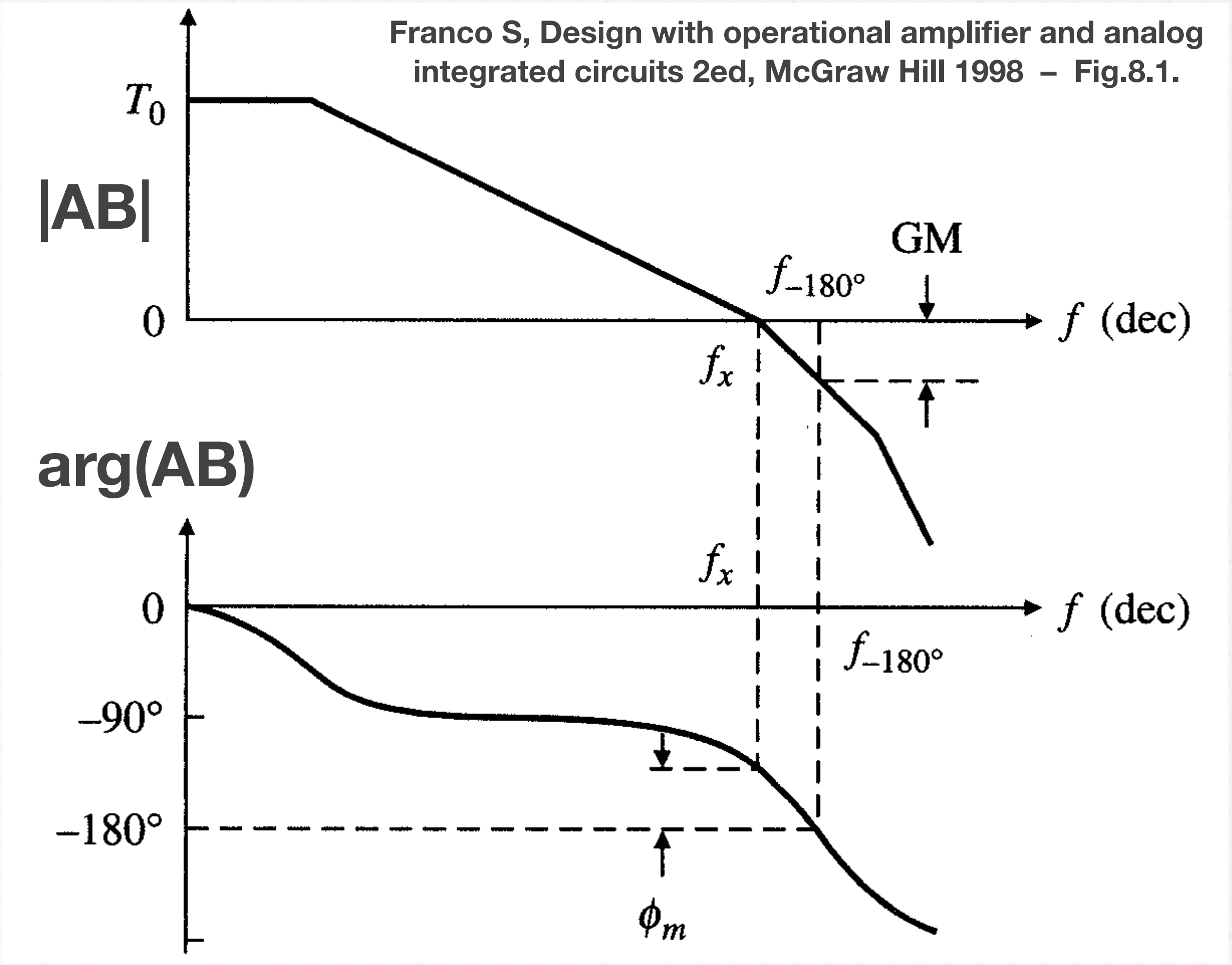

- **The control loop must be stable**
  - **|AB| < 1 at the critical frequency where arg(AB) = π**
  - **In practice, ≥ π/4 (45º) phase margin is needed**
- **Higher dc gain provides higher accuracy**

Pound-detector transfer function

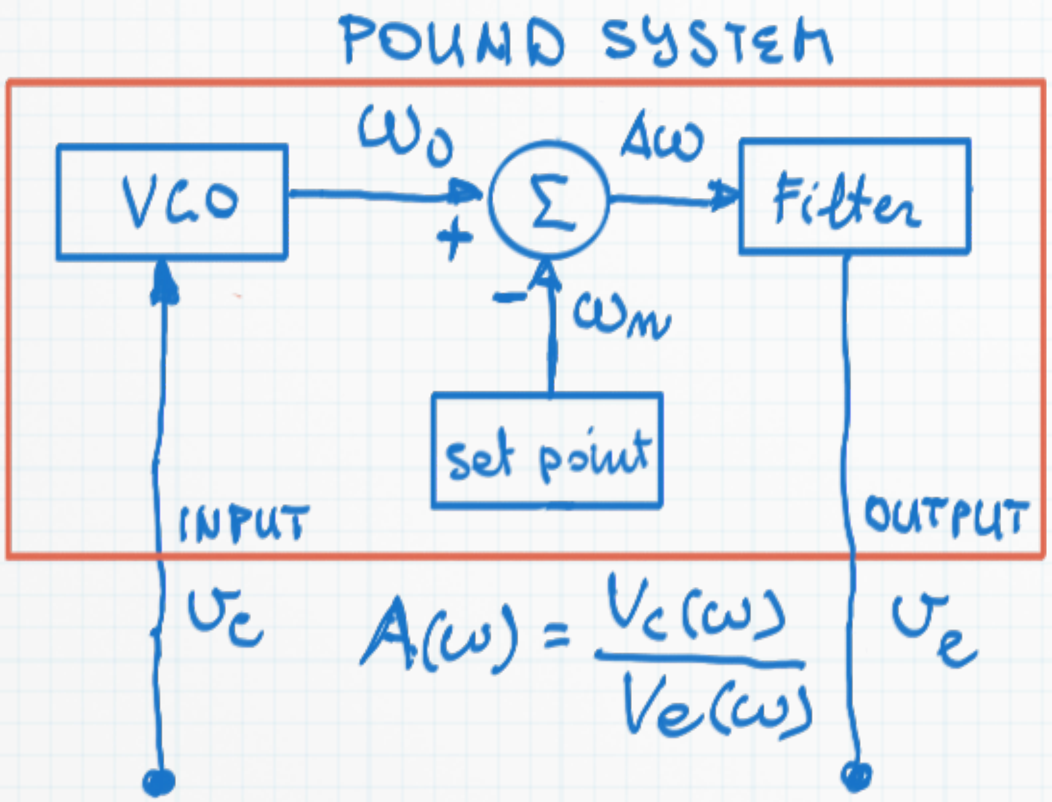

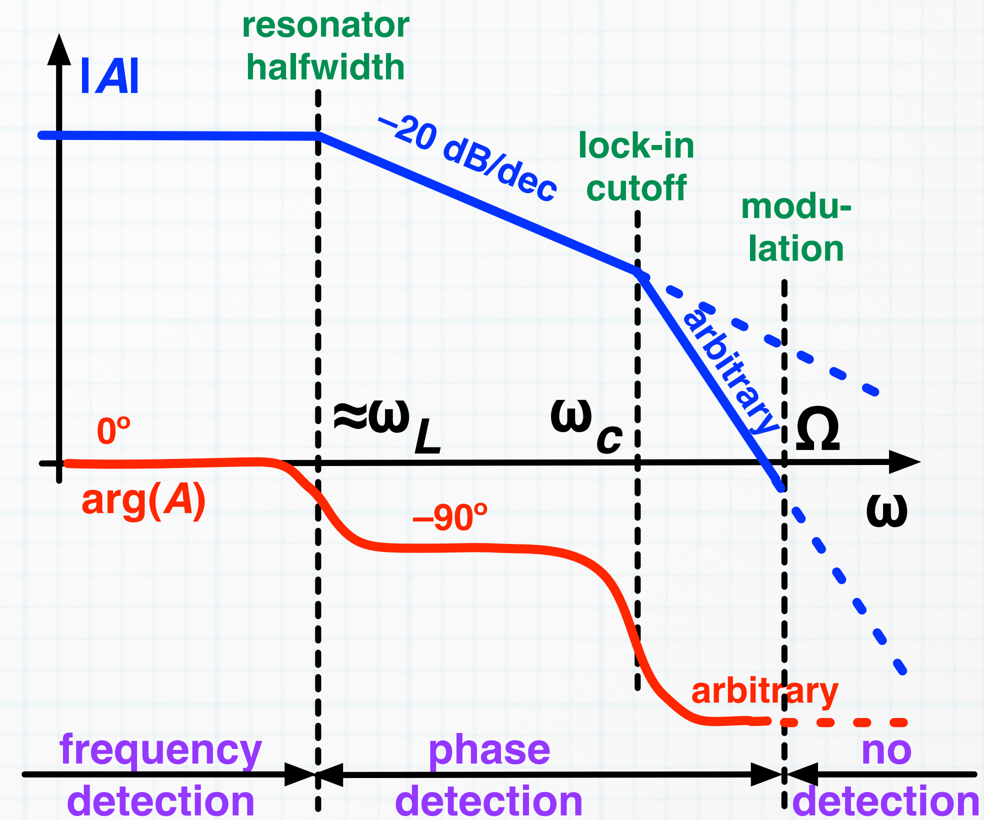

- **Quasi-static operation at $\omega < \omega_L$ (resonator half-width)**
  - **Oscillator frequency-noise detection (as discussed)**
- **At $\omega > \omega_L$, the resonator reflects the noise sidebands**
  - **Oscillator phase-noise detection at $\omega_L < \omega < \Omega$ (integrator)**
  - **The internal lock-in filter rolls off at $\omega > \omega_c$**
  - **The lock-in amplifier stops working at $\omega \approx \Omega$ and beyond**

Simple servo-loop design

Proceed from right to left

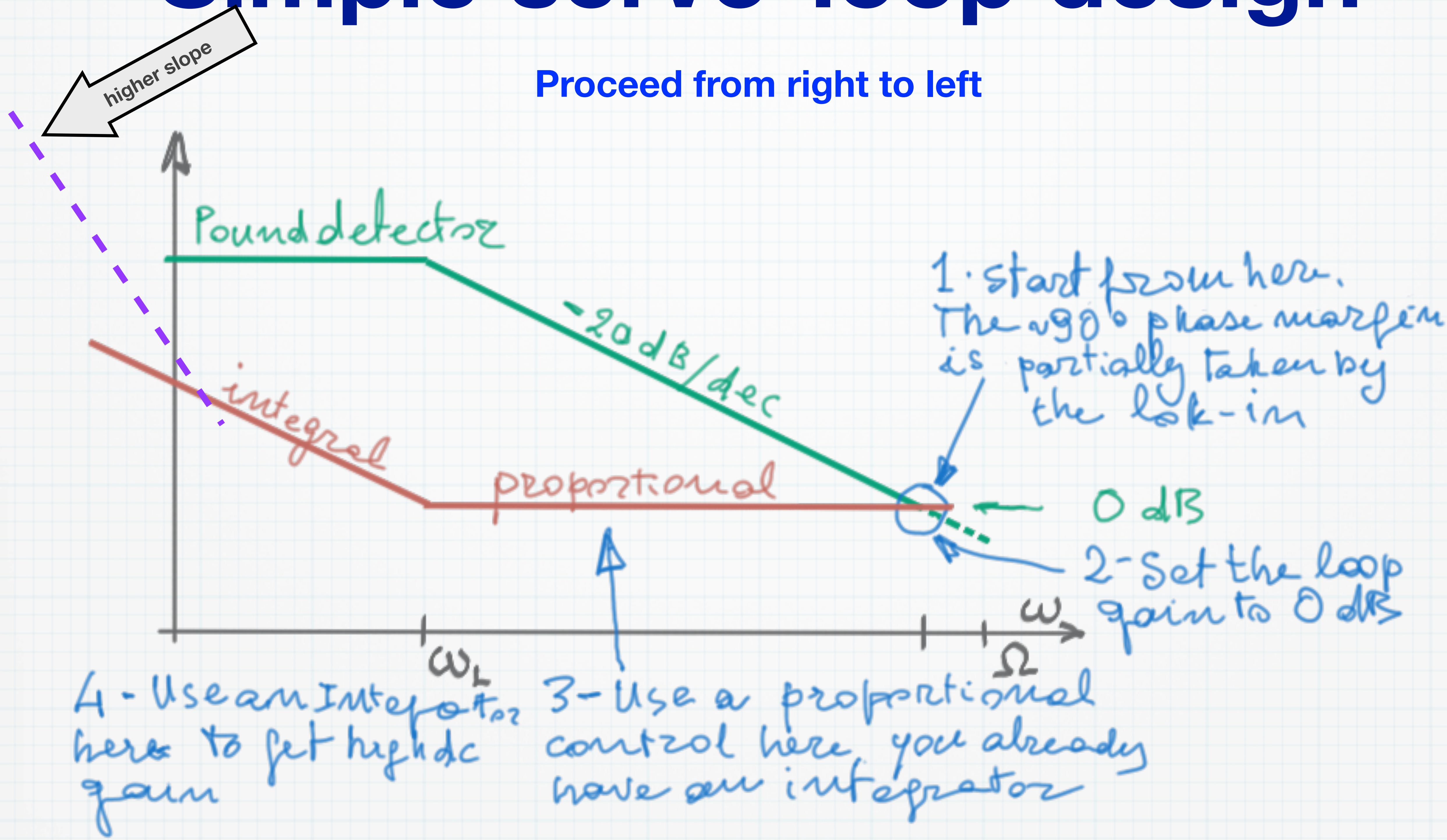

- Start from Ω (or ω_c) and go leftwards
  - Set phase margin ≈ π/4 (45º)
- Design the transfer function

Improved servo loop

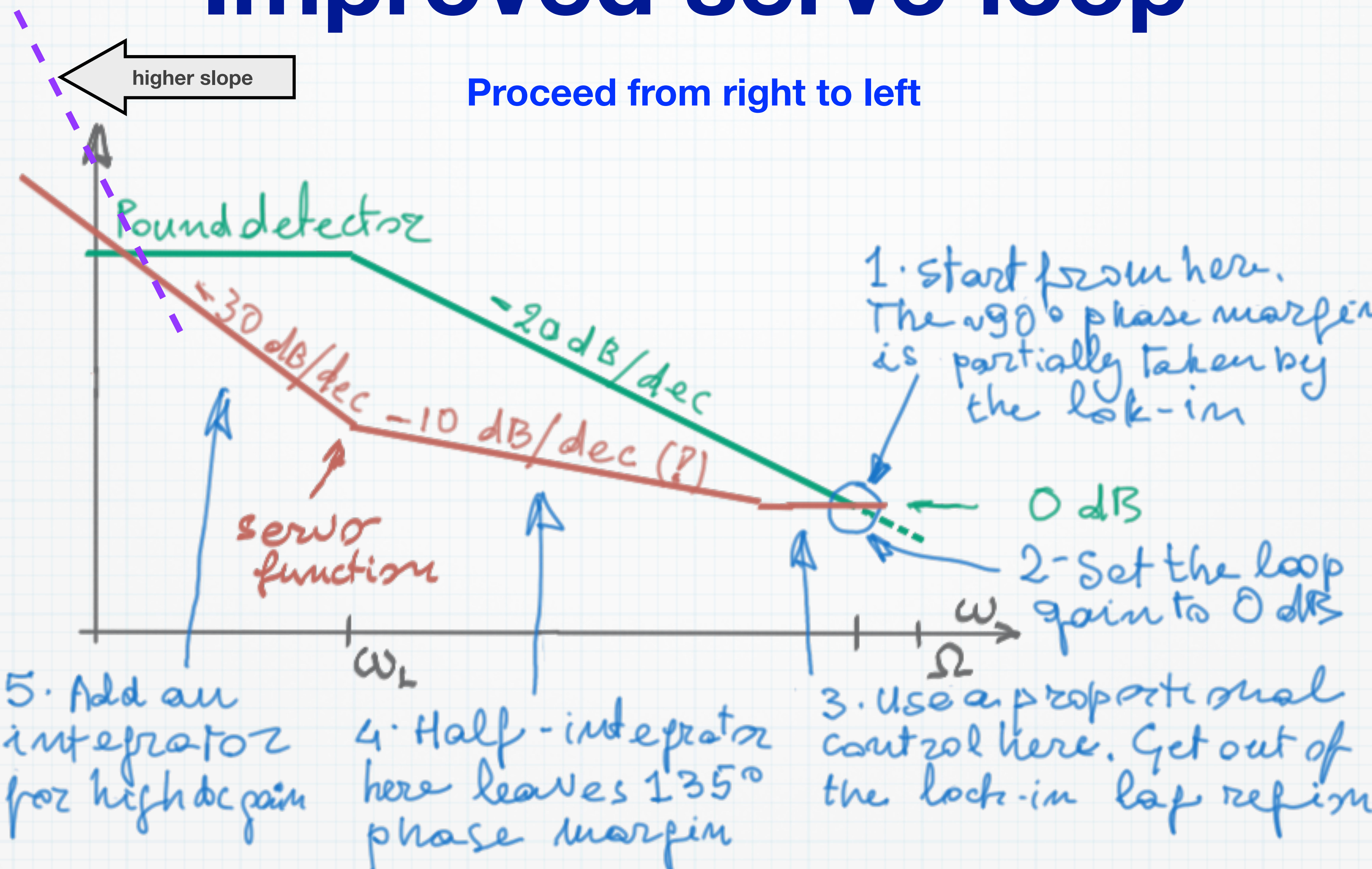

- Resonator –20 dB/decade –> 90º phase lag
- Half integrator 10 dB/decade –> 45º phase lag
- 45º phase margin (to 180º), independent of gain

Acousto-optic modulator delay

– Warning –

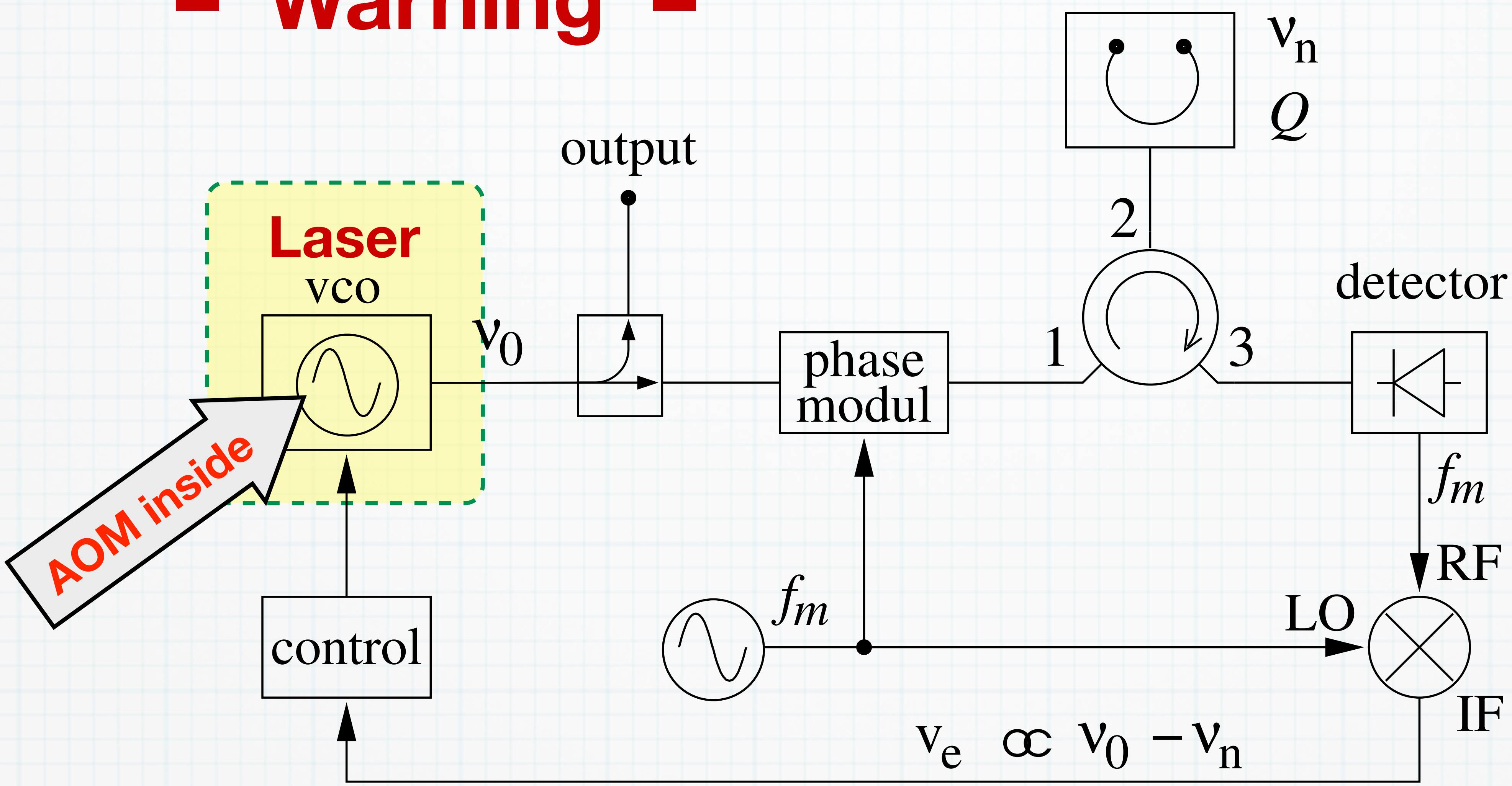

Figure from E. Rubiola, Phase noise and frequency stability in oscillators, © Cambridge University Press

- Acousto-optic modulators are often used to control the laser frequency (together with piezo modulators
- The AOM introduces a delay – a few μs typical
- The delay limits the maximum speed of the control

Resonator stability

Temperature and flicker

Temperature compensation

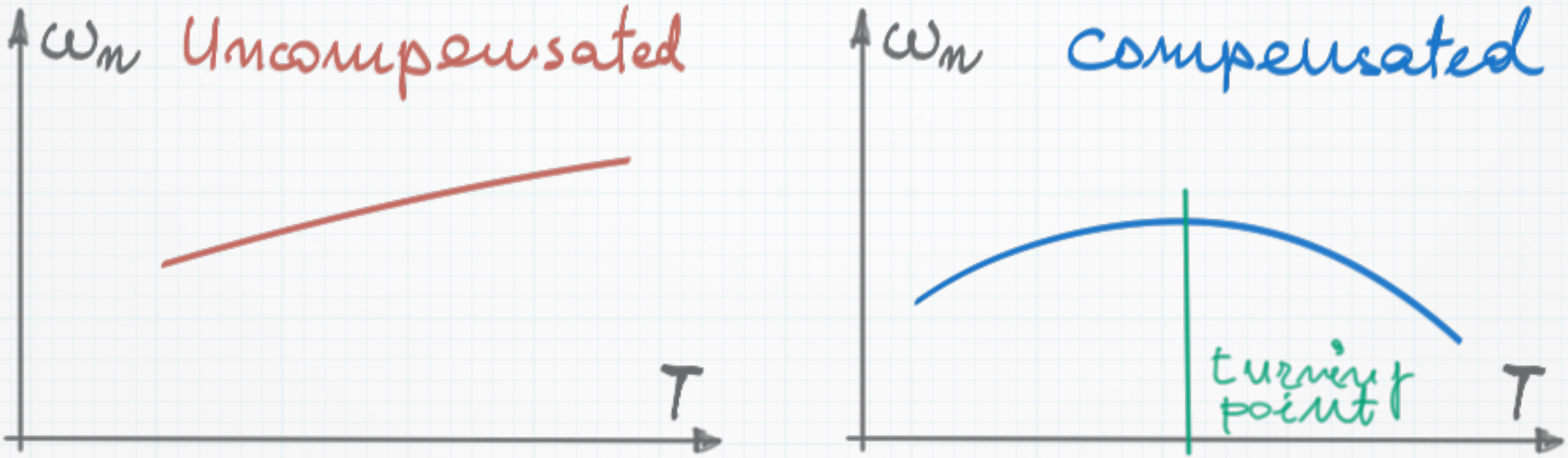

- Most solids (room temperature)
  - dielectric permittivity ε –> coefficient of 5–100 ppm/K
  - length –> coefficient of 5–25 ppm/K
- Temperature stability < 10–100 µK challenging / impossible
- A turning point is mandatory for high stability

Thermal compensation – examples

Thermo-mechanical

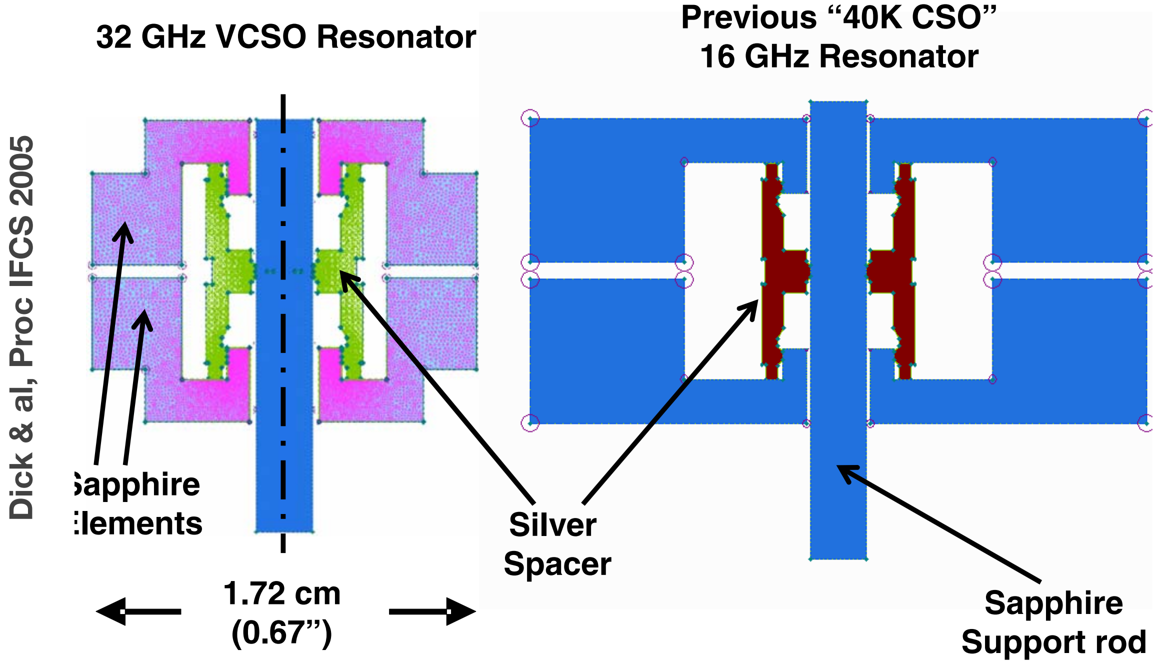

JPL Sapphire (J.Dick)
Derived from the old Lampkin oscillator

Paramagnetic

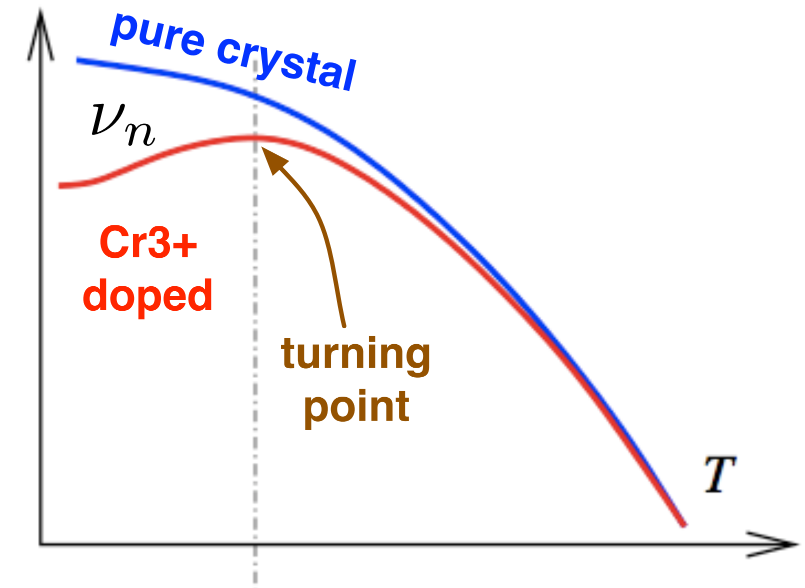

Sapphire Cr3+ impurities @ 6K (V.Giordano / M.Tobar)
Also rutile/sapphire compound @ 80 K (V.Giordano)

Natural – Refraction index

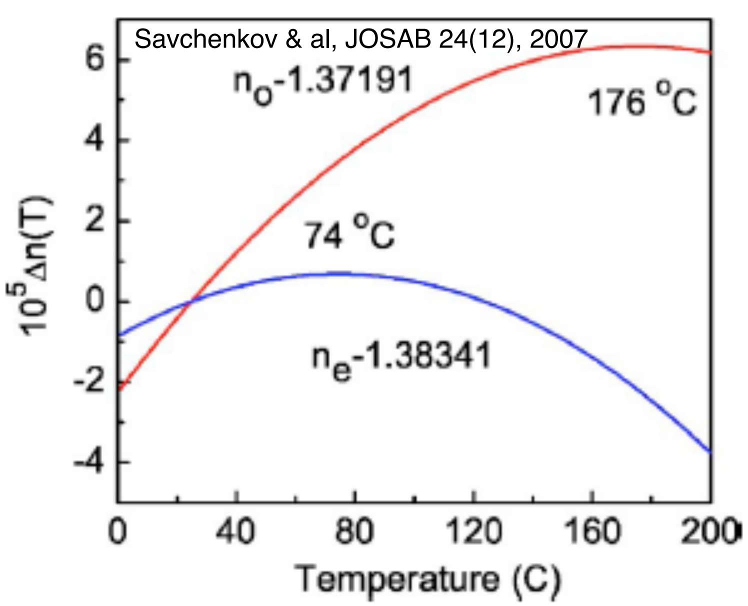

MgF2 whispering gallery (A. Savchenkov)

Natural – Thermal expansion

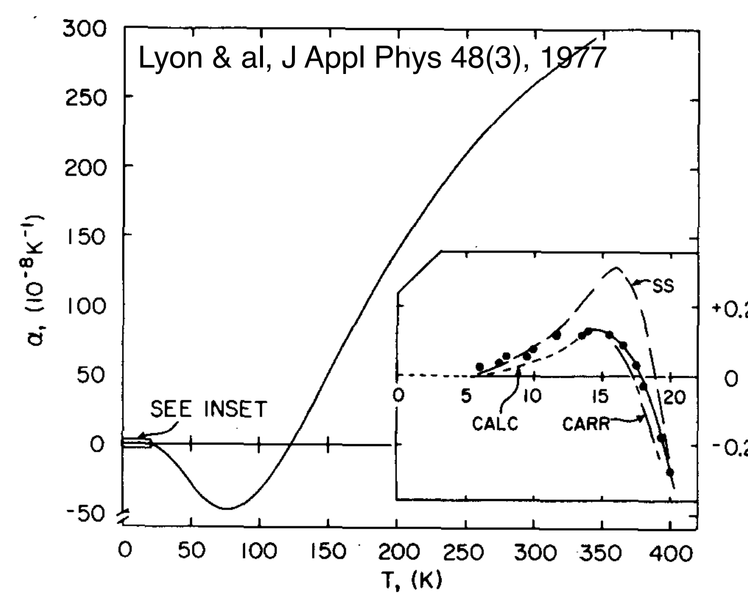

Semiconductor-grade Si @ 124 K (PTB)
@ 17 K (In progress)

Kessler & al, ArXiv 1112.3854, 2012

In some fortunate cases, the origin of 1/*f* frequency noise is known

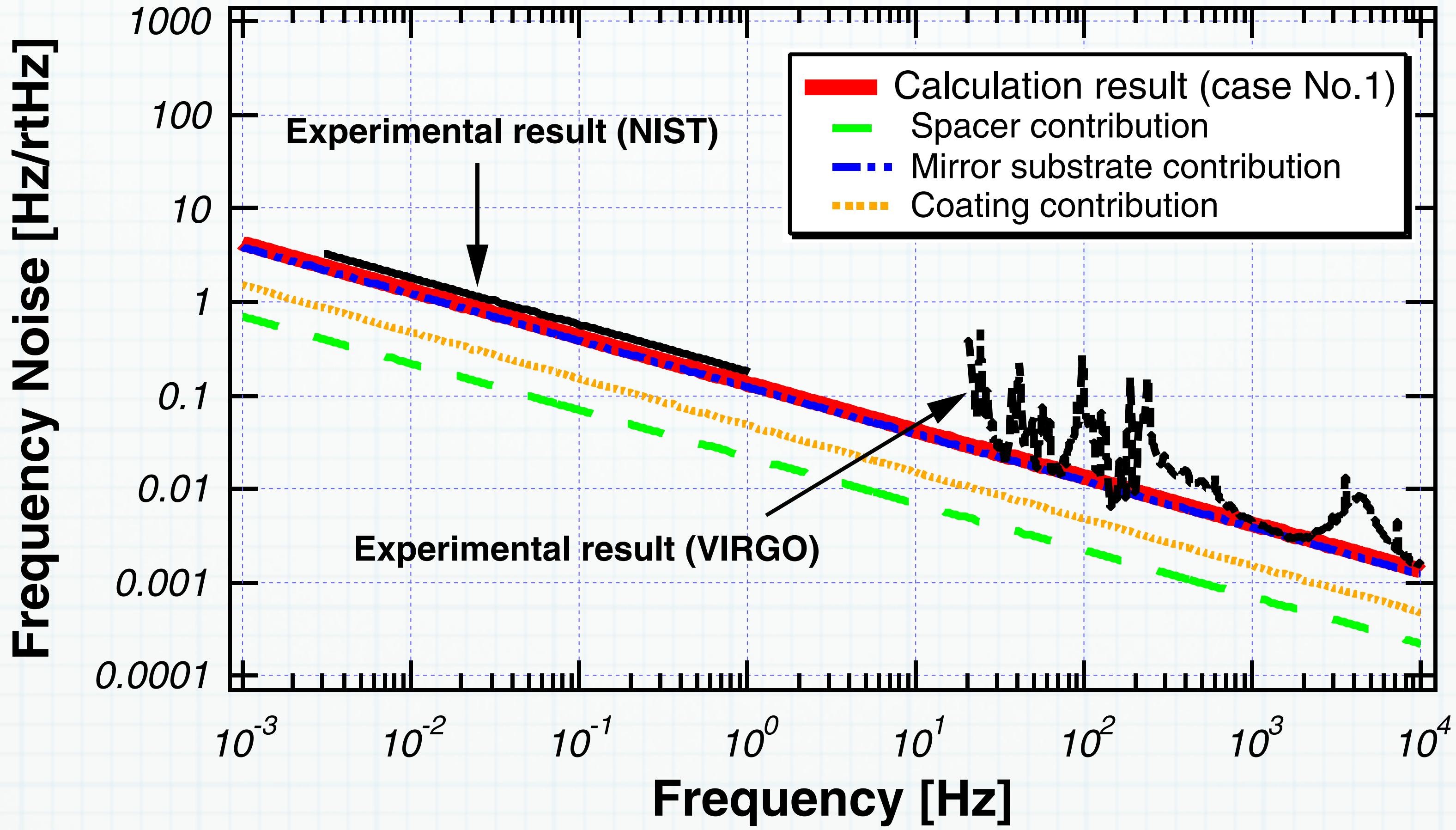

Numata K, Kemery A, Camp J, Thermal-noise limit in the frequency stabilization of lasers with rigid cavities, PRL 93(25) 250602, Dec 2004

T. Kessler, T. Legero, U. Sterr, Thermal noise in optical cavities revisited, JOSA-B 29(1), 2012

1/*f* noise – structural damping

$$\ddot{x} + 2\xi\omega_n\dot{x} + \omega_n^2 x = 0$$ homogeneous

dry friction

$F = -c\,\mathrm{sgn}(\dot{x})$

viscous

$F = -H\dot{x}$

Structural dissipation

$\approx$ in-phase with x

1/ƒ noise and FD theorem

Flicker (1/ƒ) dimensional fluctuation is powered by thermal energy

Debye-Einstein theory
for heath capacity

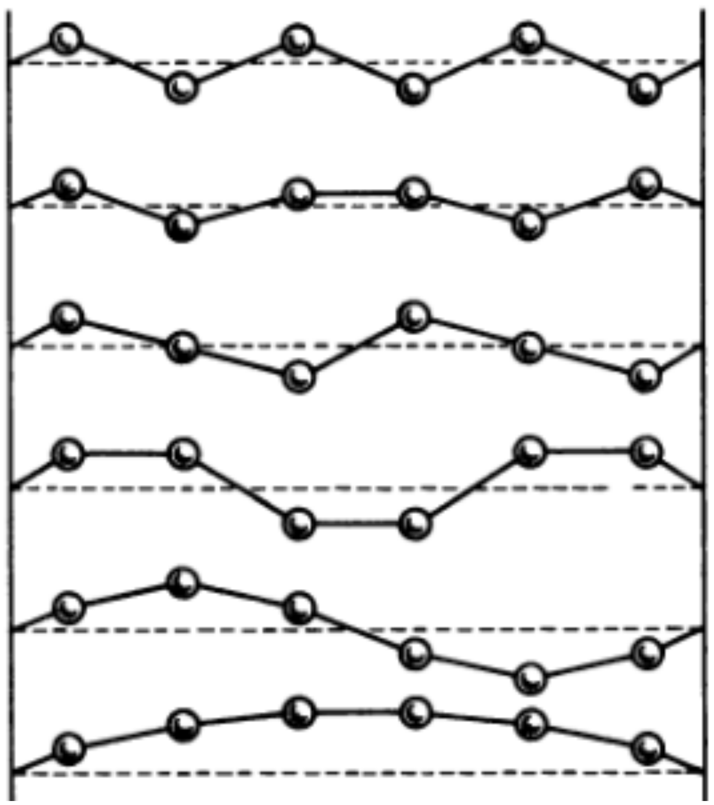

A. Holden A, The nature of solids, Dover 1965

A single theory explains
- Heath capacity
- Elasticity
- Thermal expansion

… and its fluctuations

Fluctuation Dissipation theorem in a nutshell

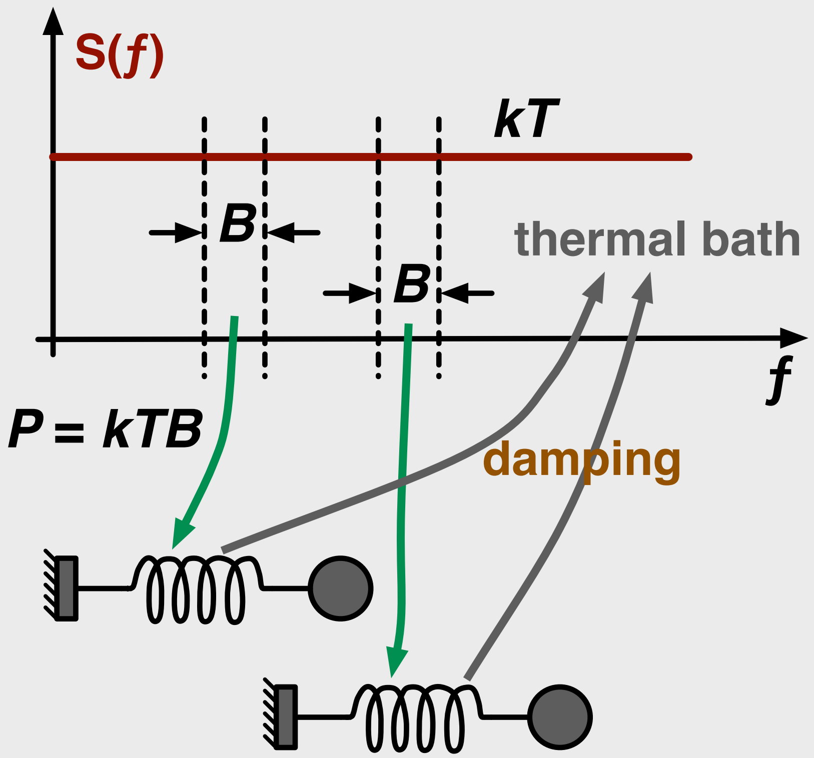

Thermal equilibrium applies
to all portions of spectrum

Thermal 1/f from the FD theorem

Look at one vibration mode

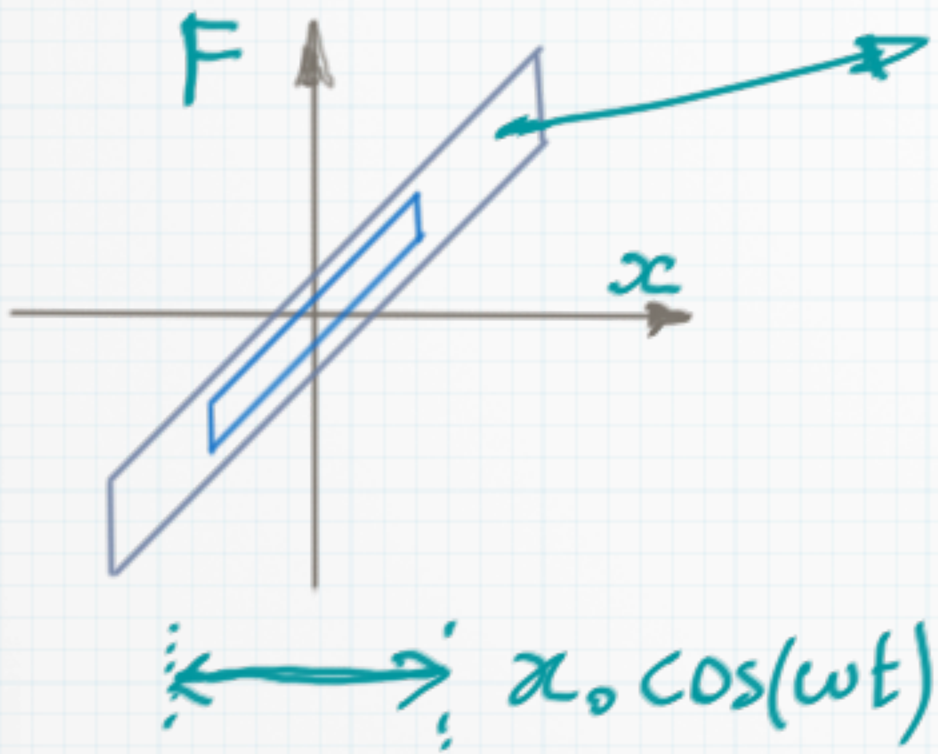

Area = Energy dissipated in 1 cycle

Small-vibration regime,
The hysteresis cycle scales with x_0

$$\boxed{E = \mu x_0^2}$$

Energy in one cycle

$$\boxed{P = \frac{\omega}{2\pi} \mu x_0^2}$$

Average power

$x_0^2 \sim 1/\omega$ Flicker!

$S_x(f) \sim 1/f$

- Structural dissipation occurs at chemical-bond scale
- Virtually instantaneous
- Thermal equilibrium
  - P = kT in 1 Hz BW
  - $x^2 \sim 1/f$ –> flicker

Damping force in phase with x (not with $\dot{x}$) –> equivalent to imaginary spring constant

Optimization Issues

Critical coupling (g = 1)

- **Maximum gain.**
  Immediately seen on Im{Γ}

$$\Gamma \simeq \frac{g-1}{g+1} - i\frac{4Q_0 g}{(g+1)^2}\frac{\Delta\omega}{\omega_n}$$

close to ω_n

- **Lowest "useless" power in the quadratic detector.**
  Immediately seen on Re{Γ}

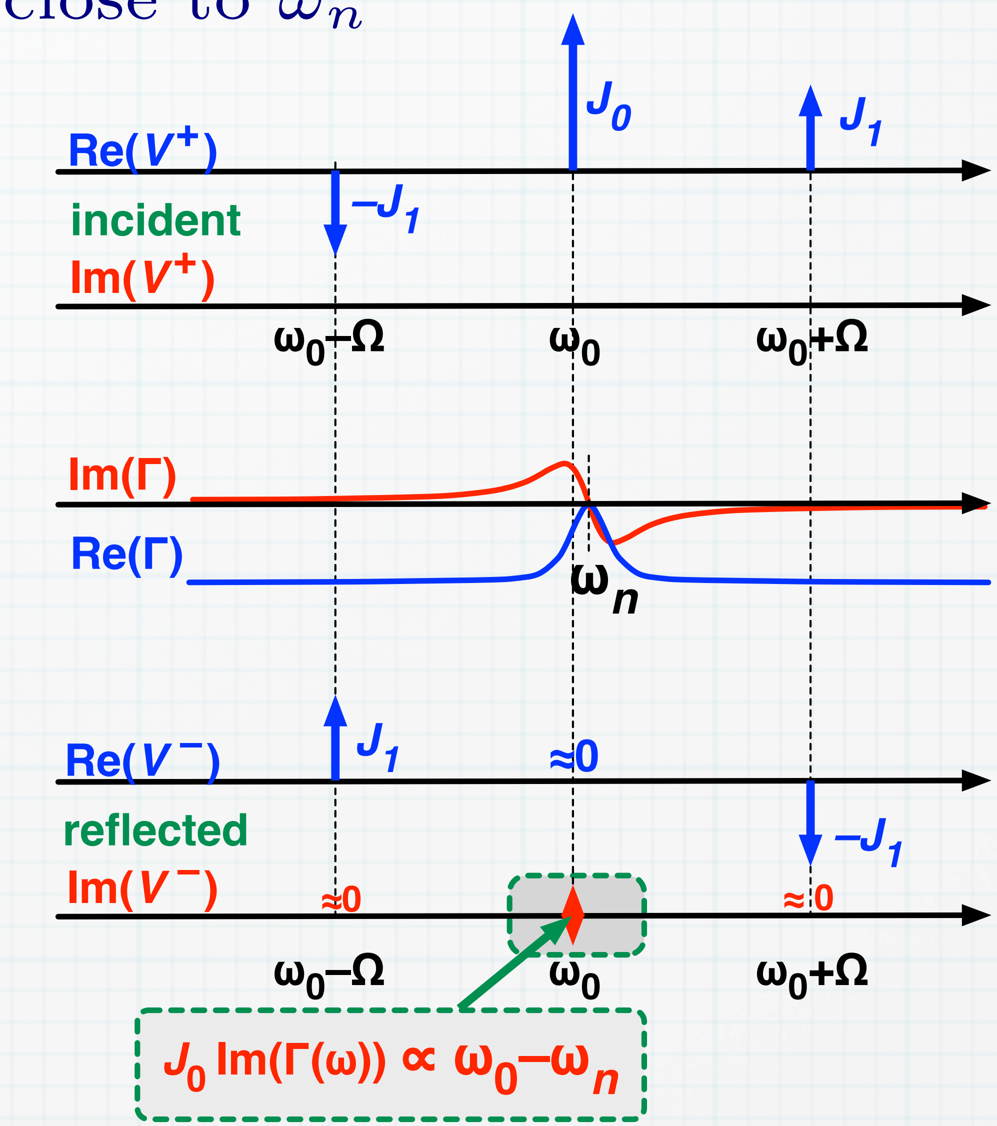

- **The frequency error due to residual AM vanishes**
  Some maths – not shown

Detector responsivity

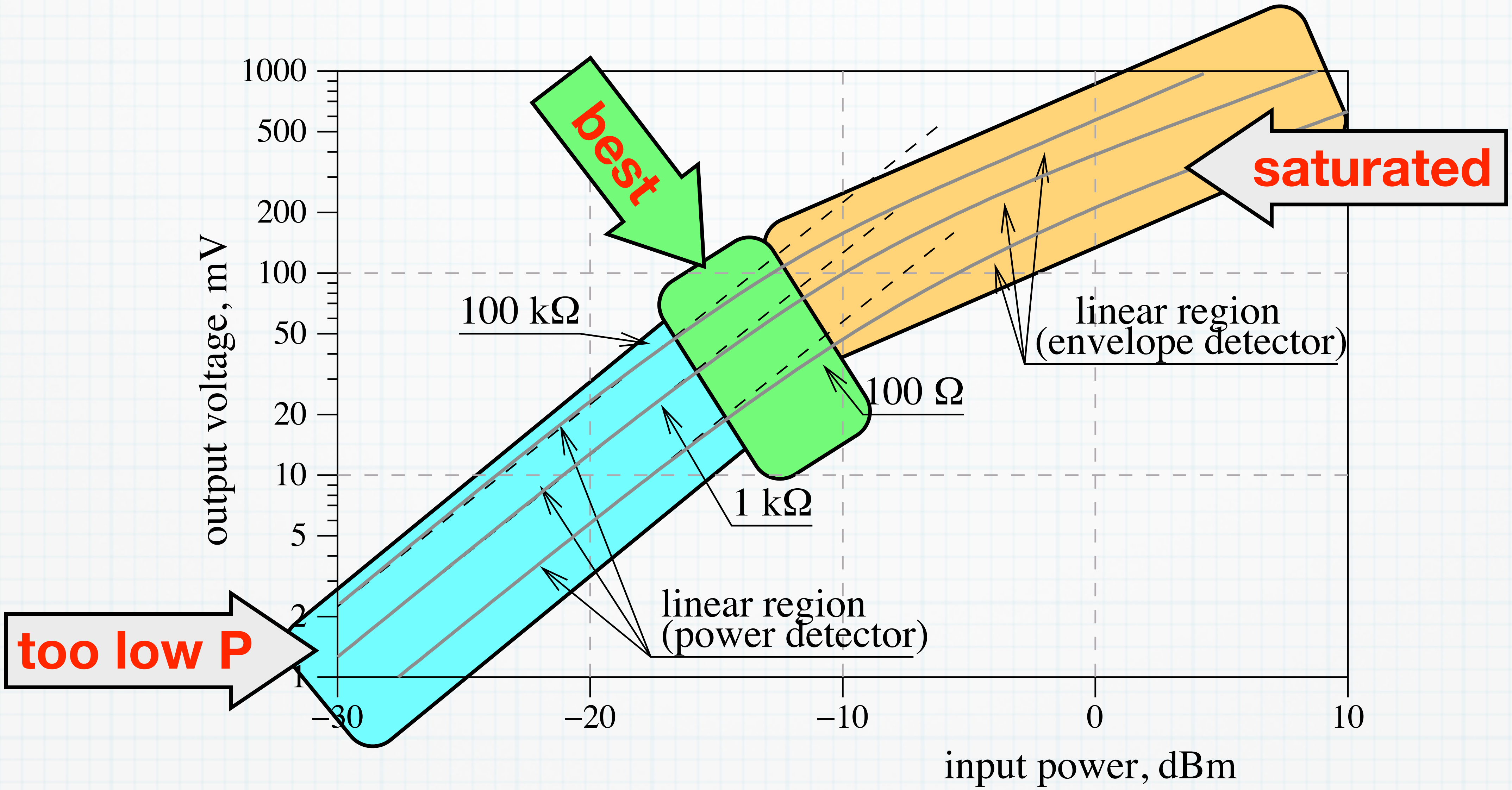

$$(a+b+c)^2 = a^2 + b^2 + c^2 + 2ab + 2ac + 2bc$$

- **The error signal comes from the 2ac + 2bc terms**
- **Highest sensitivity just below the corner**

Maximum power in the resonator

- Dissipated P –> Thermal instability (obvious)
- Traveling P –> Instability
    - Dielectric constant
    - Radiation-pressure
      Chang & al., …radiation pressure effect…, PRL 79(11) 1997
- Difficult to lock (ω_n runaway)
    - Control instability and failure
- "Maximum P" applies to the carrier, not to sidebands
    - The carrier gets in the resonator, the sidebands are reflected
- Look carefully at the resonator physics
    - Loss and dissipation are not the same thing

Modulation index

- The sidebands are reflected
- High modulation index –> high sideband power
  - Higher gain without increasing P inside the resonator
- Effect of higher-order sidebands (±2Ω, ±3Ω, etc.)
  - Not documented – though conceptually simple
- DSB modulation, instead of true PM
  - A pair of sidebands is simpler than true PM
  - Modulator $1/f$ noise?

Modulation frequency

Lower bound for Ω

- Total reflection at $\omega_n \pm \Omega$ is necessary
  - Thus, $\Omega \gg B/2\pi$,   B = resonator bandwidth

Why to choose the largest possible Ω

- Larger control bandwidth
  - Higher dc gain –> higher stability

Why *not* to choose the largest possible Ω

- Avoid dispersion (PM –> AM conversion)
- Technical issues / Design issues

My experience – at Femto-ST

- 95–99 kHz for the sapphire oscillators (10 GHz, B=10 Hz)
- 22 MHz for the optical FP (193 THz, $B \approx 30$ kHz)

Residual AM

- Residual AM yields a detected signal at the modulation frequency Ω
  - Generally poorer operation
  - Frequency error –> $\omega_0 \neq \omega_n$ at the null point
  - Frequency fluctuation if the AM fluctuates

Basu R, Wang R, Dick GJ, Novel design of an all-cryogenic RF Pound circuit, Proc IEEE IFCS 2005
Marra G & al, Reduction of residual amplitude modulation …, Proc. EFTF 2004

Removing the residual AM

- Additional detector enables nulling the AM in closed loop
- The power detector is reversible
- Reversed, is used as a variable stub

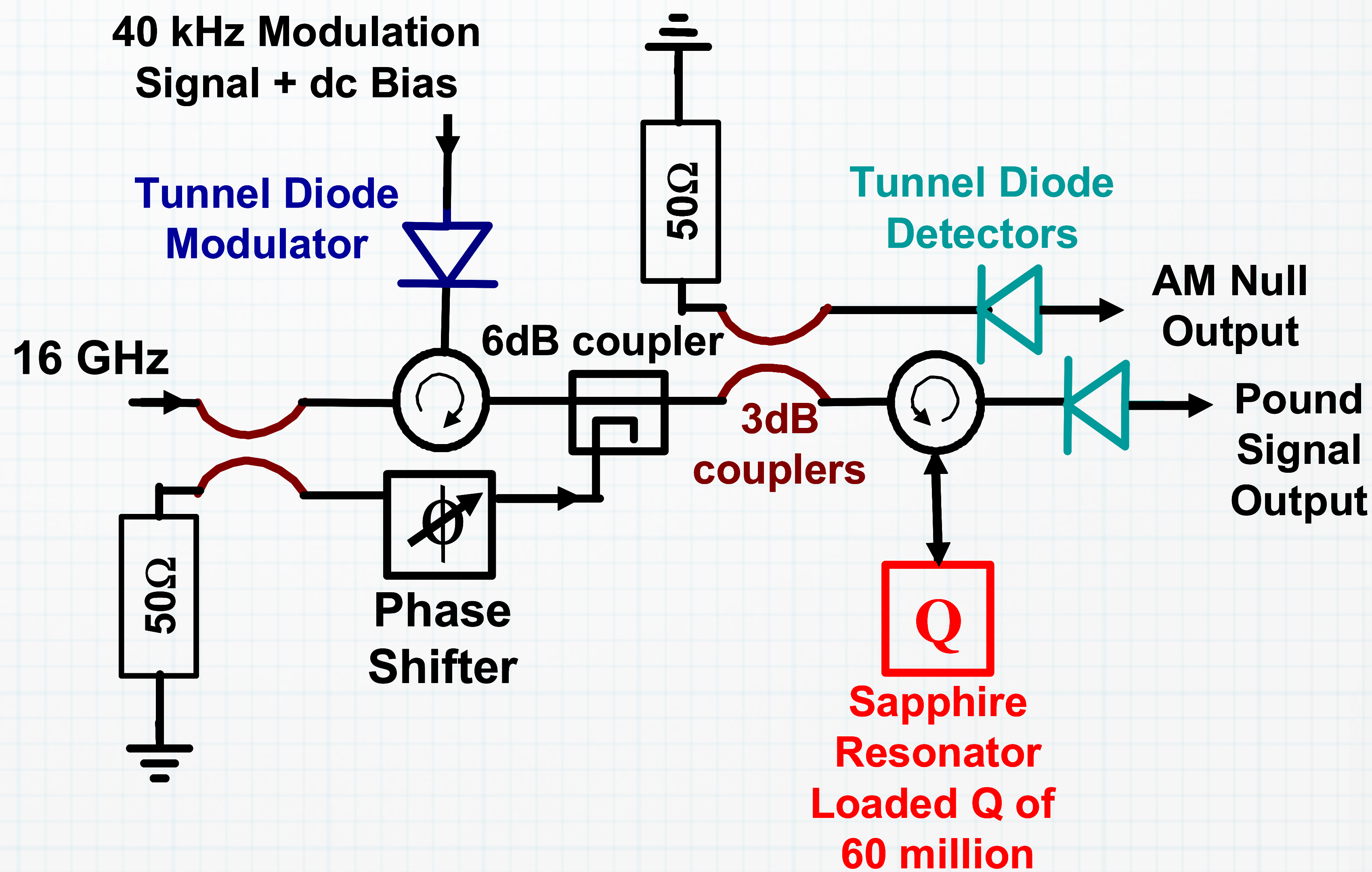

Basu R, Wang R, Dick GJ, Novel design of an all-cryogenic RF Pound circuit, Proc IEEE IFCS 2005

Filter the detector output

dc terms

$$P = \frac{|V_0|^2}{2R_0}\left\{J_1^2(m) + \frac{1}{2}J_0^2(m)\left[\frac{g-1}{g+1}\right]^2 + \frac{1}{2}J_0^2(m)\left[\frac{4Q_0}{g+1}\frac{\Delta\omega}{\omega_n}\right]^2\right\} +$$

$$-\frac{|V_0|^2}{2R_0}J_1^2(m)\cos(2\Omega t) + \frac{|V_0|^2}{2R_0}2J_0(m)J_1(m)\frac{4Q_0}{g+1}\frac{\Delta\omega}{\omega_n}\sin(\Omega t)$$

diagnostic

error signal

Large, 2Ω

Small, Ω

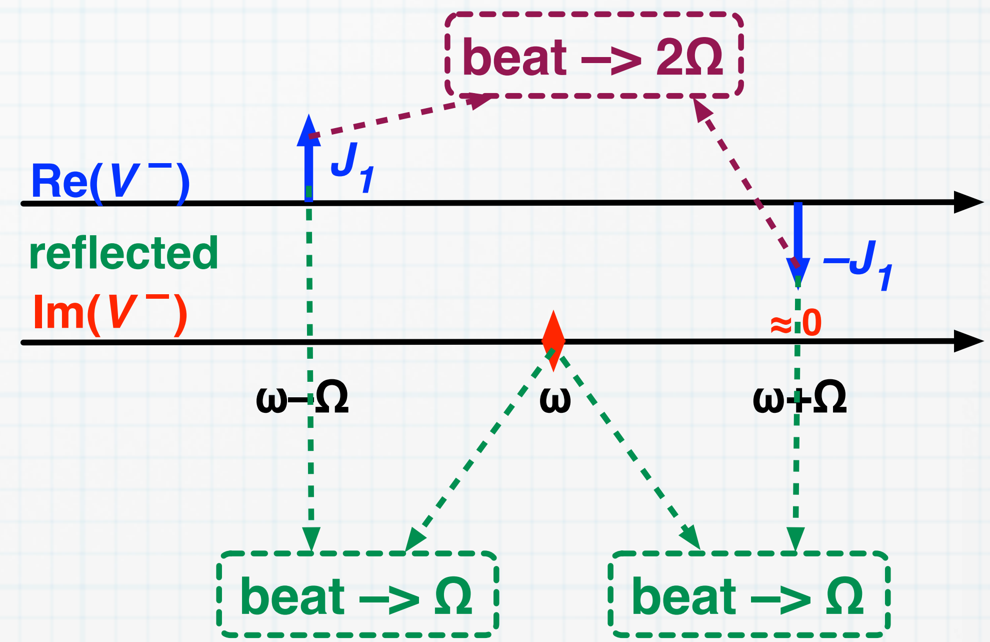

Separating the Ω and 2Ω signals with passive filter helps in getting clean, simple and effective electronics

More optimization issues

- Given the laser power –> best modulation index (Eric Black)
- Detector saturation power –> best modulation scheme
- Resonator max power –> best modulation
- Quadrature modulation (μwaves) – does it really make sense?

Applications

Resonators and oscillators

Microwaves

Whispering gallery resonator

Geometrical optics interpretation

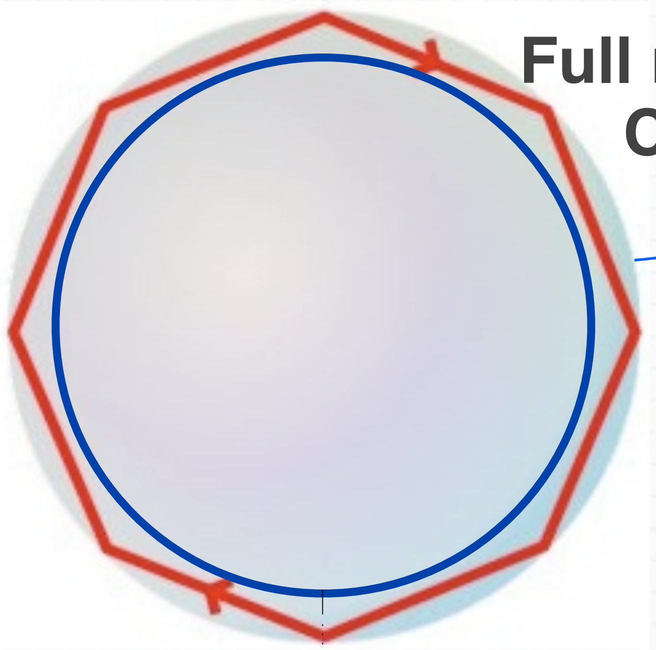

Full reflexion

Confinement inside the dielectric

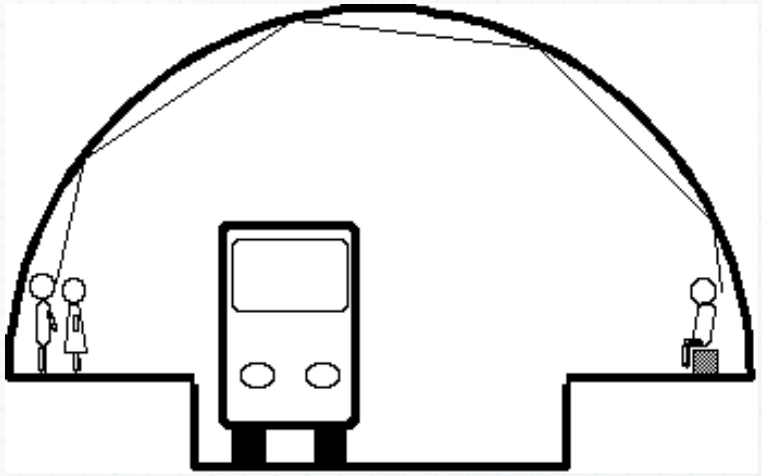

Electromag. fields

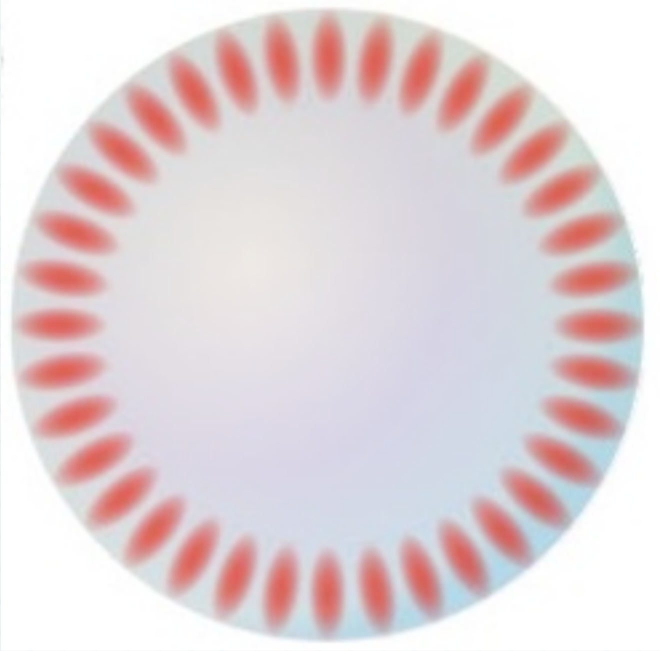

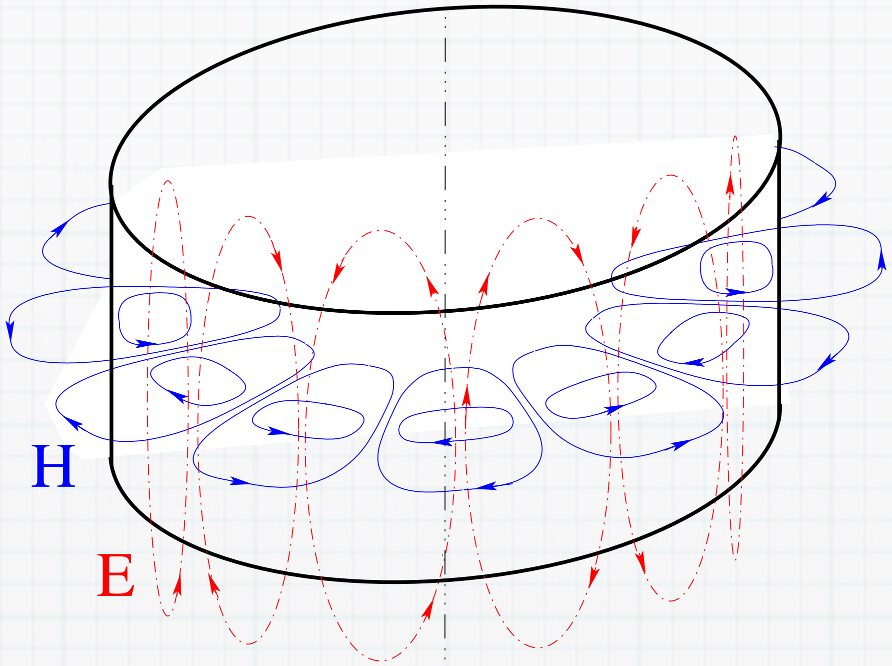

WGH mode

$$Q_0 \sim \frac{1}{\mathrm{tg}\delta} \quad \rightarrow \quad \sim 10^9 \text{ @ } 4\mathrm{K}$$

Temperature compensation

Compensation exploiting impurities, ≈6 K

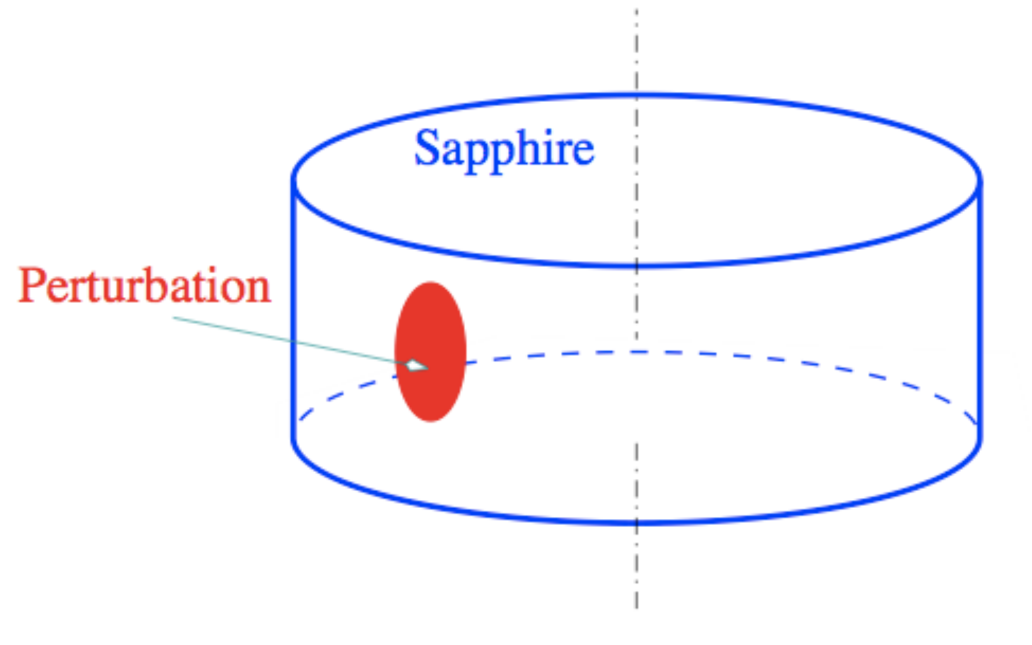

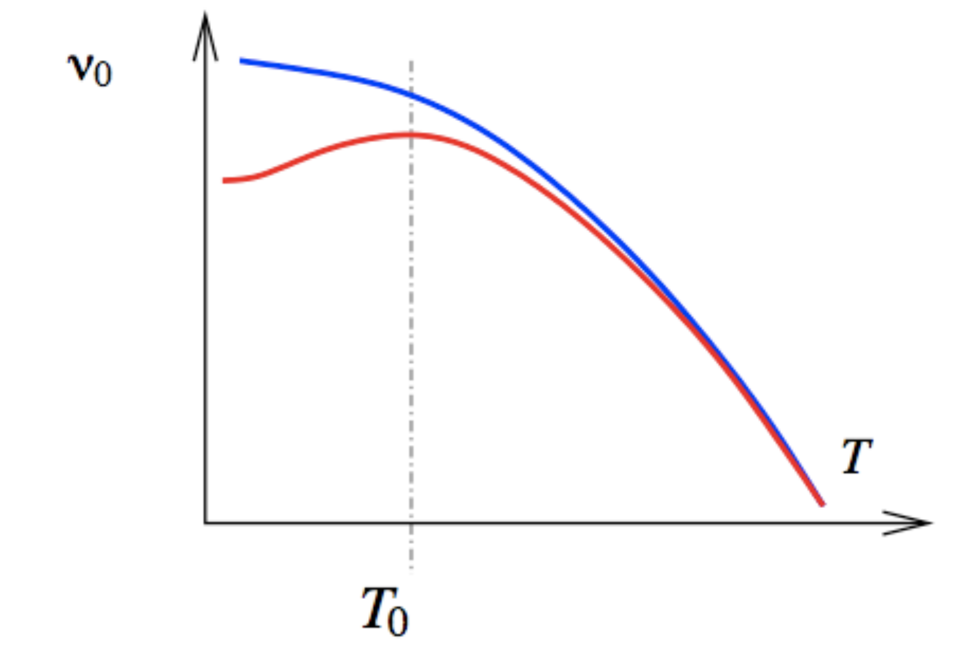

two ideas tested above 30K

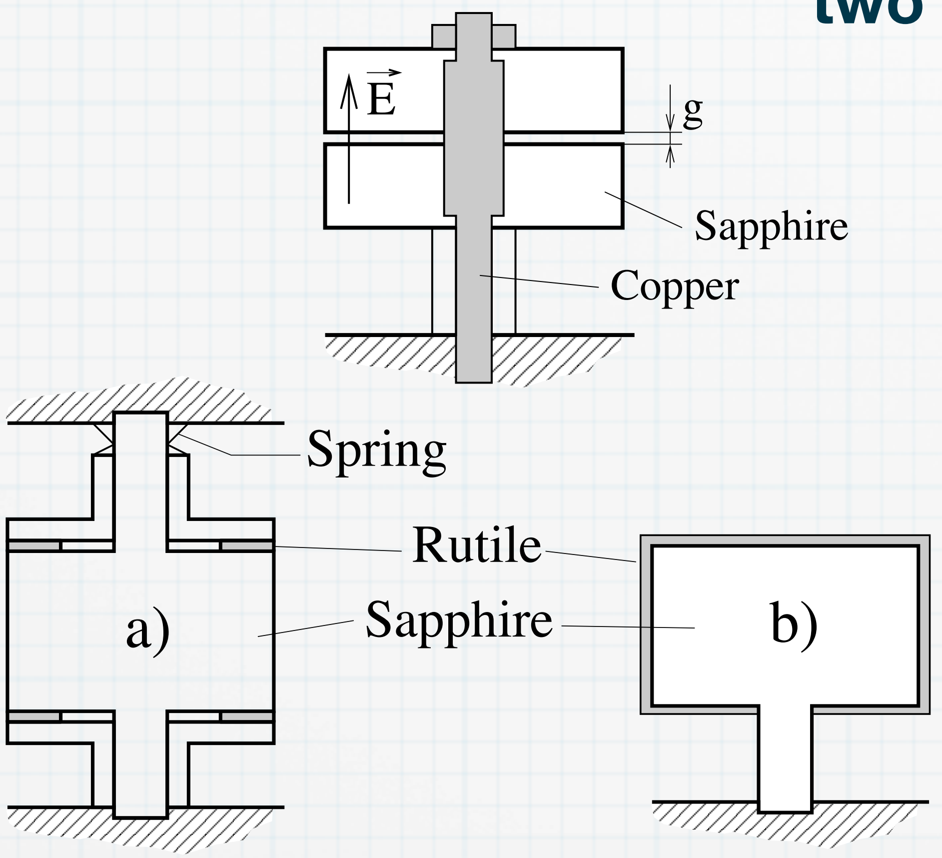

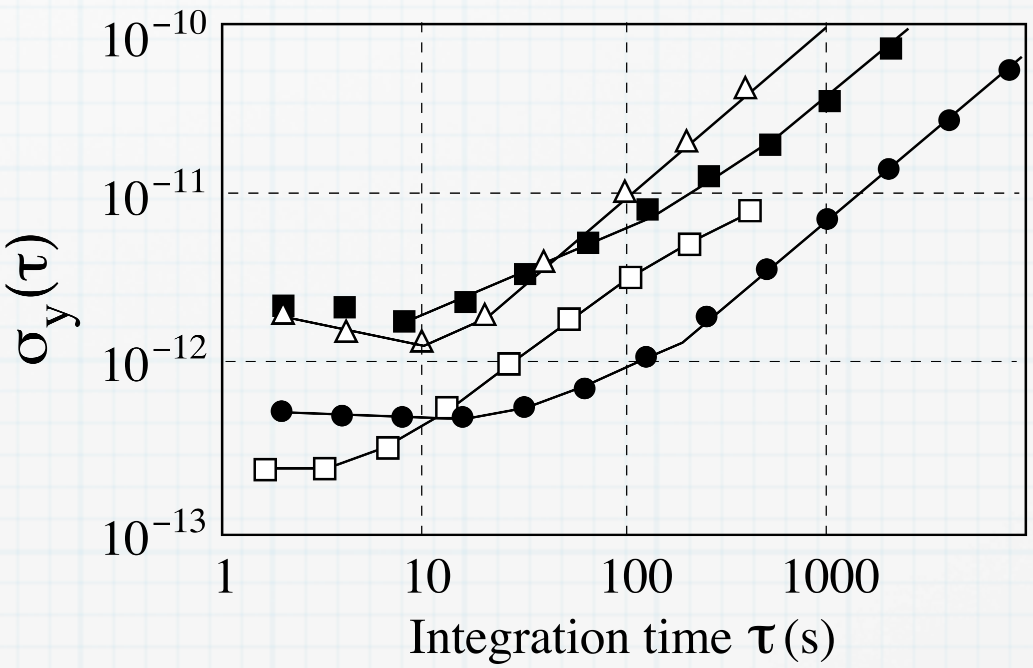

Temperature compensation

paramagnetic impurities: Fe3+ Cr3+, Mo3+, Ti3+

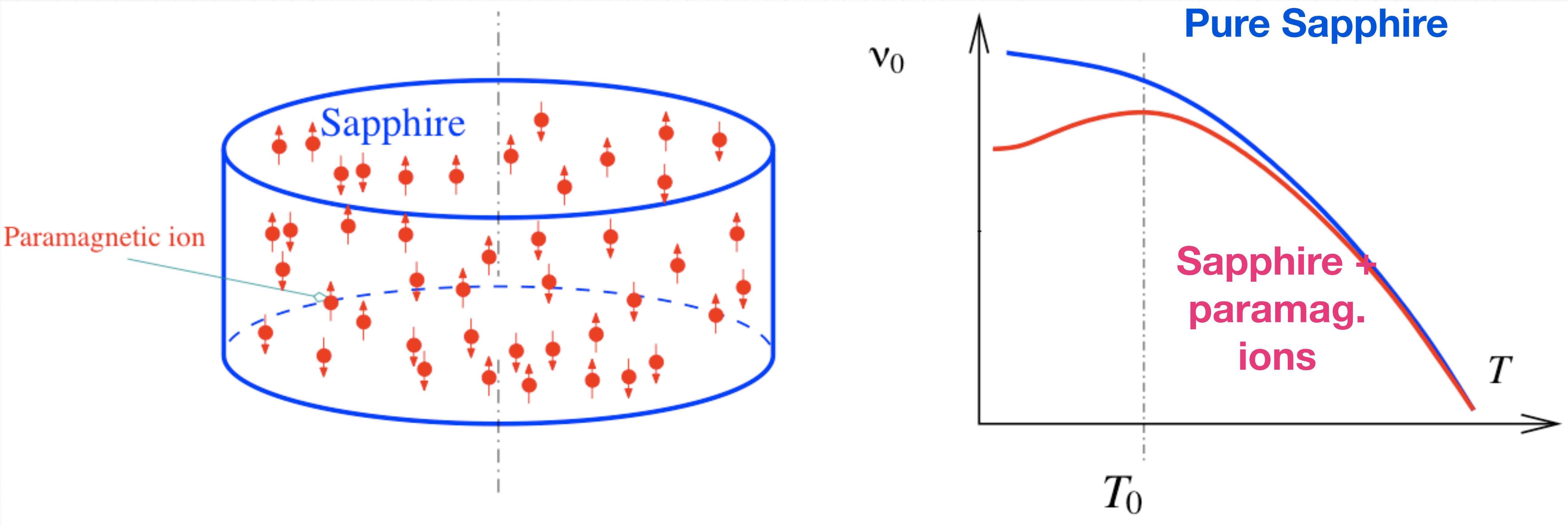

$$T_0 \sim 6\ \mathrm{K}$$

Elisa, before going to Argentina

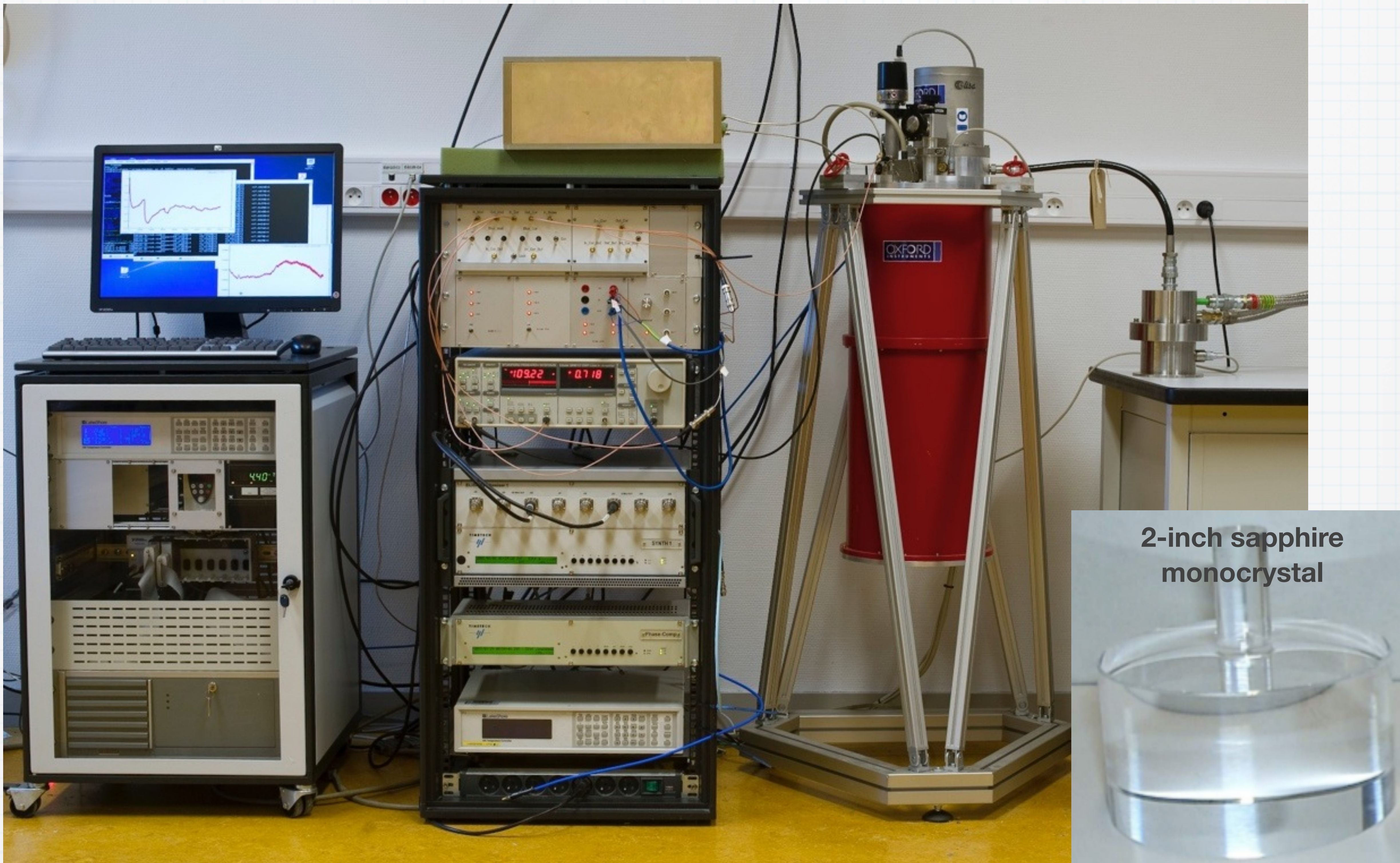

Uliss

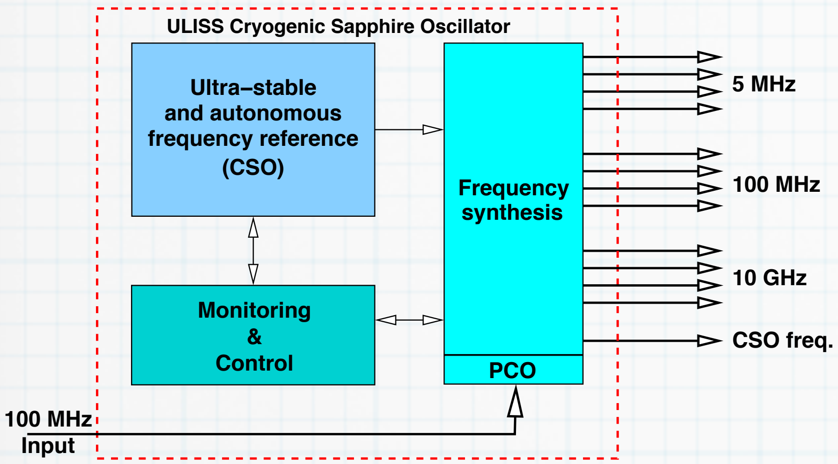

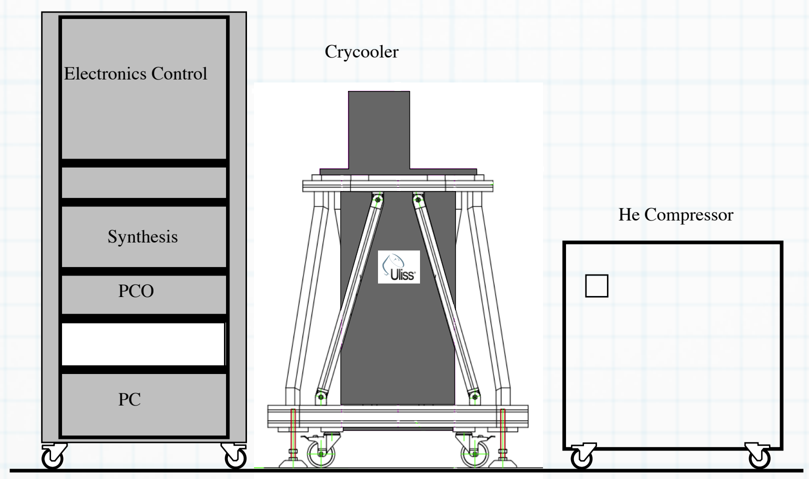

ADEV measurement ELISA/ULISS

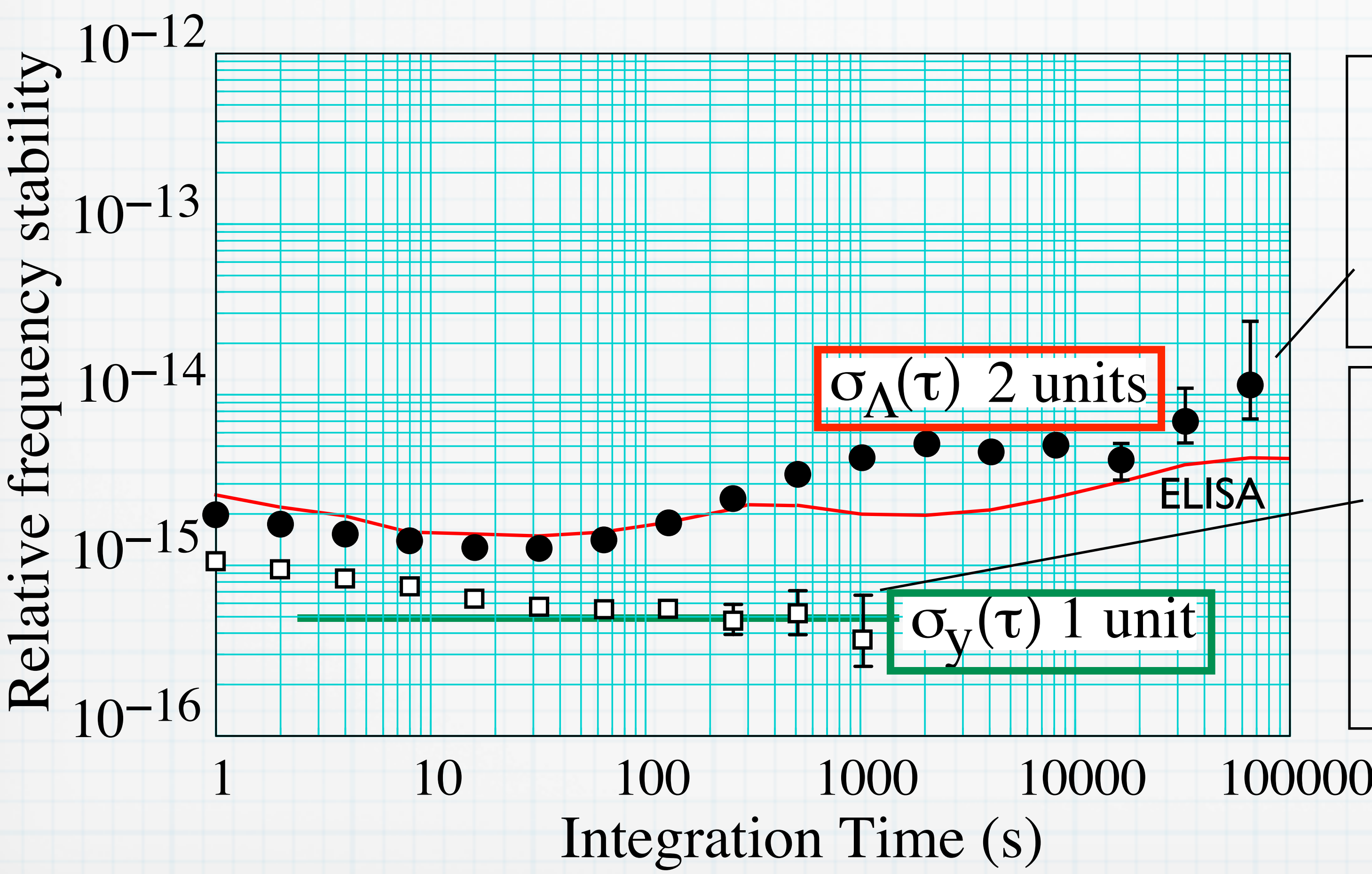

3 days measurement without post-processing
Perturbed environment:
- Technical university (ENSMM), ≥ 800 students
- Air conditioning still not operational during measurements

3 hours extracted from the entire data set
- Quiet environment, nighttime
- Take away 3dB for two equal units
- Λ-counter compensated: for flicker: $\sigma_\Lambda(\tau) \simeq 1.3 \times \sigma_y(\tau)$

flicker floor: 4×10^{-16} 10 s < τ < 1,000 s

Flory-Taber Bragg resonator

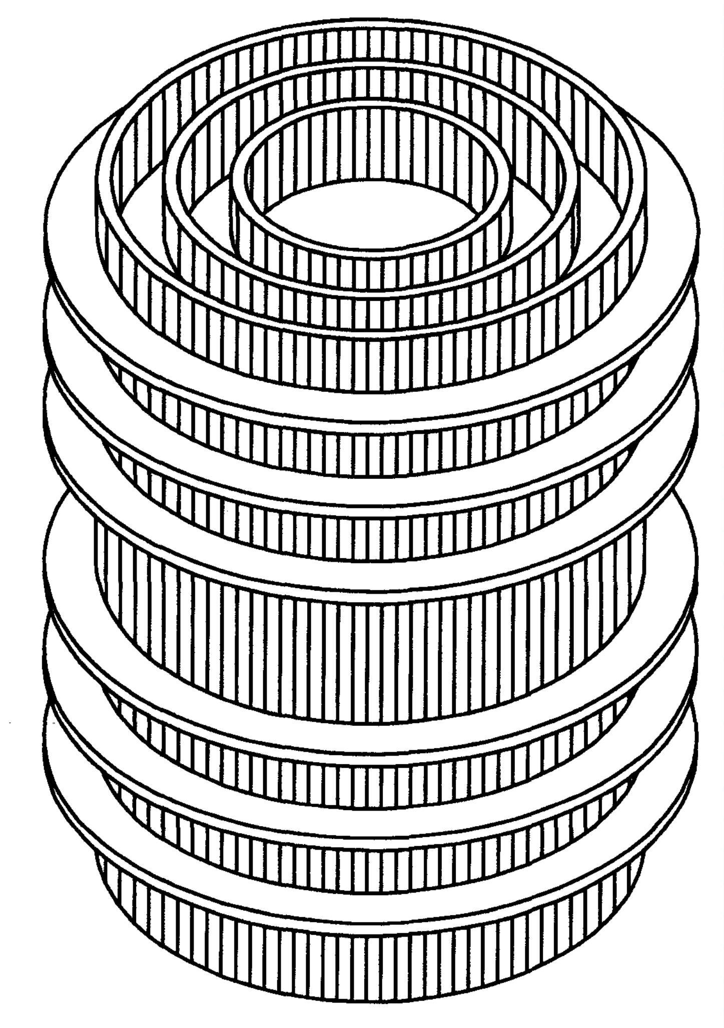

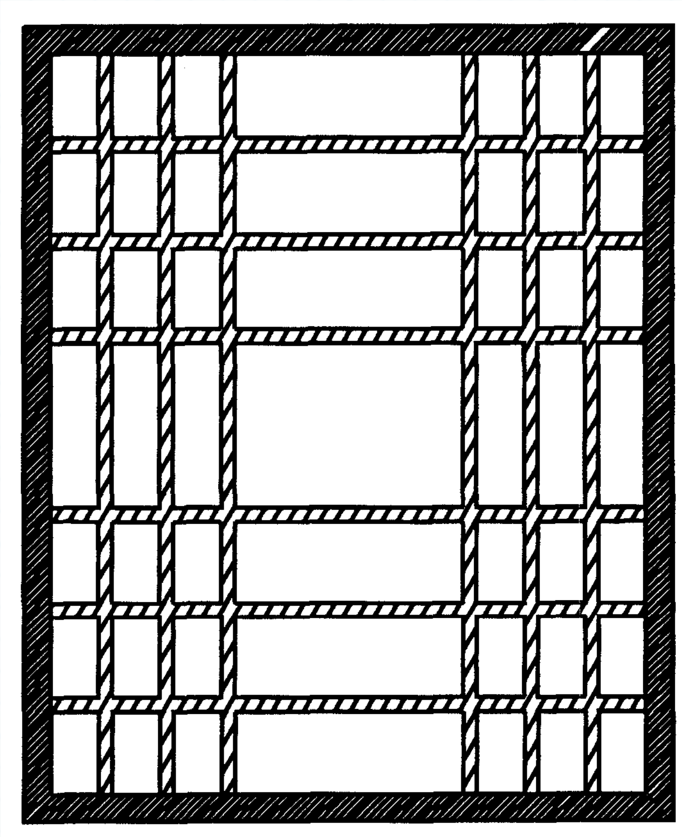

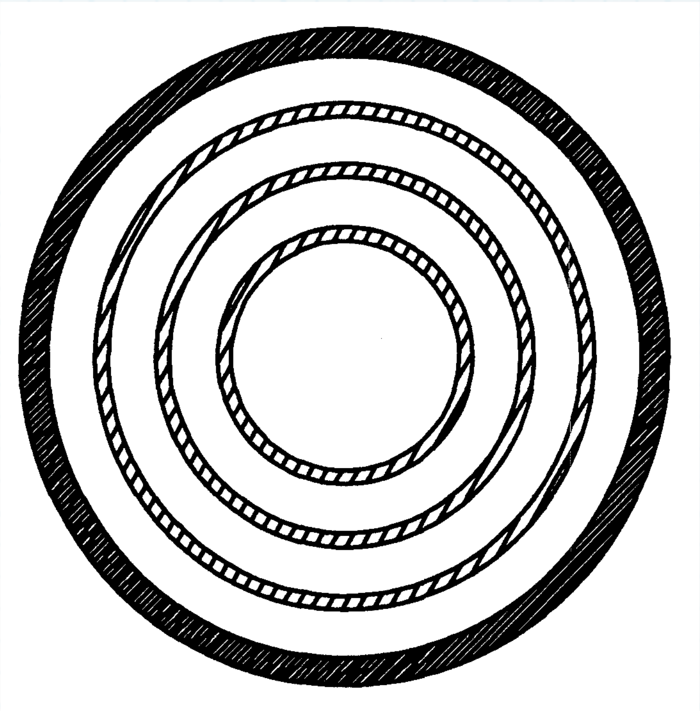

- Measured Q = 6.5×10^5 at 9 GHz, and 4.5×10^5 at 13.2 GHz
- Oscillator stability and noise not reported (yet)
- Project dropped

Flory CA, Taber RC, IEEE T UFFC 44(2), March 1997

The Bale-Everard Aperiodic Bragg resonator

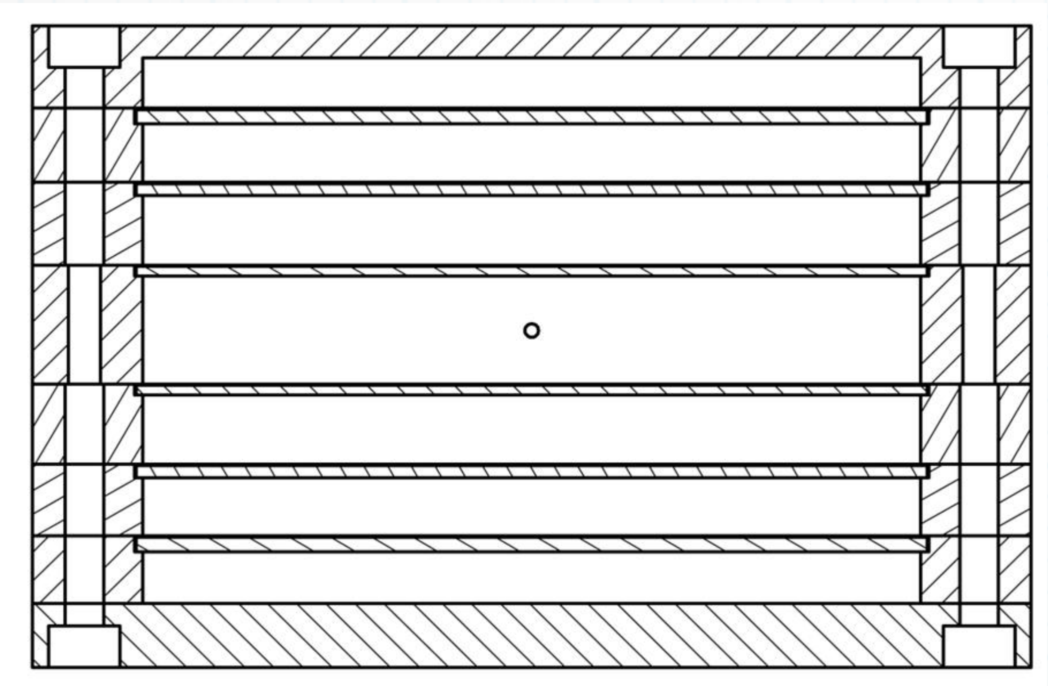

Suitable to Pound lock

- 6-plates 10 GHz resonator
  - Q > 3×10^5 (simulated)
  - Q ≈ 2×10^5 (measured)
- Oscillator stability and noise not reported yet

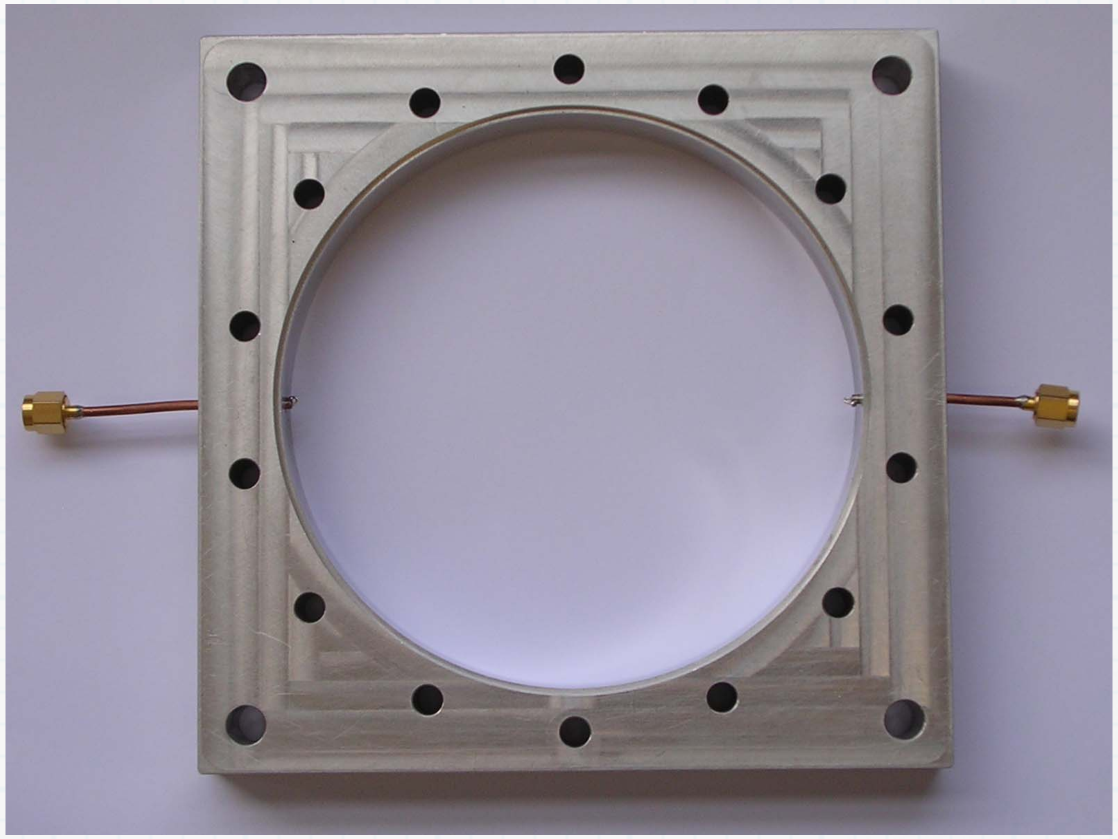

Bale S, Everard J - High Q X-band distributed Bragg resonator utilising an aperiodic alumina plate arrangement - Proc IFCS-EFTF 2009
Everard J, Proc. IFCS-EFTF 2015

Small superconducting resonator

Superconducting resonator (NPL, UK)

Nb on Al2O3, 300x300 μm2. 7.5 GHz, Q = 5E4,

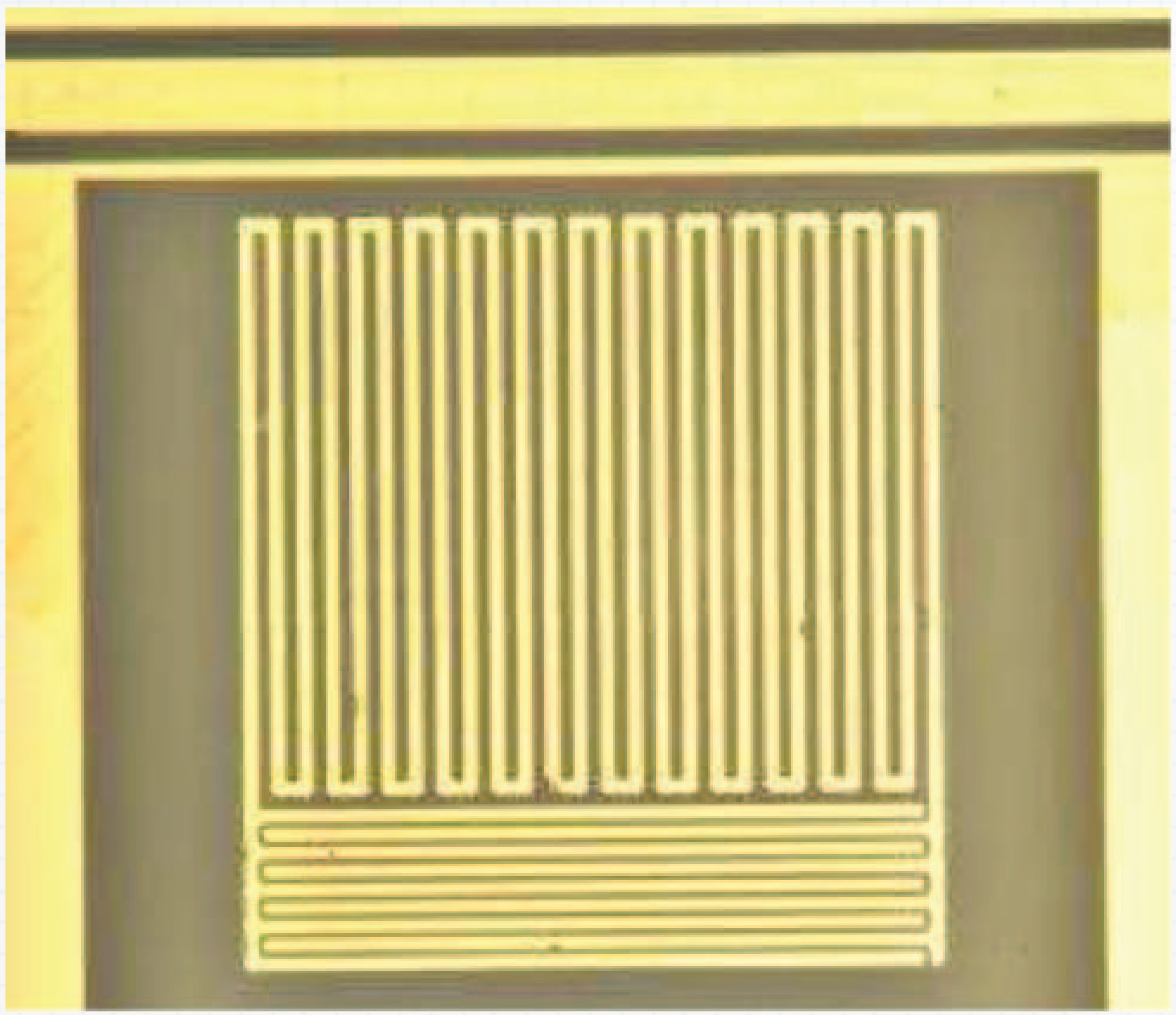

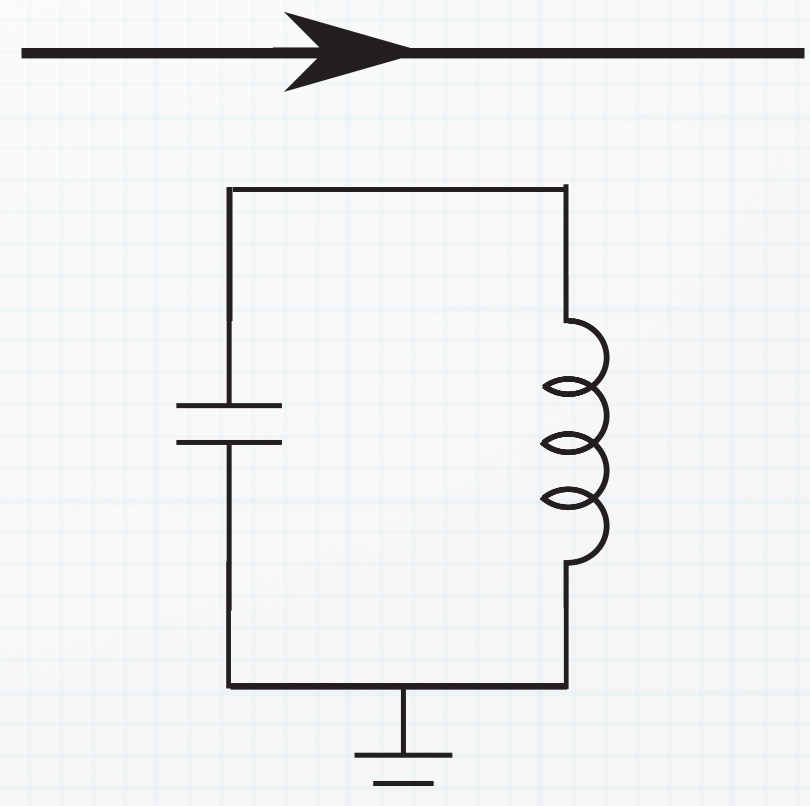

Lindstrom, Oxborrow & al, Rev Sci Instrum 82, 104706 (2011)

Optics

Stabilization of the FS comb

The FS comb enables frequency synthesis from RF/µwaves to optics

- Major breakthrough
- 2005 Nobel prize, R.Glauber, J.Hall, T.Haensch

Stability and noise

- Low noise in the sub-millisecond region
- Drift and walk
- Need stabilization

Common practice

- CW laser stabilized to a FP etalon
- PDH control – of course
- Compare/stabilize the FS comb to the CW laser

Featured book

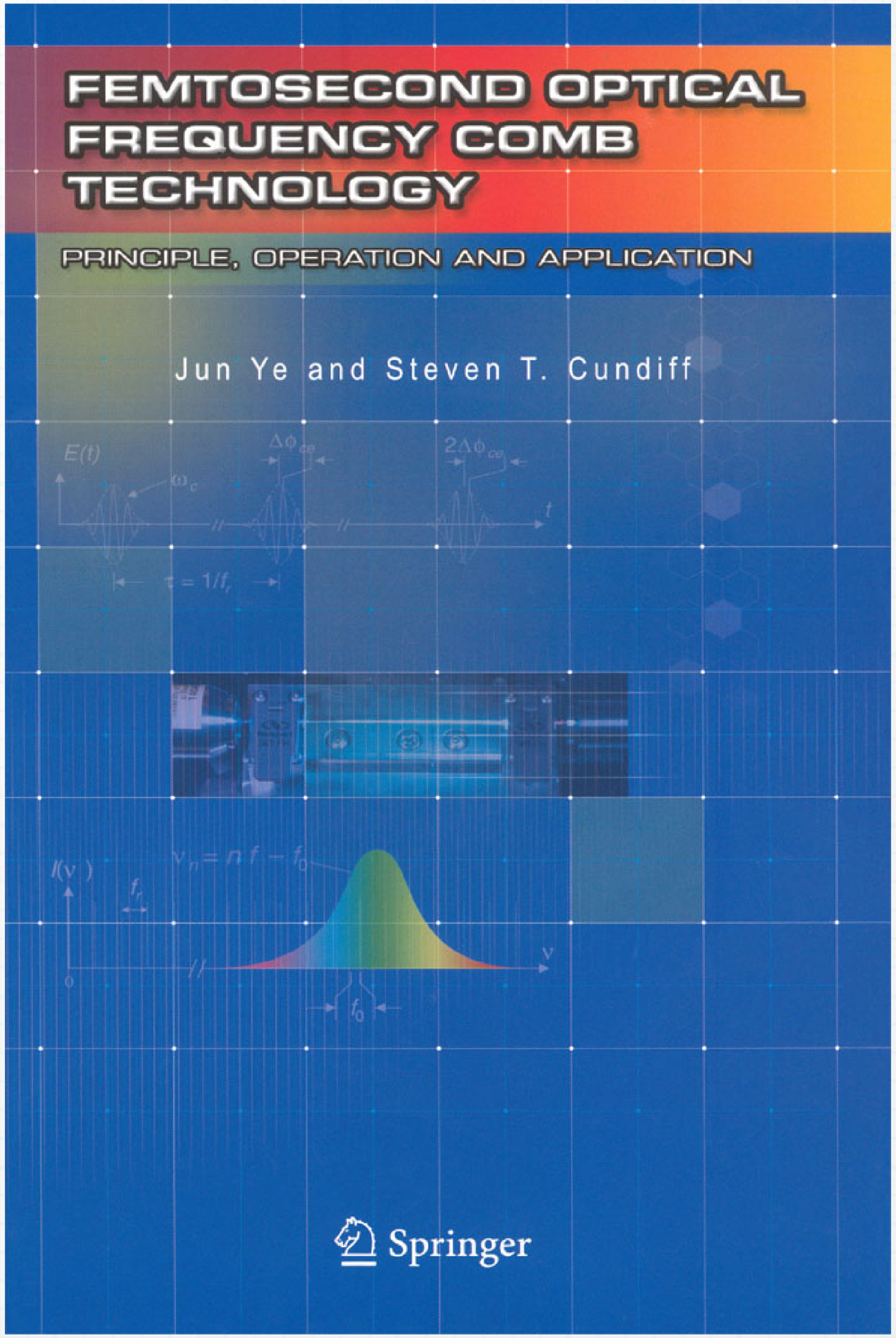

Fabry Perot cavity

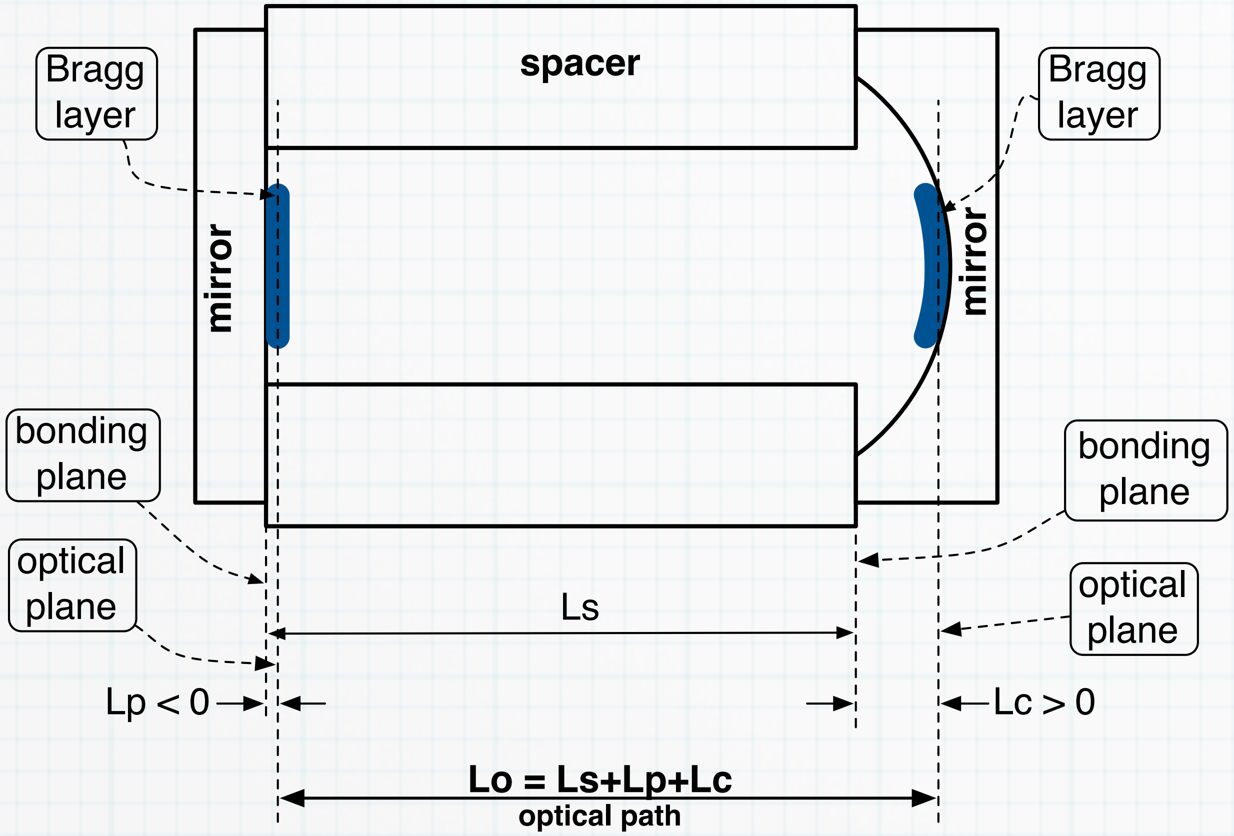

Optical transmission

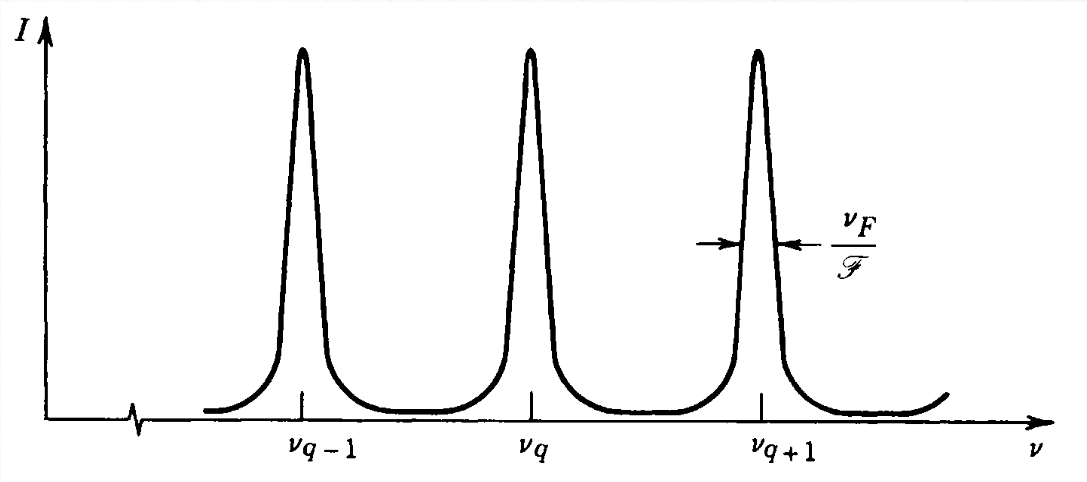

- Smart design of the spacer provides
  - Low sensitivity to acceleration
  - Temperature compensation
    - ULE and Zerodur
    - Many materials (Si, Ge, …) have natural turning point
- High Q is possible, ≥ 10^{10} (≈10 kHz optical bandwidth)

The JILA bicone spacer

March 15, 2007 / Vol. 32, No. 6 / OPTICS LETTERS 641

Compact, thermal-noise-limited optical cavity for diode laser stabilization at 1×10^{-15}

A. D. Ludlow, X. Huang,* M. Notcutt, T. Zanon-Willette, S. M. Foreman, M. M. Boyd, S. Blatt, and J. Ye

JILA, National Institute of Standards and Technology, and University of Colorado Department of Physics, University of Colorado, Boulder, Colorado 80309-0440, USA

Received October 30, 2006; accepted November 25, 2006; posted December 20, 2006 (Doc. ID 76598); published February 15, 2007

We demonstrate phase and frequency stabilization of a diode laser at the thermal noise limit of a passive optical cavity. The system is compact and exploits a cavity design that reduces vibration sensitivity. The subhertz laser is characterized by comparison with a second independent system with similar fractional frequency stability (1×10^{-15} at 1 s). The laser is further characterized by resolving a 2 Hz wide, ultranarrow optical clock transition in ultracold strontium. © 2007 Optical Society of America

OCIS codes: 140.2020, 030.1640, 300.6320.

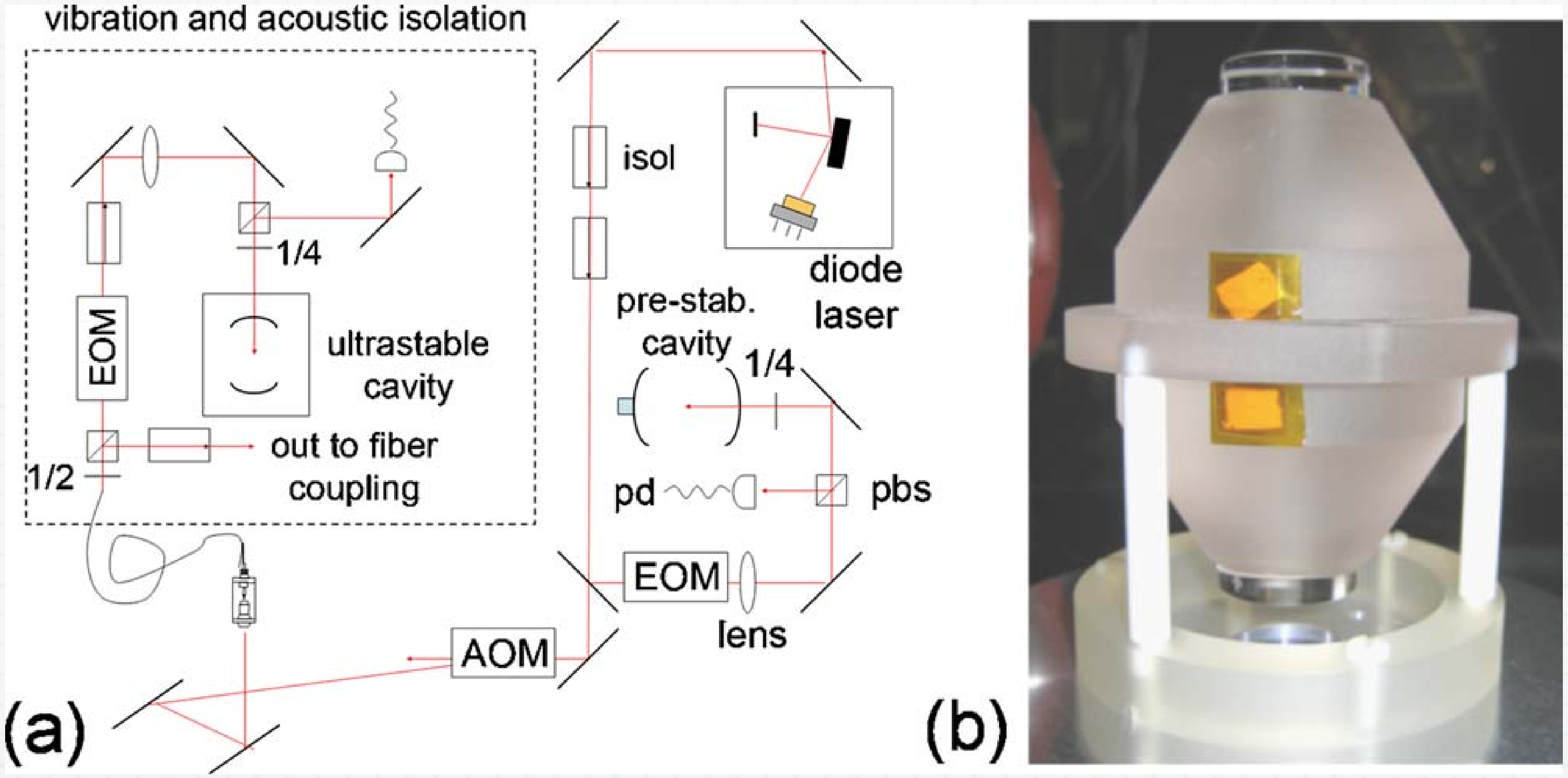

NIST spherical spacer

Field-test of a robust, portable, frequency-stable laser

David R. Leibrandt,* Michael J. Thorpe, James C. Bergquist, and Till Rosenband
National Institute of Standards and Technology, 325 Broadway Street, Boulder, Colorado 80305, USA
**david.leibrandt@nist.gov*

Abstract: We operate a frequency-stable laser in a non-laboratory environment where the test platform is a passenger vehicle. We measure the acceleration experienced by the laser and actively correct for it to achieve a system acceleration sensitivity of $\Delta f/f = 11(2) \times 10^{-12}$/g, $6(2) \times 10^{-12}$/g, and $4(1) \times 10^{-12}$/g for accelerations in three orthogonal directions at 1 Hz. The acceleration spectrum and laser performance are evaluated with the vehicle both stationary and moving. The laser linewidth in the stationary vehicle with engine idling is 1.7(1) Hz.

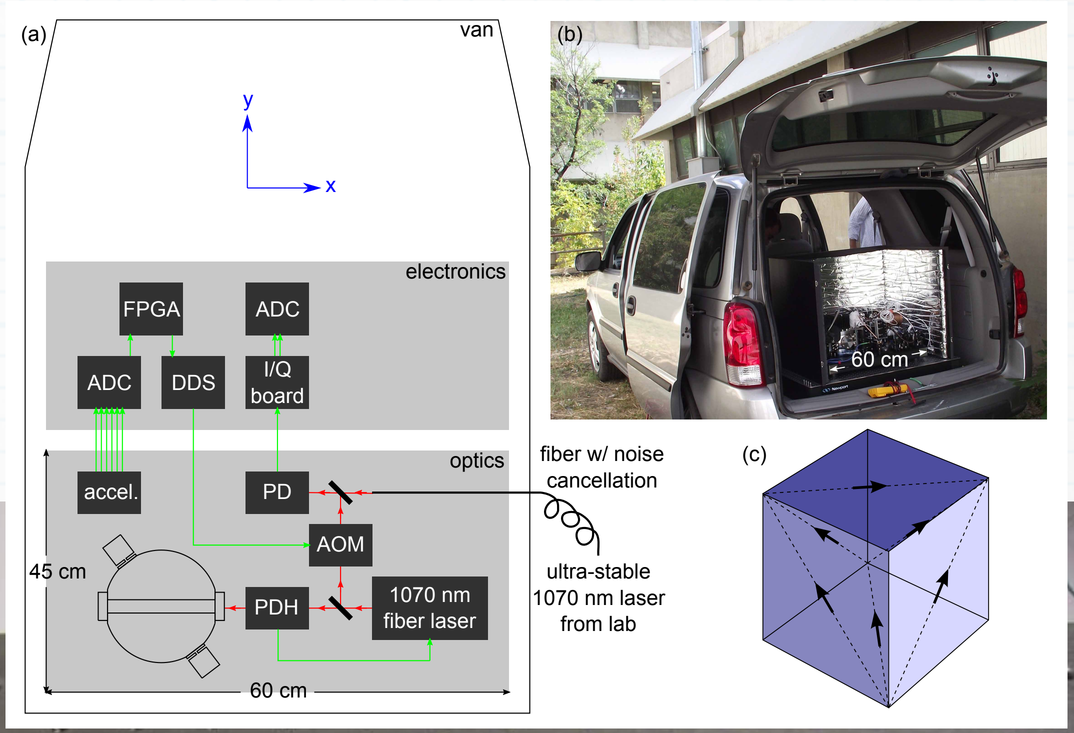

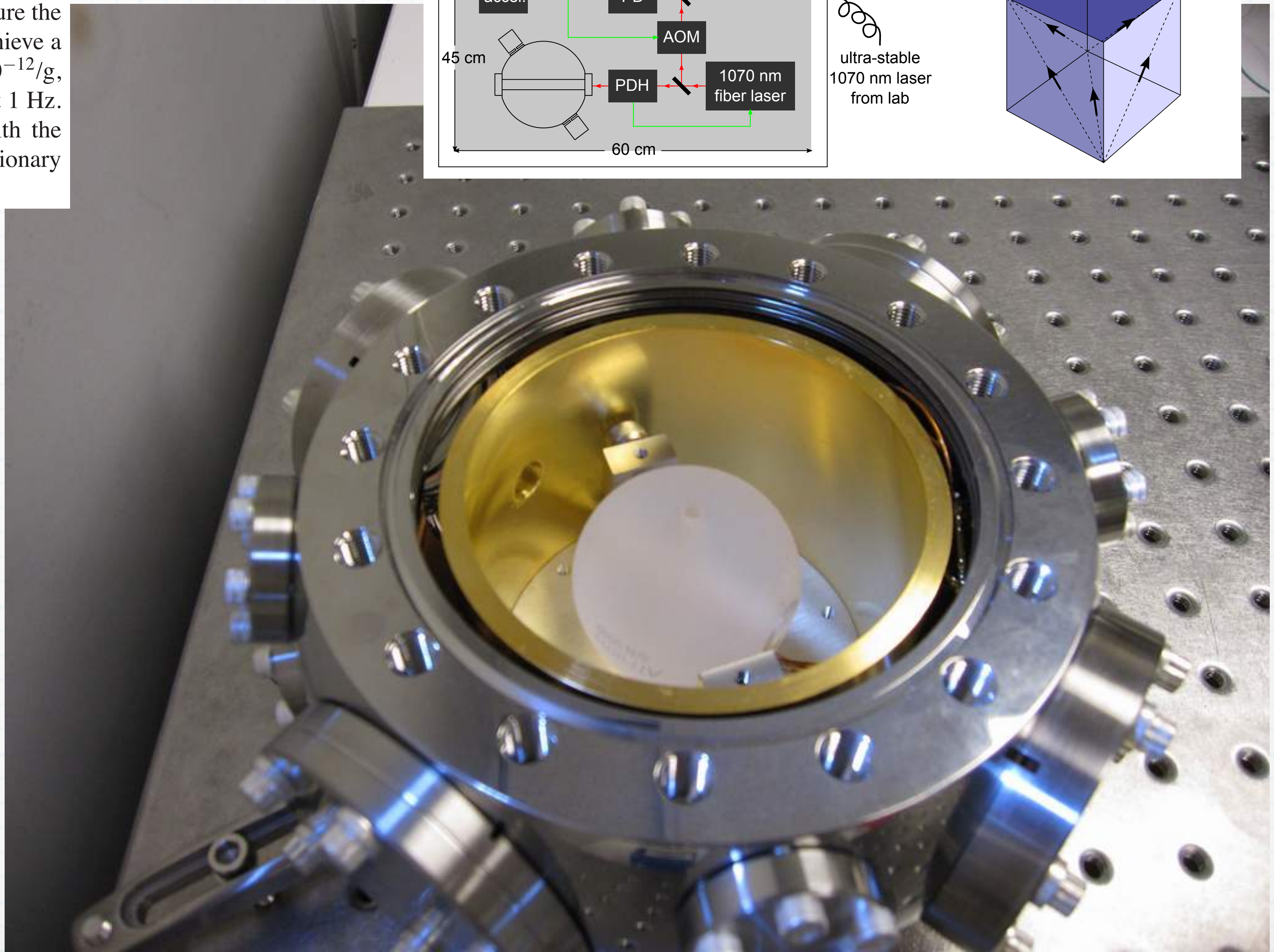

NIST improved spherical spacer

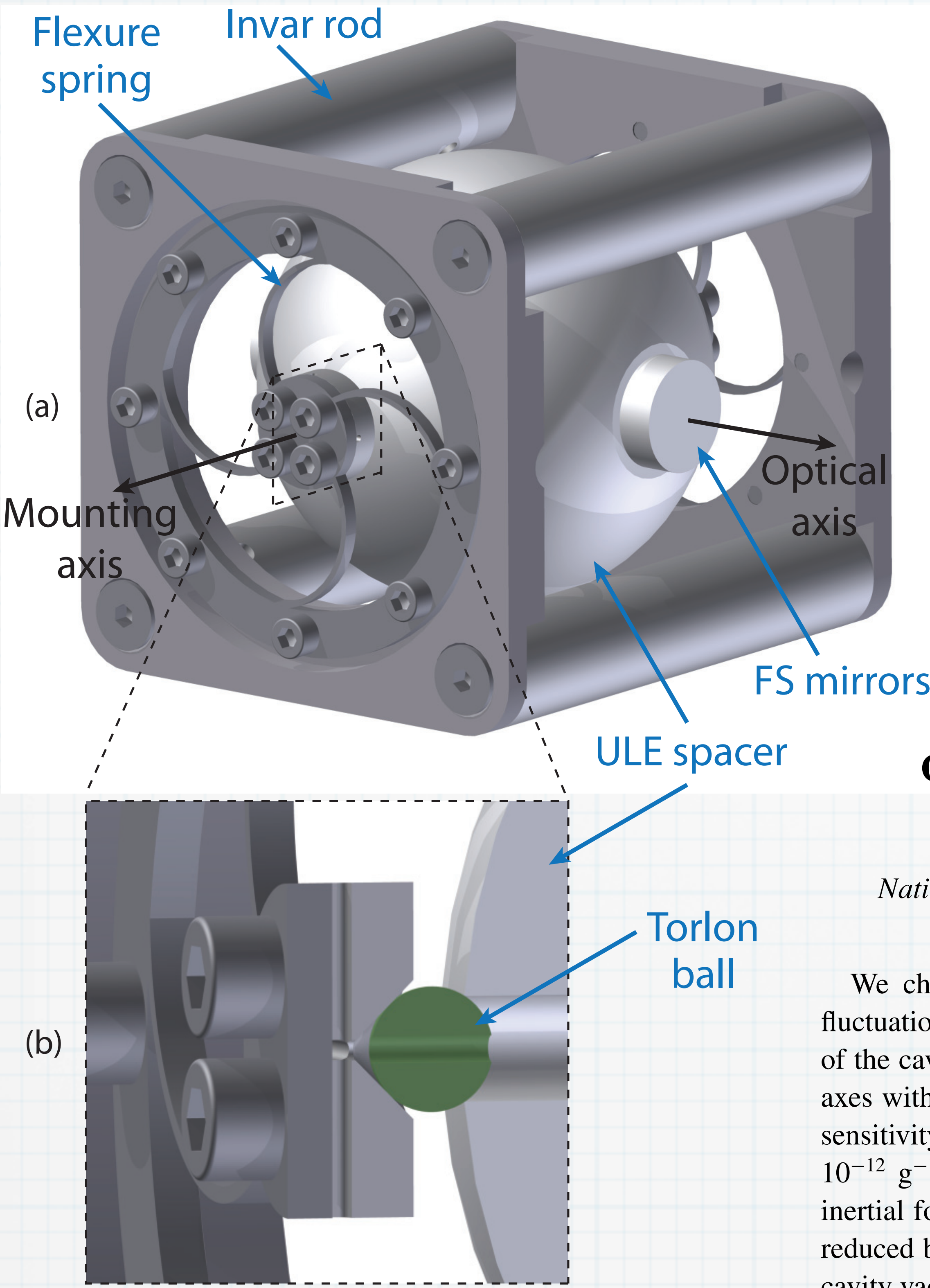

PHYSICAL REVIEW A **87**, 023829 (2013)

Cavity-stabilized laser with acceleration sensitivity below 10^{-12} g^{-1}

David R. Leibrandt,* James C. Bergquist, and Till Rosenband
National Institute of Standards and Technology, 325 Broadway Street, Boulder, Colorado 80305, USA
(Received 31 December 2012; published 21 February 2013)

We characterize the frequency sensitivity of a cavity-stabilized laser to inertial forces and temperature fluctuations, and perform real-time feedforward to correct for these sources of noise. We measure the sensitivity of the cavity to linear accelerations, rotational accelerations, and rotational velocities by rotating it about three axes with accelerometers and gyroscopes positioned around the cavity. The worst-direction linear acceleration sensitivity of the cavity is $2(1) \times 10^{-11}$ g^{-1} measured over 0–50 Hz, which is reduced by a factor of 50 to below 10^{-12} g^{-1} for low-frequency accelerations by real-time feedforward corrections of all of the aforementioned inertial forces. A similar idea is demonstrated in which laser frequency drift due to temperature fluctuations is reduced by a factor of 70 via real-time feedforward from a temperature sensor located on the outer wall of the cavity vacuum chamber.

DOI: 10.1103/PhysRevA.87.023829 PACS number(s): 42.62.Eh, 42.60.Da, 46.40.−f, 07.07.Tw

NPL horizontal cavity

PHYSICAL REVIEW A **75**, 011801(R) (2007)

Vibration insensitive optical cavity

S. A. Webster, M. Oxborrow, and P. Gill
National Physical Laboratory, Hampton Road, Teddington, Middlesex, TW11 0LW, United Kingdom
(Received 31 October 2006; published 9 January 2007)

An optical cavity is designed and implemented that is insensitive to vibration in all directions. The cavity is mounted with its optical axis in the horizontal plane. A minimum response of 0.1 (3.7) $\mathrm{kHz/ms^{-2}}$ is achieved for low-frequency vertical (horizontal) vibrations.

DOI: 10.1103/PhysRevA.75.011801 PACS number(s): 42.60.Da, 07.60.Ly, 06.30.Ft

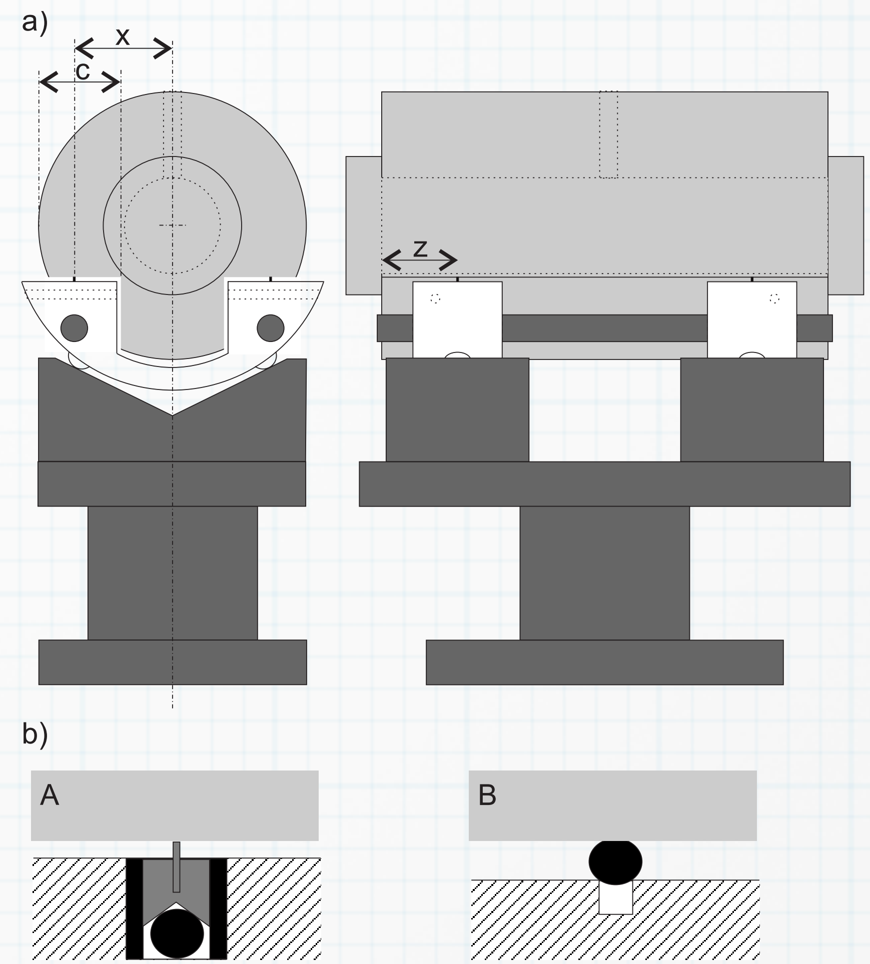

PHYSICAL REVIEW A **77**, 033847 (2008)

Thermal-noise-limited optical cavity

S. A. Webster,[1] M. Oxborrow,[1] S. Pugla,[2] J. Millo,[3] and P. Gill[1]
[1]*National Physical Laboratory, Hampton Road, Teddington, Middlesex, TW11 0LW, United Kingdom*
[2]*Blackett Laboratory, Imperial College London, South Kensington Campus, London, SW7 2BZ, United Kingdom*
[3]*SYRTE, Observatoire de Paris, 61, Avenue de l'Observatoire, 75014, Paris, France*
(Received 31 October 2007; published 27 March 2008)

A pair of optical cavities are designed and set up so as to be insensitive to both temperature fluctuations and mechanical vibrations. With the influence of these perturbations removed, a fundamental limit to the frequency stability of the optical cavity is revealed. The stability of a laser locked to the cavity reaches a floor $<2\times10^{-15}$ for averaging times in the range 0.5–100 s. This limit is attributed to Brownian motion of the mirror substrates and coatings.

DOI: 10.1103/PhysRevA.77.033847 PACS number(s): 42.60.Da, 07.60.Ly, 07.10.Fq, 06.30.Ft

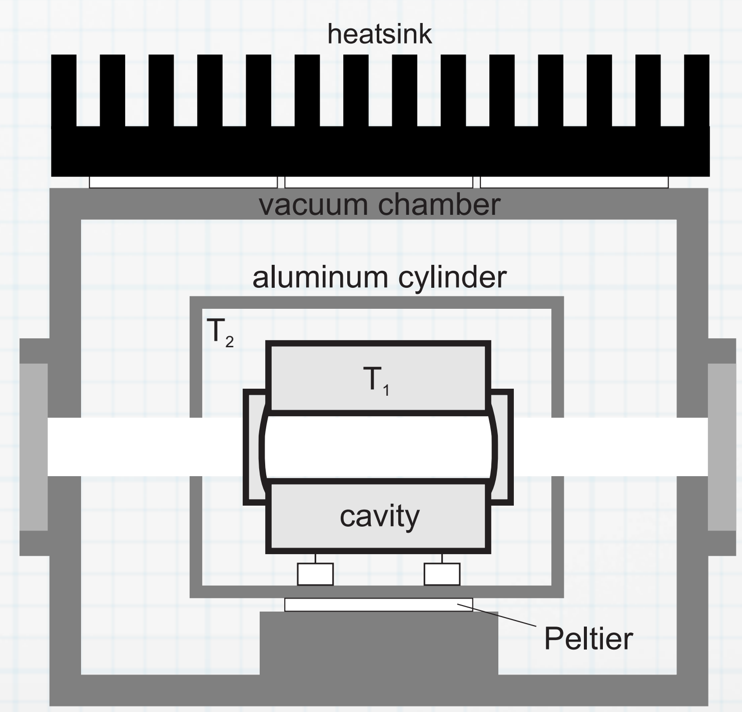

NPL small cubic cavity

Force-insensitive optical cavity

Stephen Webster* and Patrick Gill
National Physical Laboratory, Hampton Road, Teddington, Middlesex, TW11 0LW, UK
**Corresponding author: stephen.webster@npl.co.uk*

Received June 20, 2011; revised August 11, 2011; accepted August 11, 2011;
posted August 12, 2011 (Doc. ID 149376); published September 9, 2011

We describe a rigidly mounted optical cavity that is insensitive to inertial forces acting in any direction and to the compressive force used to constrain it. The design is based on a cubic geometry with four supports placed symmetrically about the optical axis in a tetrahedral configuration. To measure the inertial force sensitivity, a laser is locked to the cavity while it is inverted about three orthogonal axes. The maximum acceleration sensitivity is $2.5 \times 10^{-11}/g$ (where $g = 9.81\,\mathrm{ms}^{-2}$), the lowest passive sensitivity to be reported for an optical cavity.

OCIS codes: 140.4780, 140.3425, 120.3940, 120.6085.

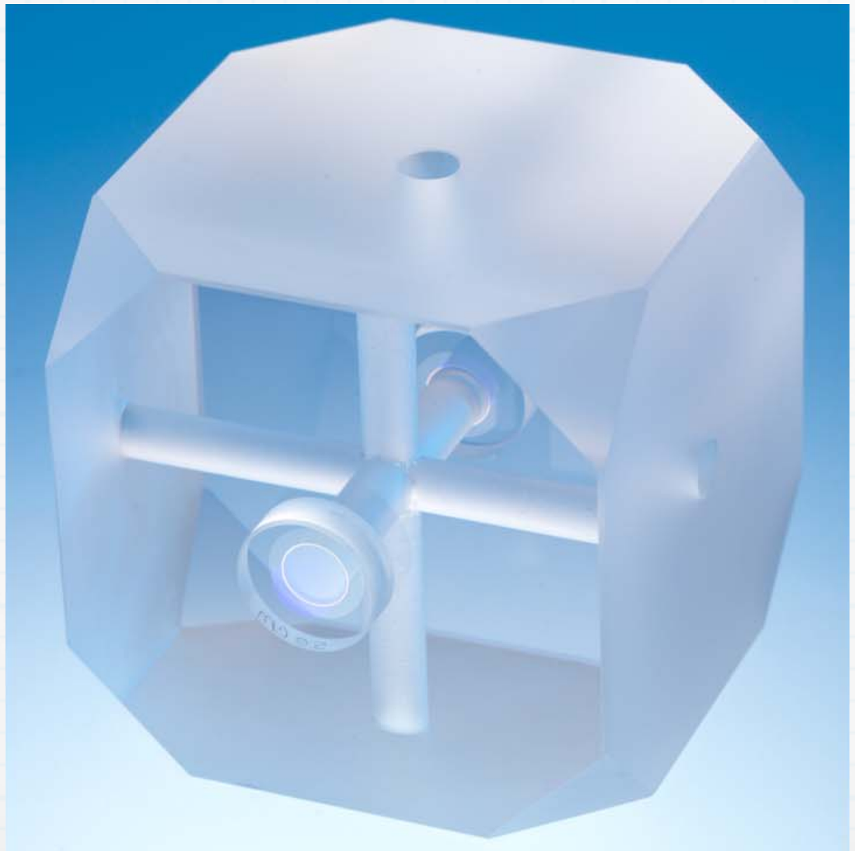

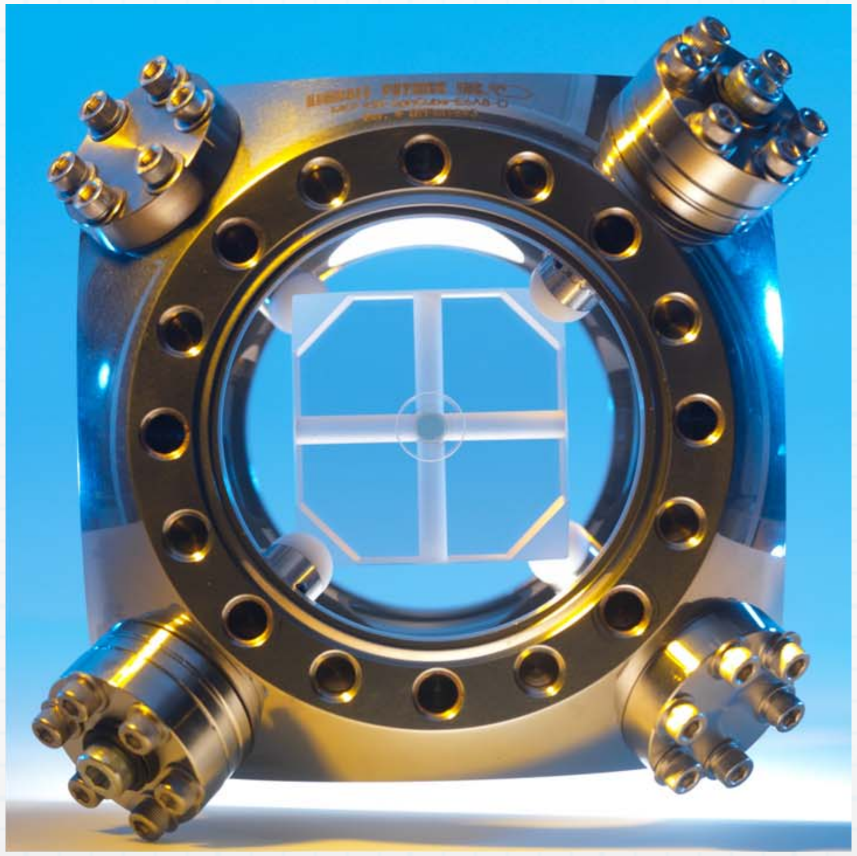

SYRTE horizontal cavity

PHYSICAL REVIEW A **79**, 053829 (2009)

Ultrastable lasers based on vibration insensitive cavities

J. Millo, D. V. Magalhães, C. Mandache, Y. Le Coq, E. M. L. English,* P. G. Westergaard, J. Lodewyck, S. Bize, P. Lemonde, and G. Santarelli

LNE-SYRTE, Observatoire de Paris, CNRS, UPMC, 61 Avenue de l'Observatoire, 75014 Paris, France

(Received 5 February 2009; published 18 May 2009)

We present two ultrastable lasers based on two vibration insensitive cavity designs, one with vertical optical axis geometry, the other horizontal. Ultrastable cavities are constructed with fused silica mirror substrates, shown to decrease the thermal noise limit, in order to improve the frequency stability over previous designs. Vibration sensitivity components measured are equal to or better than $1.5 \times 10^{-11}/\text{m s}^{-2}$ for each spatial direction, which shows significant improvement over previous studies. We have tested the very low dependence on the position of the cavity support points, in order to establish that our designs eliminate the need for fine tuning to achieve extremely low vibration sensitivity. Relative frequency measurements show that at least one of the stabilized lasers has a stability better than 5.6×10^{-16} at 1 s, which is the best result obtained for this length of cavity.

DOI: 10.1103/PhysRevA.79.053829 PACS number(s): 42.60.Da, 07.60.Ly, 42.62.Fi

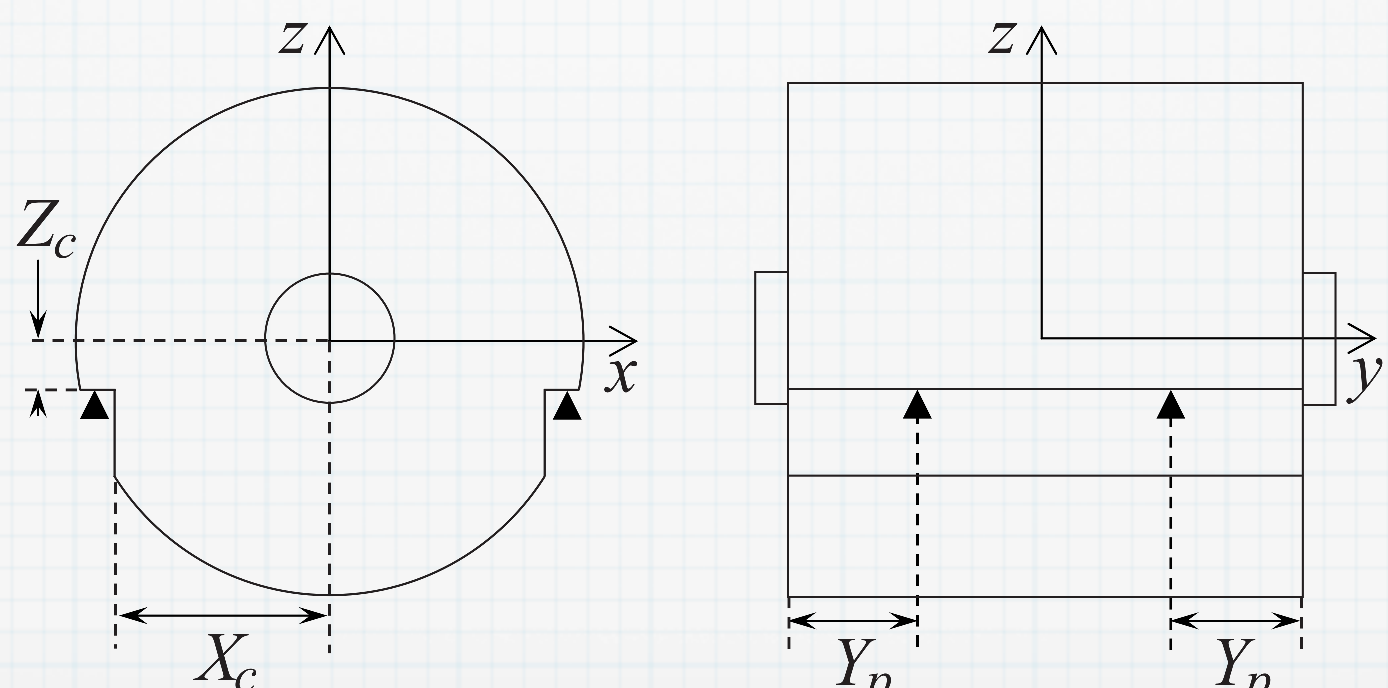

PTB transportable laser

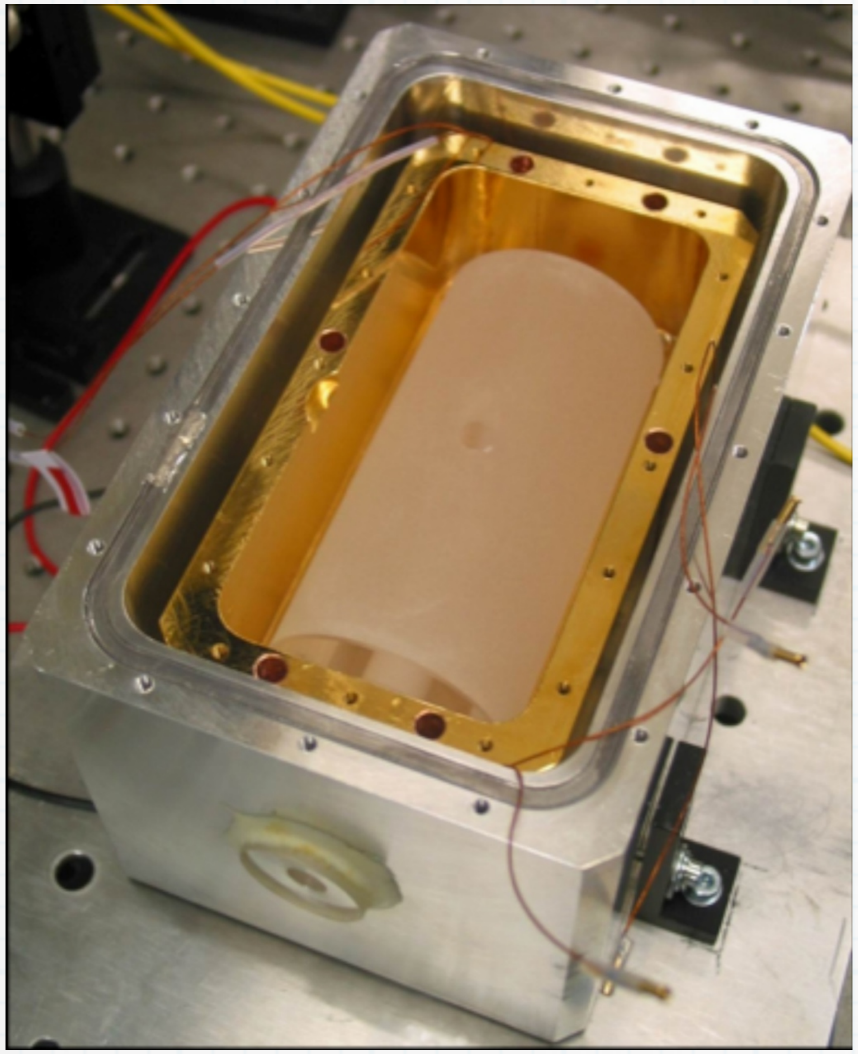

Demonstration of a Transportable 1 Hz-Linewidth Laser

Stefan Vogt, Christian Lisdat, Thomas Legero, Uwe Sterr, Ingo Ernsting, Alexander Nevsky, Stephan Schiller

APPLIED PHYSICS B: LASERS AND OPTICS
Volume 104, Number 4, 741-745, DOI: 10.1007/s00340-011-4652-7

Si has zero expansion at 17 K and 124 K

T = 124 K –> T. Kessler & al., PTB / QUEST - Proc. 2011 IFCS

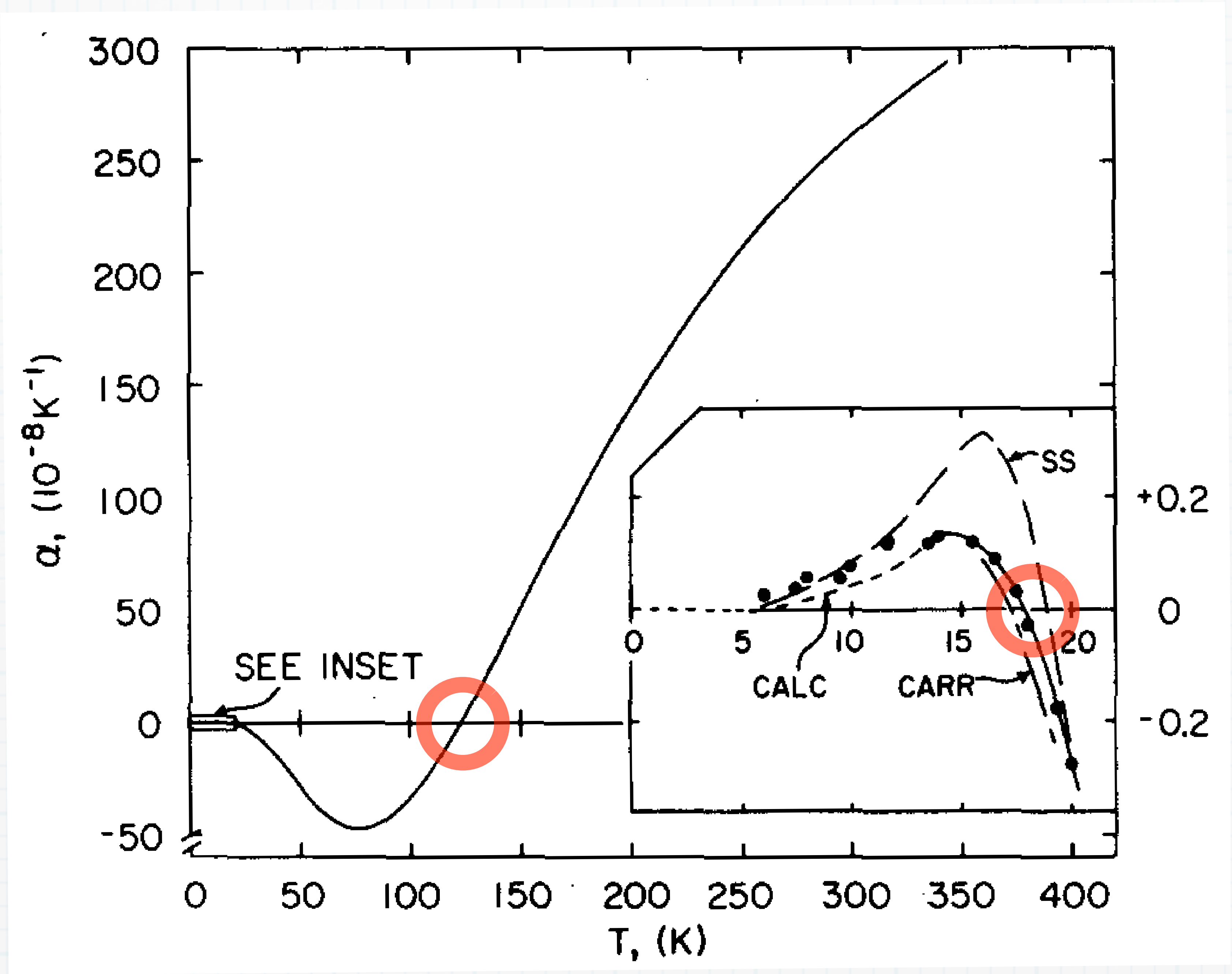

K. G Lyon & al, Linear thermal expansion measurements on silicon from 6 to 340 K - J Appl. Phys 48(3) p.865, 1977

Swenson CA - Recommended values for the thermal expansivity of Silicon from 0 to 1000 K - JPCRD 12(2), 1983

PTB 124-K Si cavity

Experimental setup

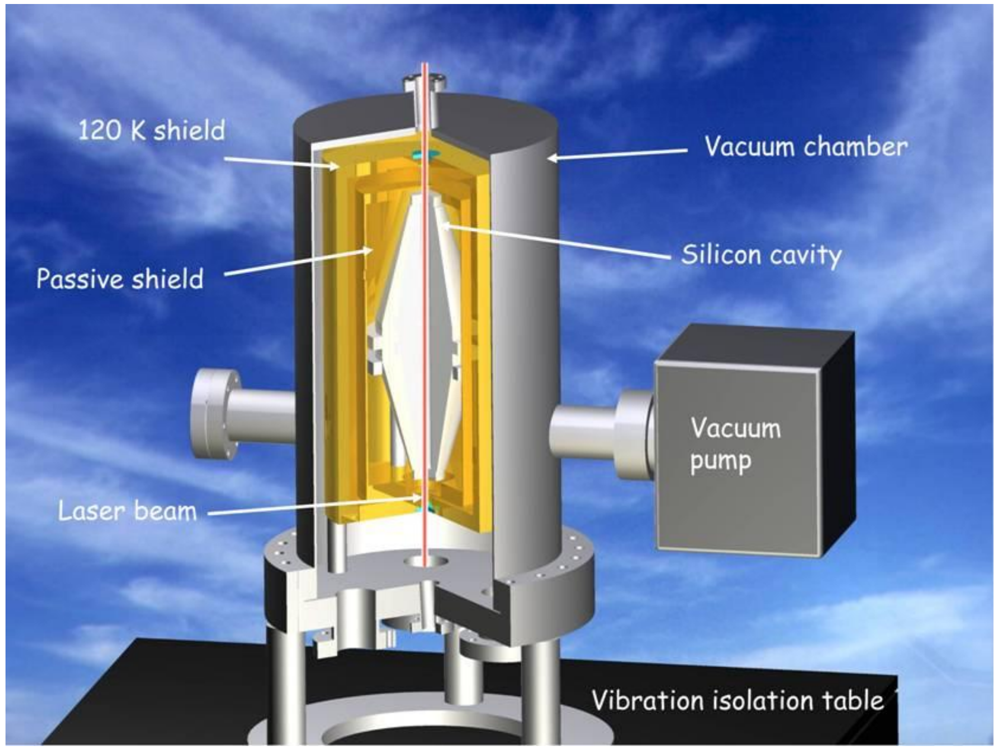

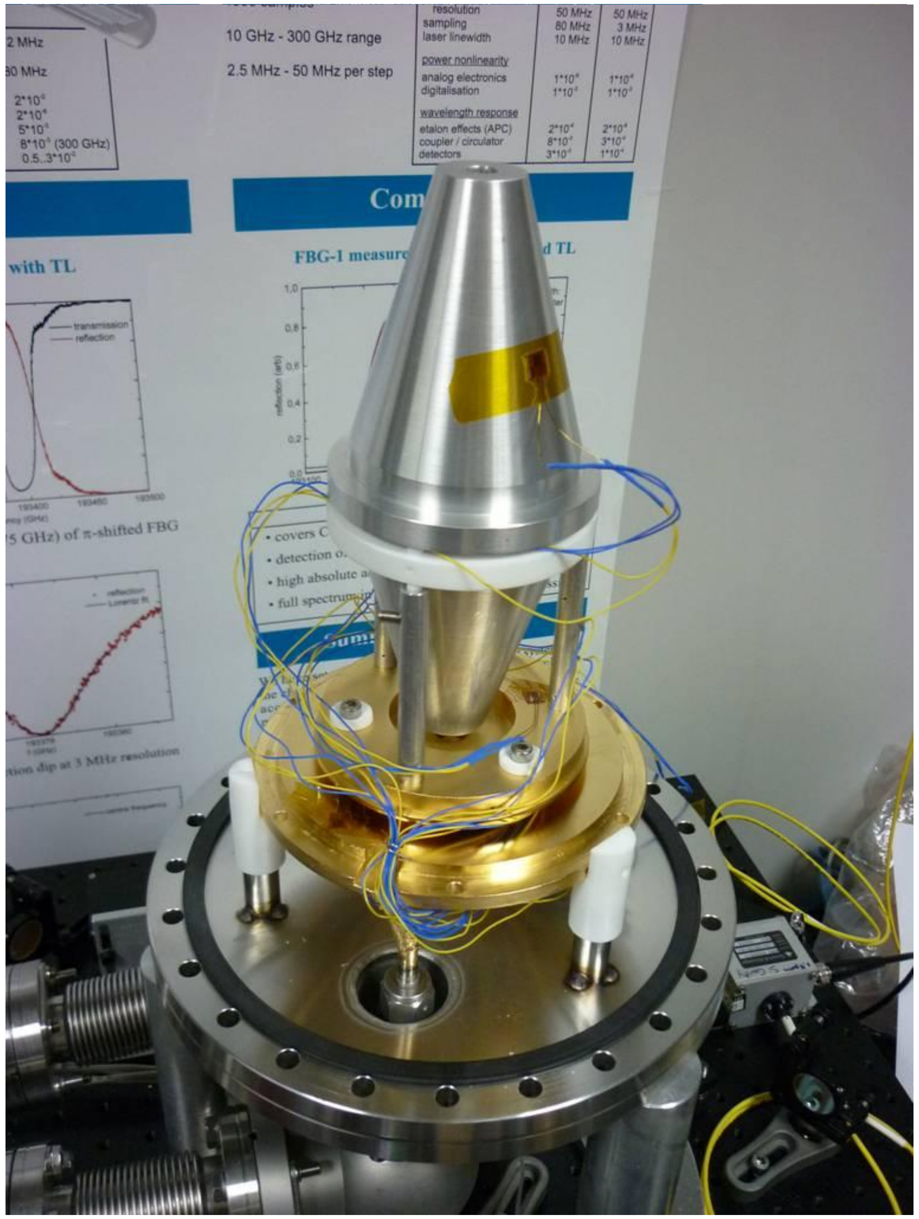

Silicon cavity is thermally isolated by two gold-plated copper shields.

Optical whispering gallery

- Pioneering work by Braginsky (Moscow)
- Made popular by Maleki and Ilchenko (JPL/OEwaves)
- Similar to a Fabry Perot
- Q = $10^9 \ldots 10^{11}$ has been reported
- Poor power handling
- Temperature compensation is challenging

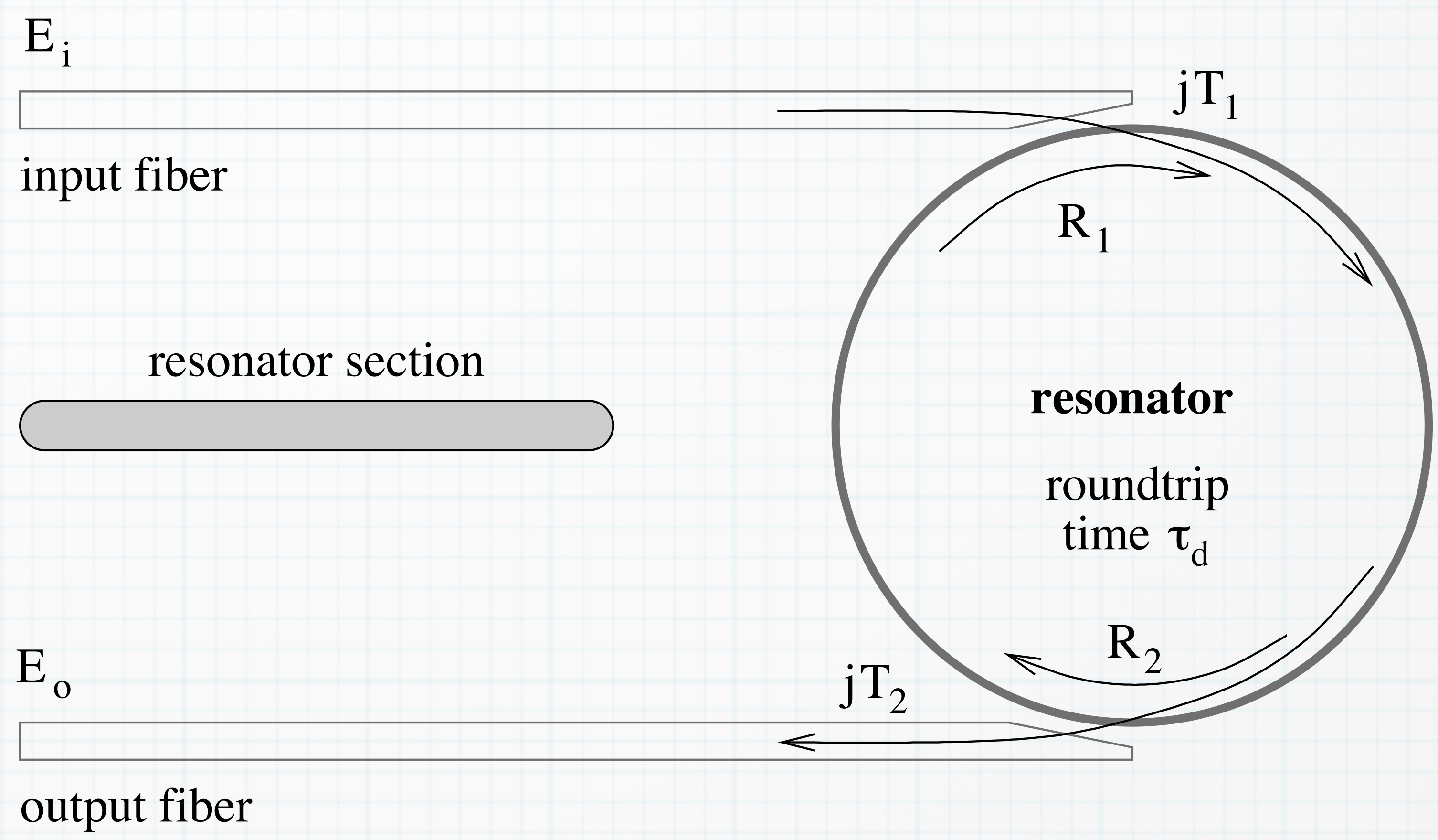

Alnis & al., PRA 4, 011804(R) (2011)

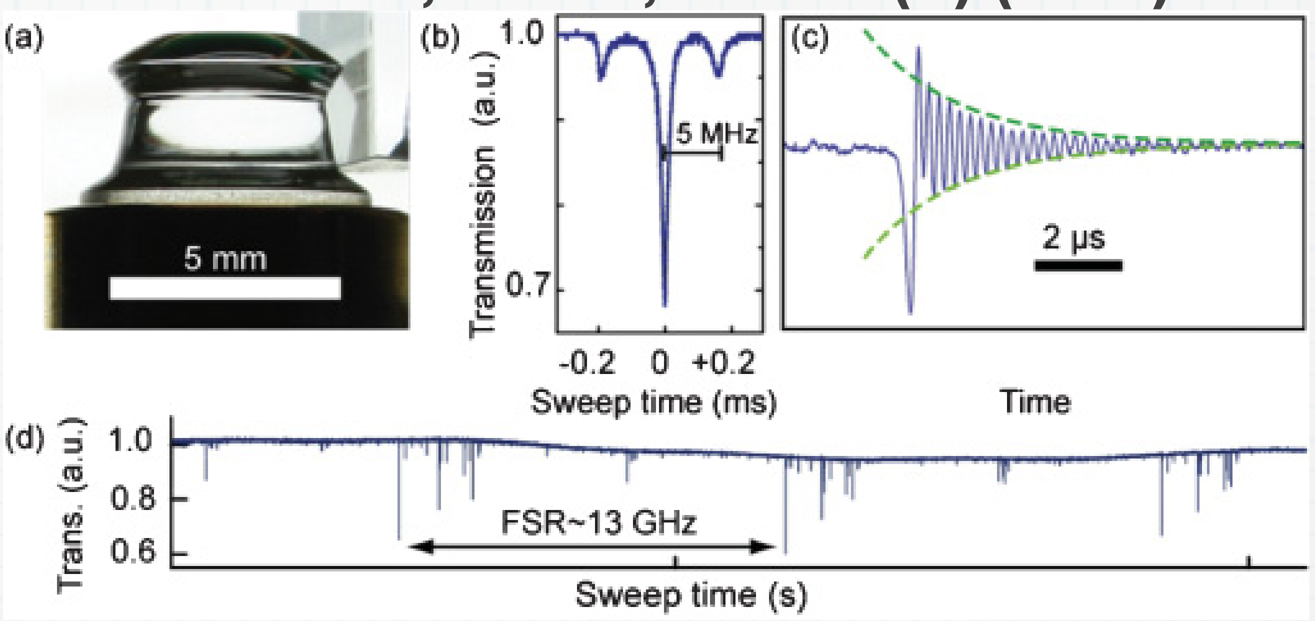

Spherical FP Etalon

Target : $\sigma_y(\tau) \approx 8\times10^{-16}$

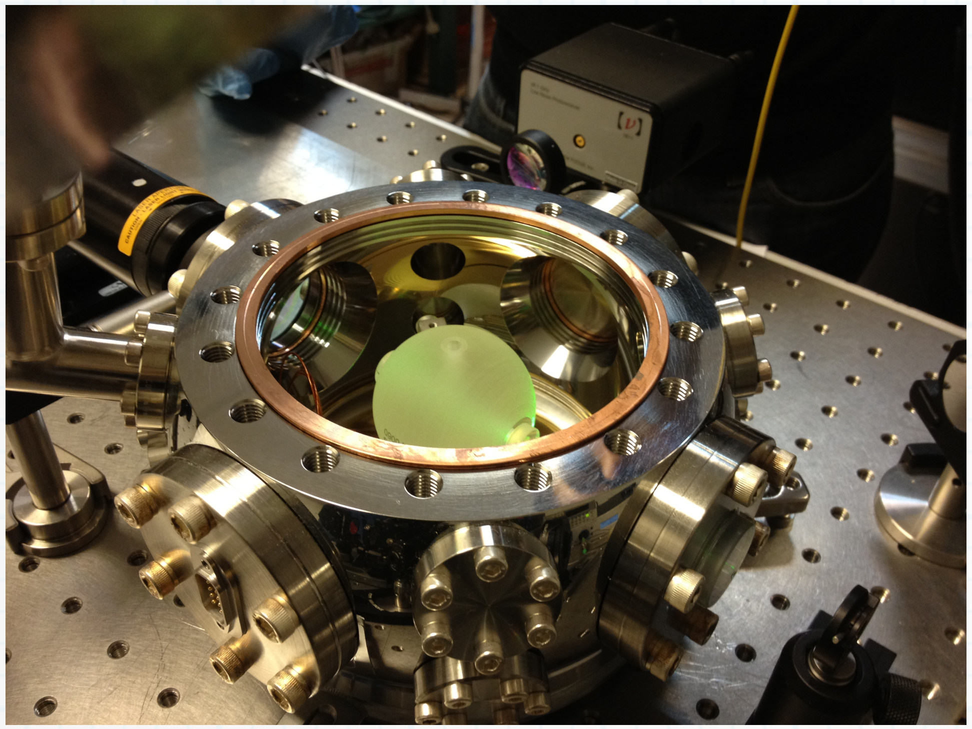

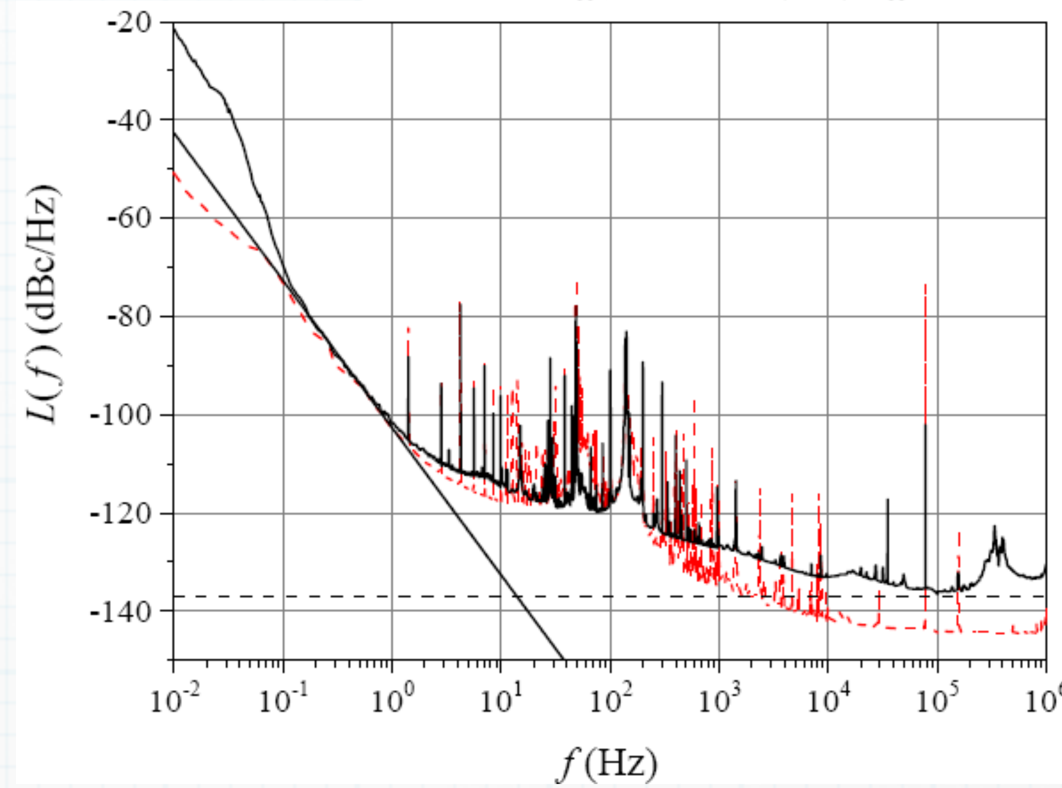

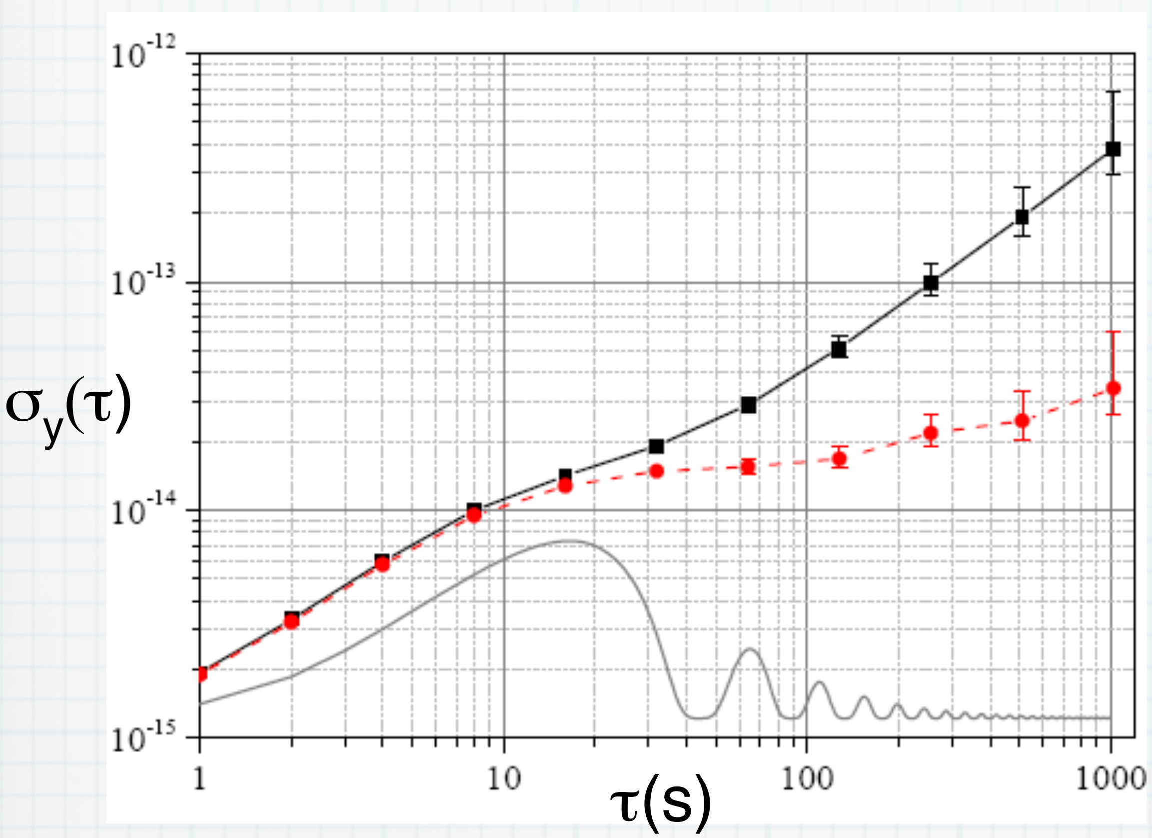

Phase noise : -104 dBc/Hz state of the art

Frequency instability limited by the lab temperature fluctuations

Compact FP Etalon

Target : $\sigma_y(\tau) \approx 2\ 10^{-15}$

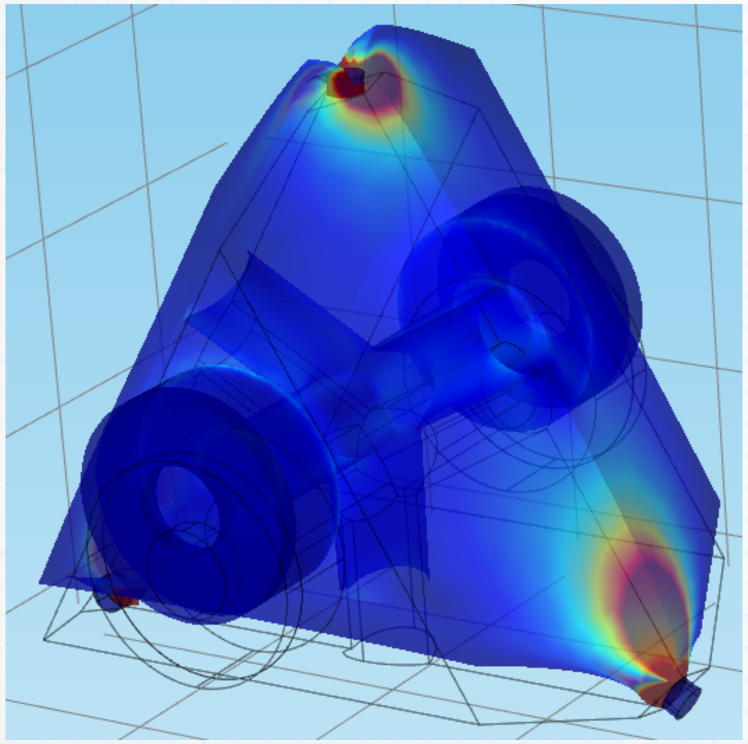

Design and machining completed

Two options for mirrors
- classical
- crystal

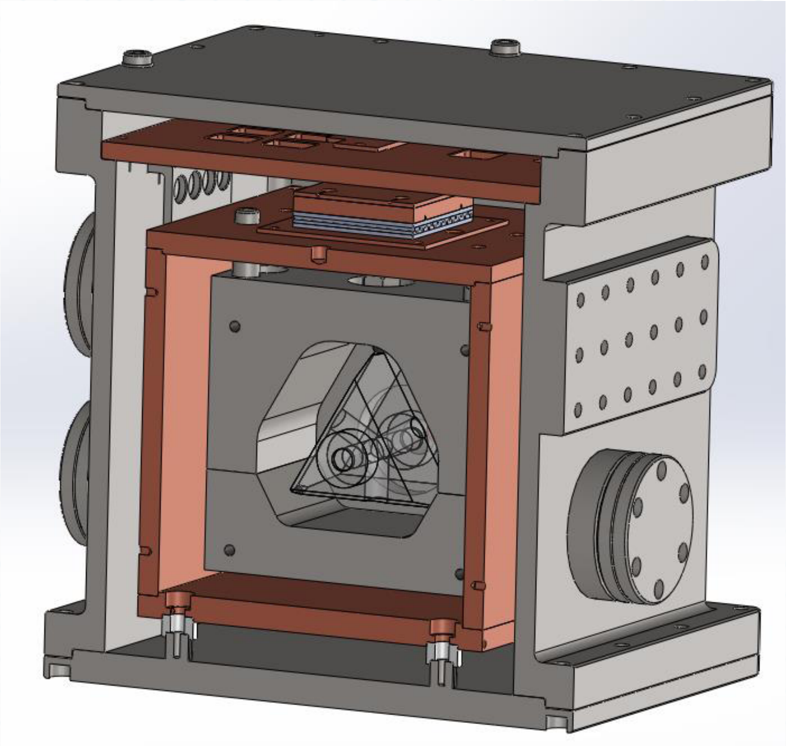

Design of vacuum chamber and thermal isolation completed

Machining will be done end November

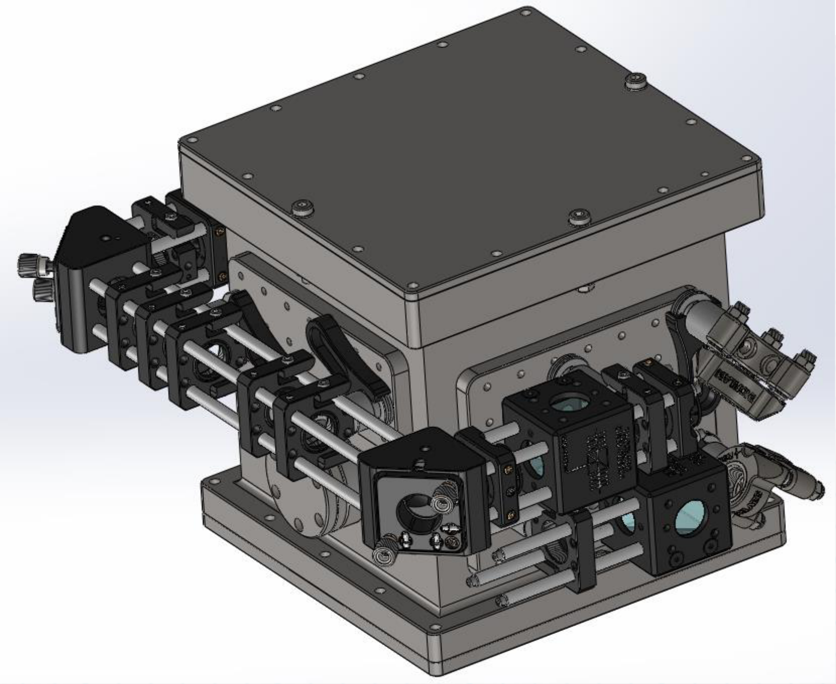

Light injection in the cavity
To be tested…

First experiments end of 2014

Silicon FP Etalon

(Also Région FC, 70 k€)

Target : $\sigma_y(\tau) \approx 3\mathrm{x}10^{-17}$

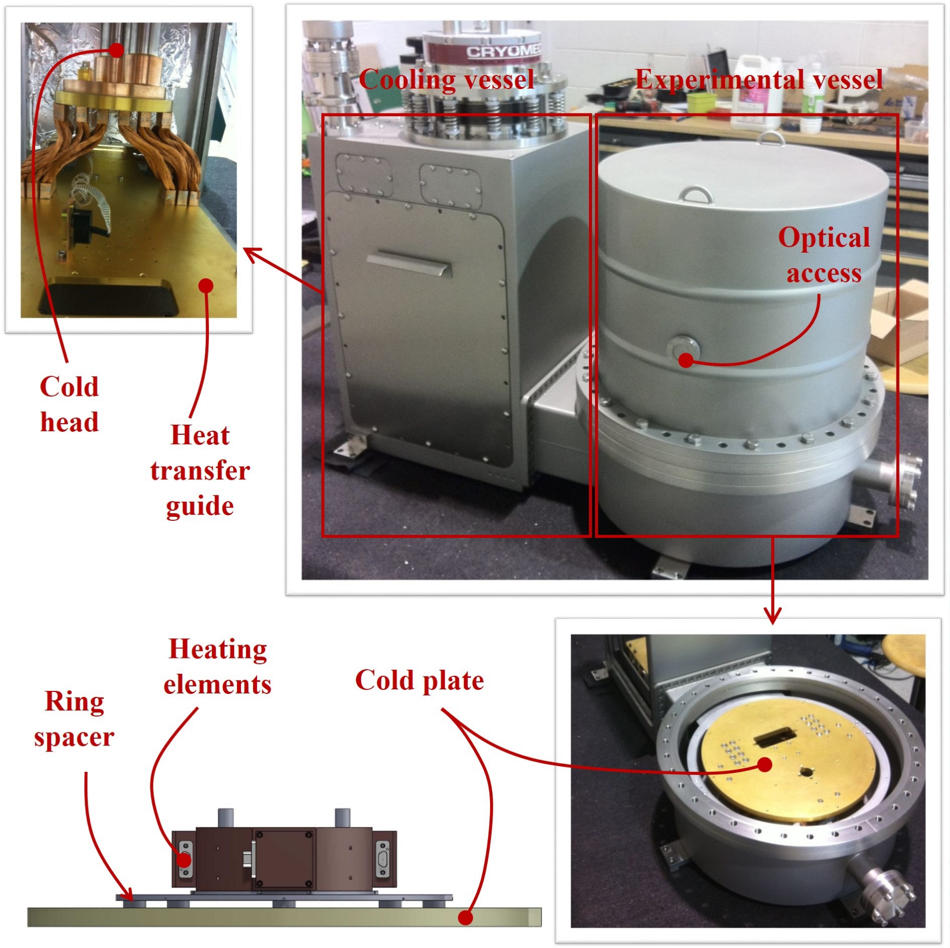

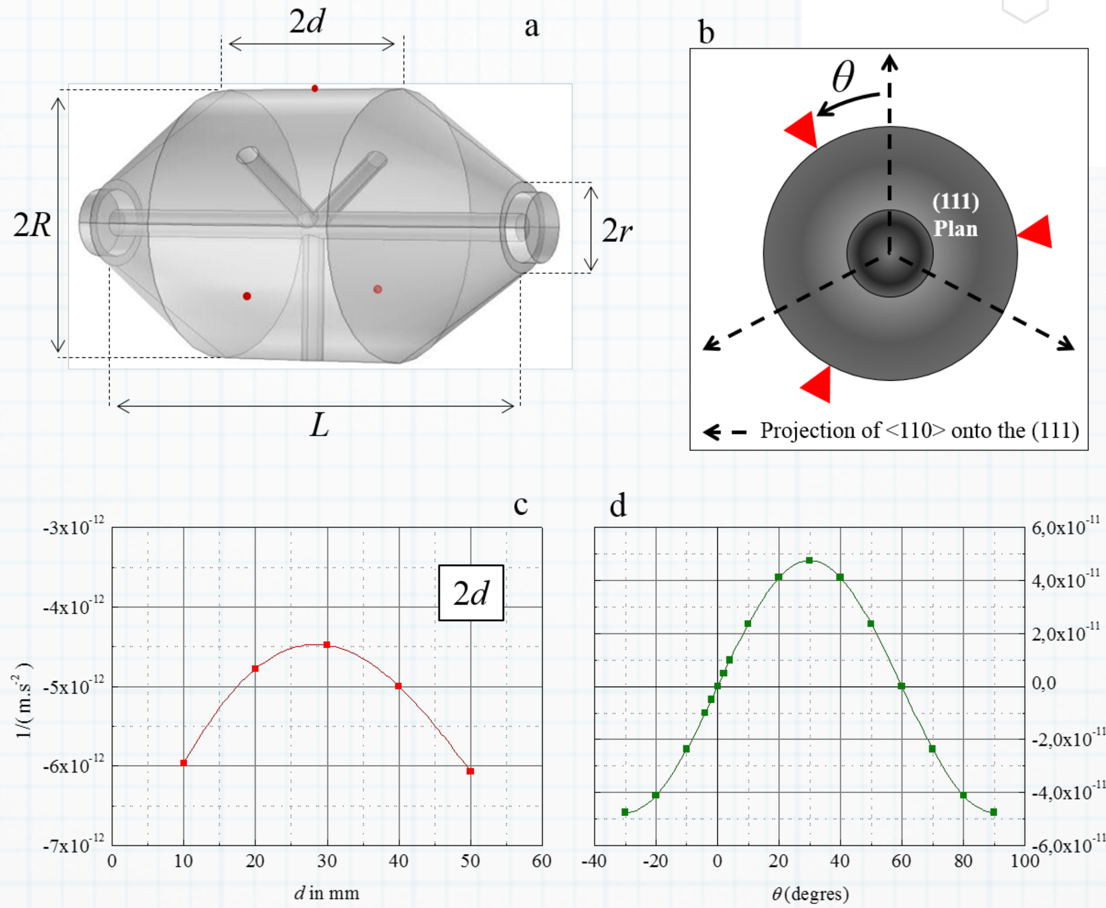

Relative frequency sensitivity to vibrations less than 4.10^{-12} / $\mathrm{m.s}^{-2}$

Low vibrations cryocooler: displacement less than 40 nm

Temperature instability less than 100 μK

Cavity

Thermal effect on frequency

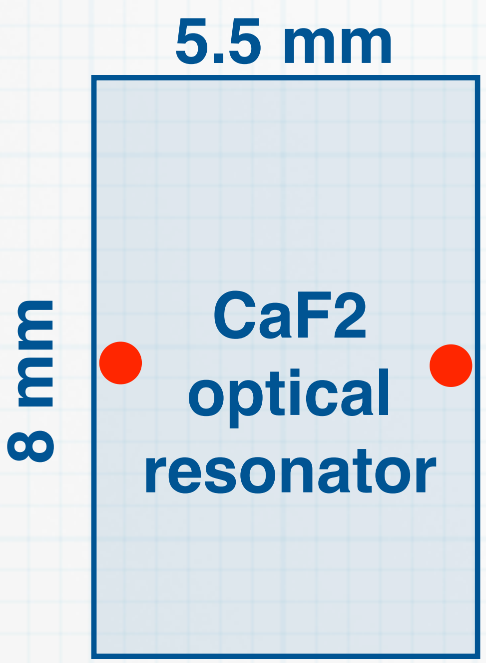

- wavelength 1.56 µm (v0=192 THz)
- Q=5x10^{9} –> BW=40 kHz
- a power of 300 µW shifts the resonant frequency by 1.2 MHz (6x10^{-9}), i.e., 37.5 x BW
- time scale about 60 µs
- [Q = 6x10^{10} demonstrated with CaF2 (I. Grudinin)]

laser scan

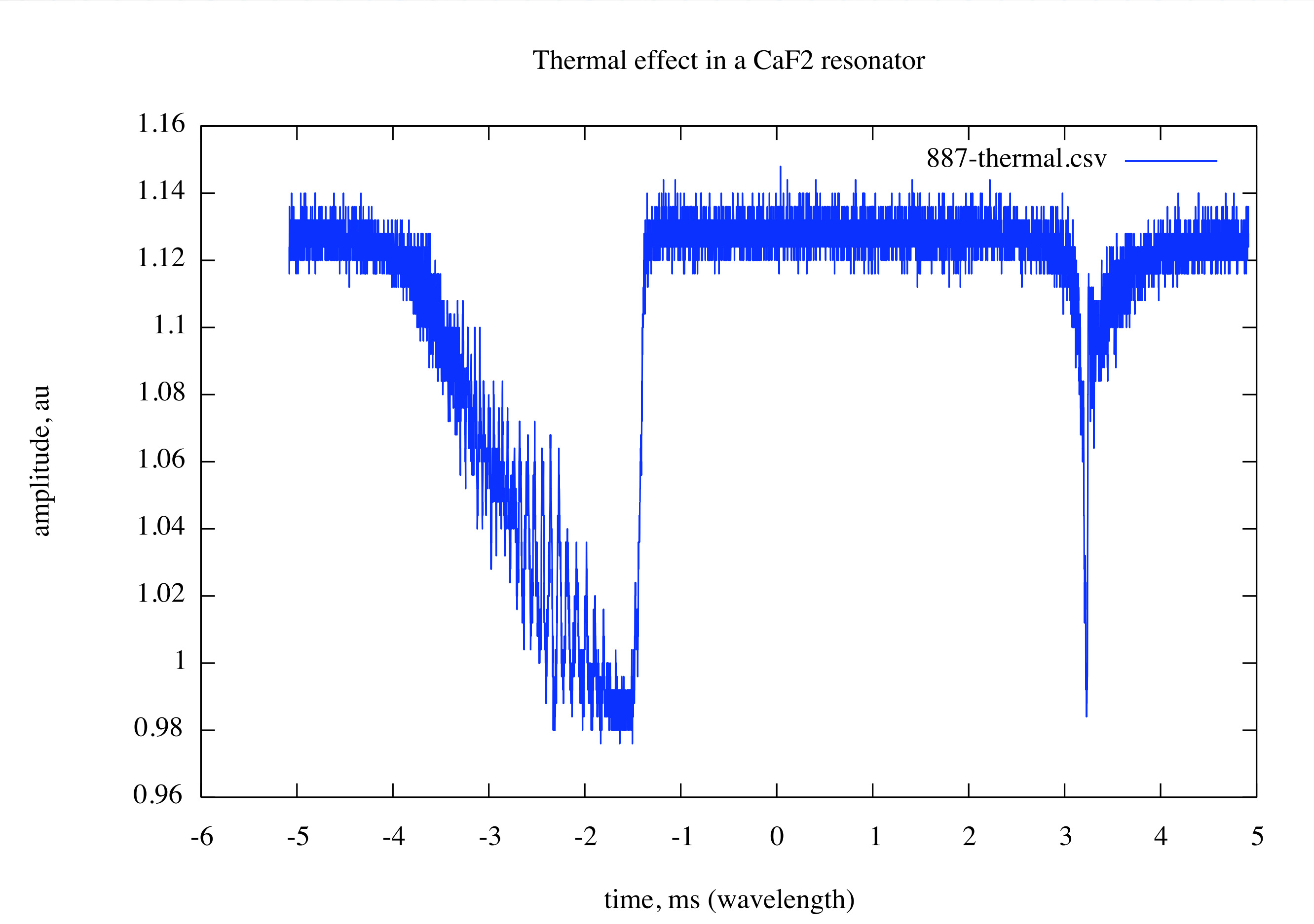

calibration (2 MHz phase modulation)

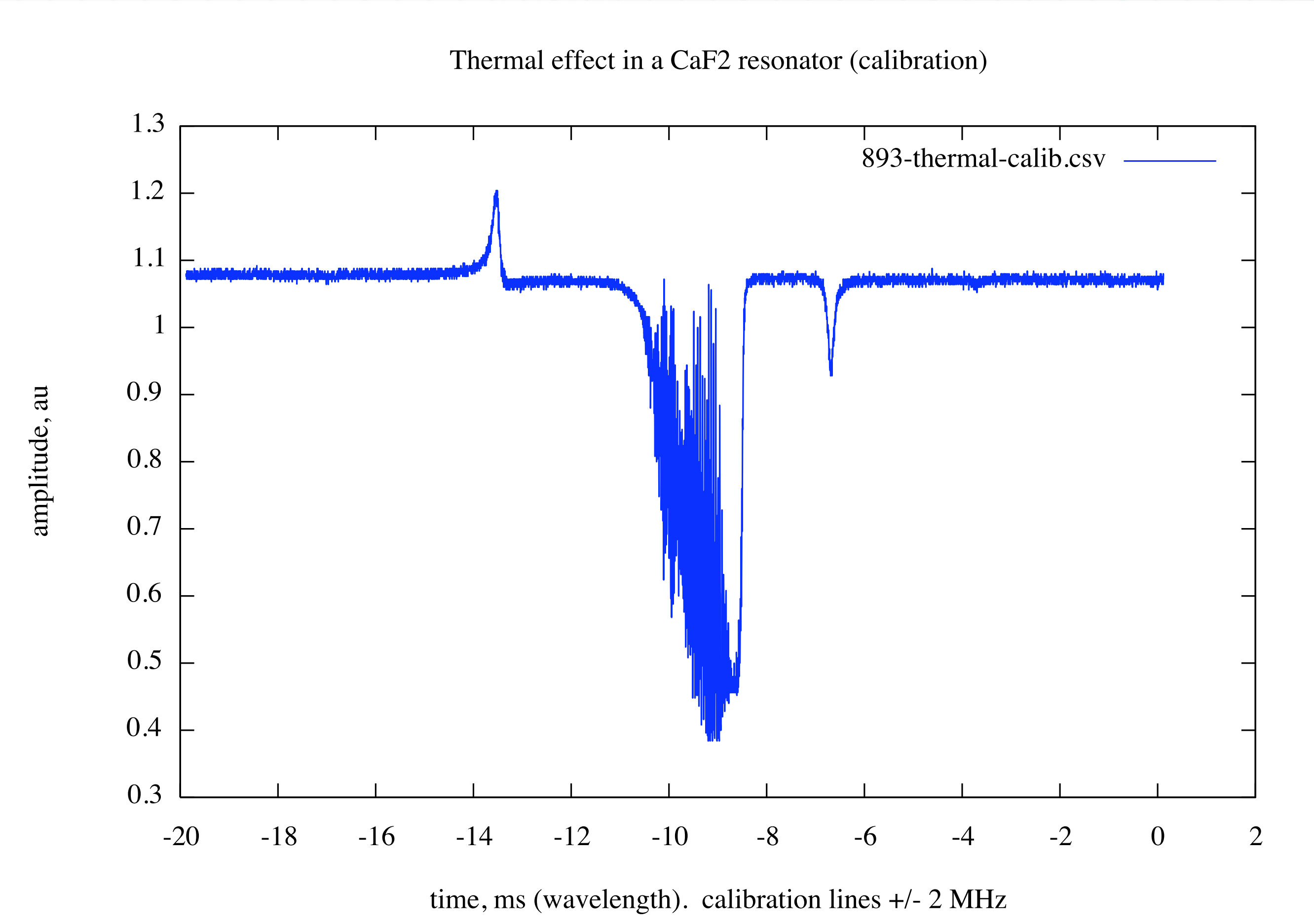

Extreme non-linearity

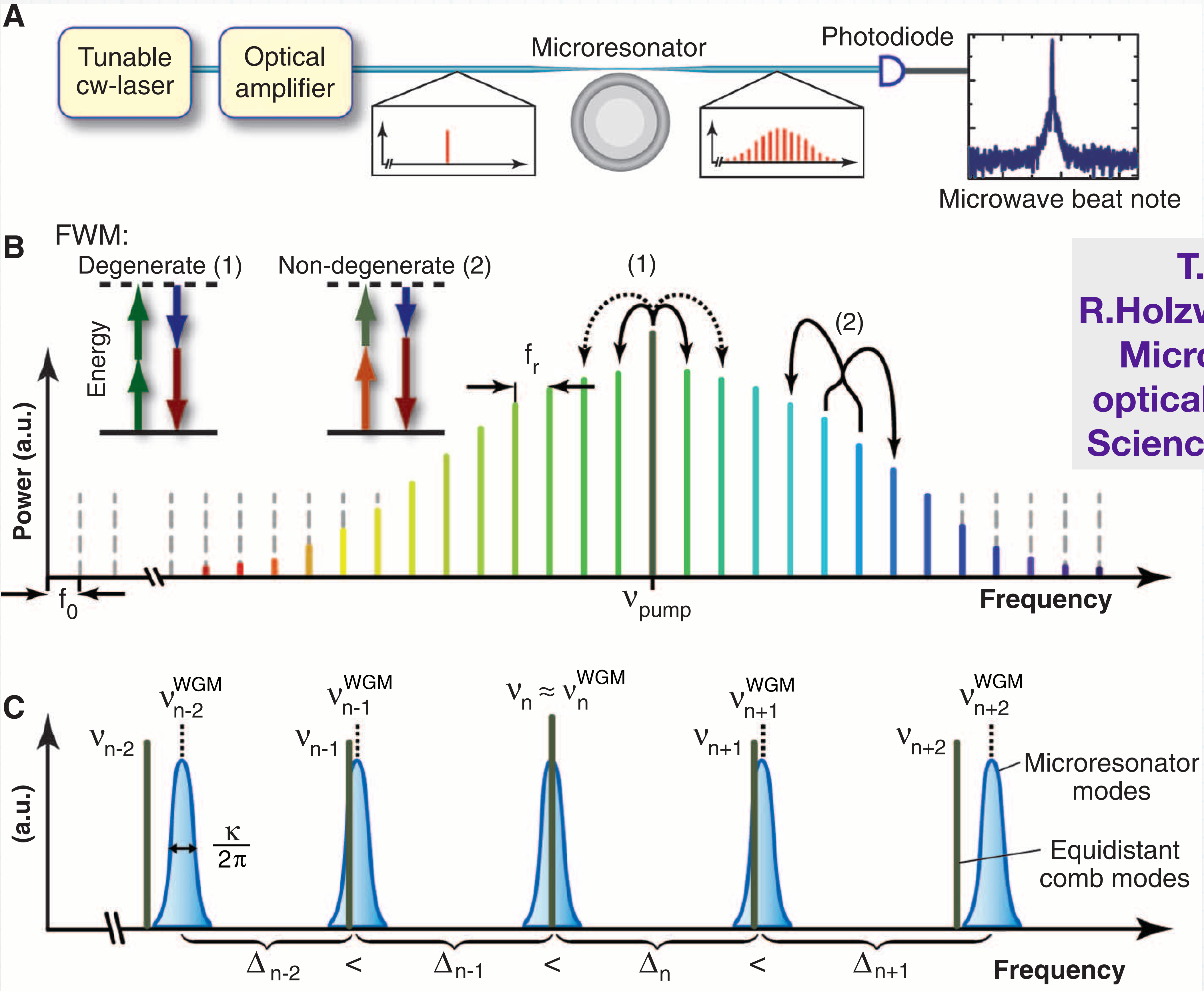

T.J.Kippenberg, R.Holzwarth, S.A.Diddams, Microresonator-based optical frequency combs, Science 332:555, Apr.2011

VIRGO – Gravitational waves

- Large Michelson interferometers detect the space-time fluctuations
- PDH control is used to lock ultra-stable lasers to the interferometer

Vinet JY ed., The VIRGO physics II, Optics and related topics, available online

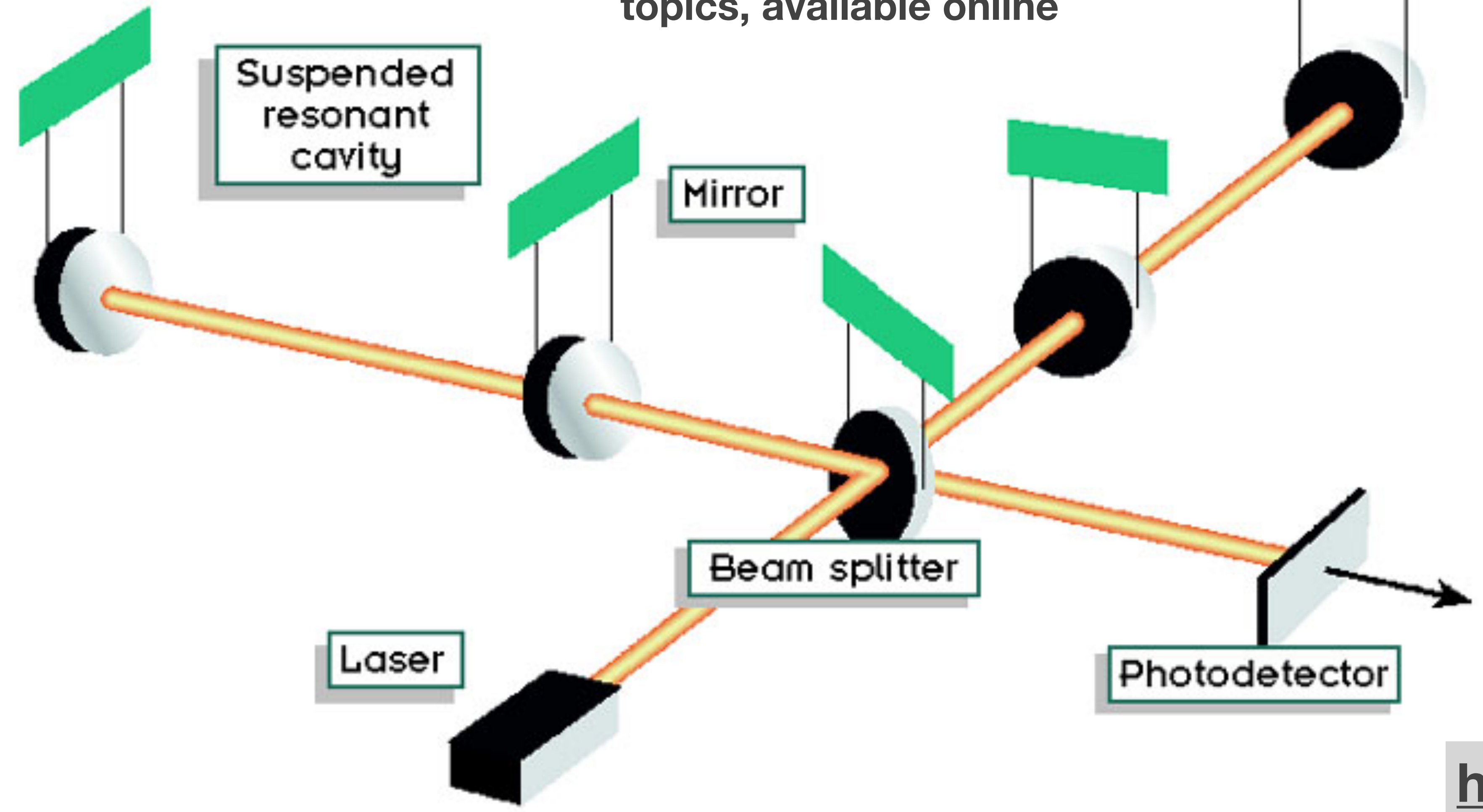

https://www.cascina.virgo.infn.it

Lorentz invariance

PHYSICAL REVIEW D **80,** 105011 (2009)

Rotating optical cavity experiment testing Lorentz invariance at the 10^{-17} level

S. Herrmann,[1,2] A. Senger,[1] K. Möhle,[1] M. Nagel,[1] E. V. Kovalchuk,[1] and A. Peters[1]
[1]*Institut für Physik, Humboldt-Universität zu Berlin, Hausvogteiplatz 5-7, 10117 Berlin*
[2]*ZARM, Universität Bremen, Am Fallturm 1, 28359 Bremen*
(Received 10 August 2009; published 12 November 2009)

We present an improved laboratory test of Lorentz invariance in electrodynamics by testing the isotropy of the speed of light. Our measurement compares the resonance frequencies of two orthogonal optical resonators that are implemented in a single block of fused silica and are rotated continuously on a precision air bearing turntable. An analysis of data recorded over the course of one year sets a limit on an anisotropy of the speed of light of $\Delta c/c \sim 1 \times 10^{-17}$. This constitutes the most accurate laboratory test of the isotropy of c to date and allows to constrain parameters of a Lorentz violating extension of the standard model of particle physics down to a level of 10^{-17}.

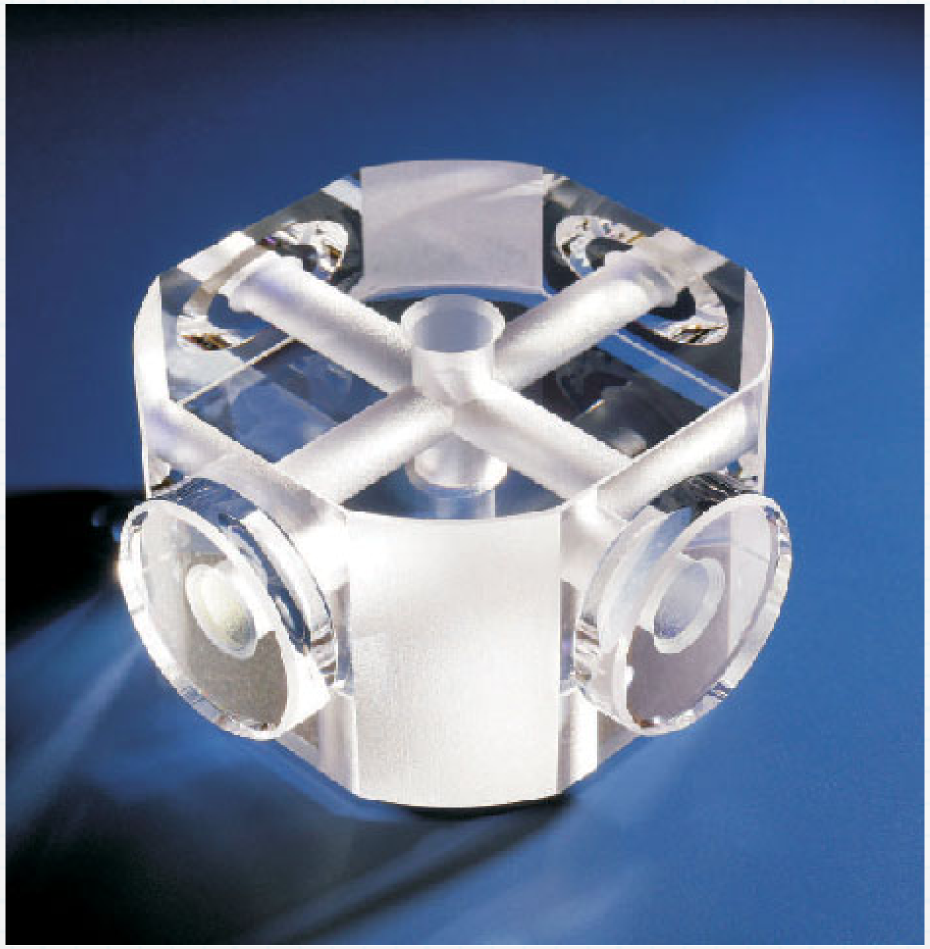

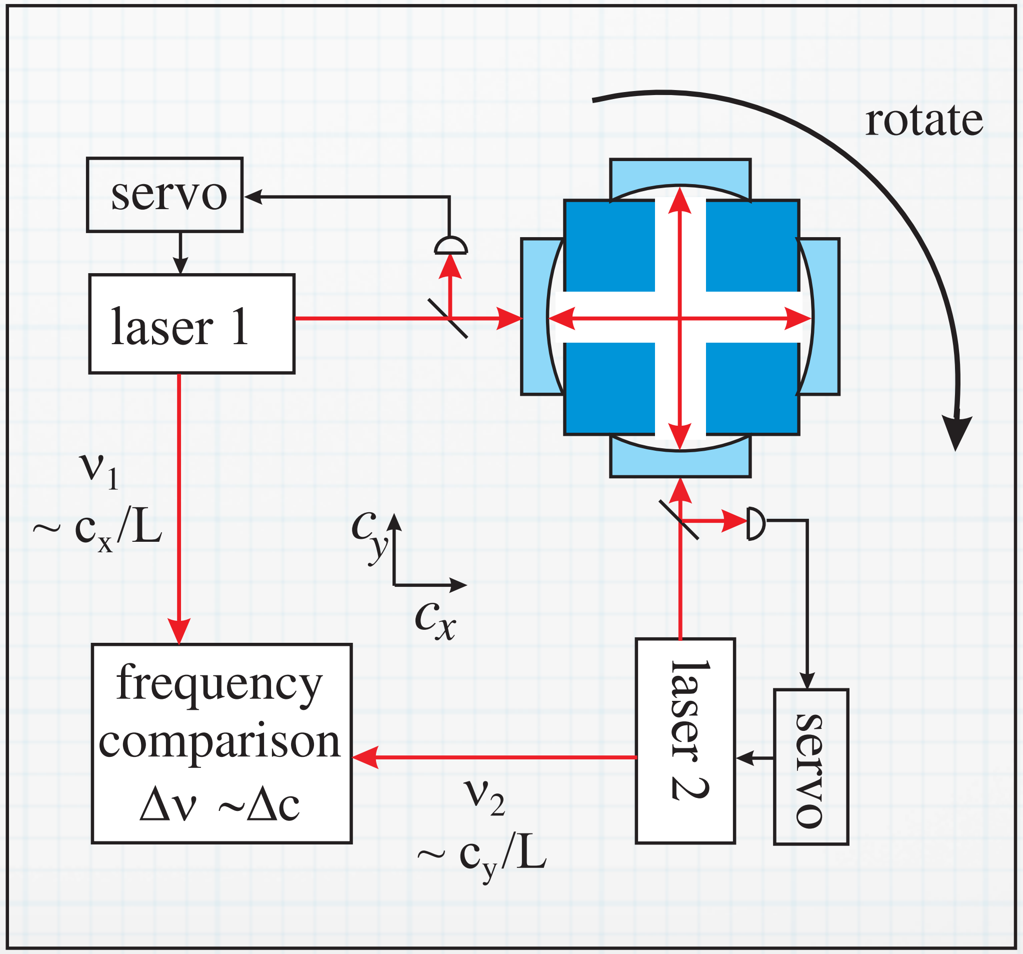

Alternate schemes

The original Pound scheme

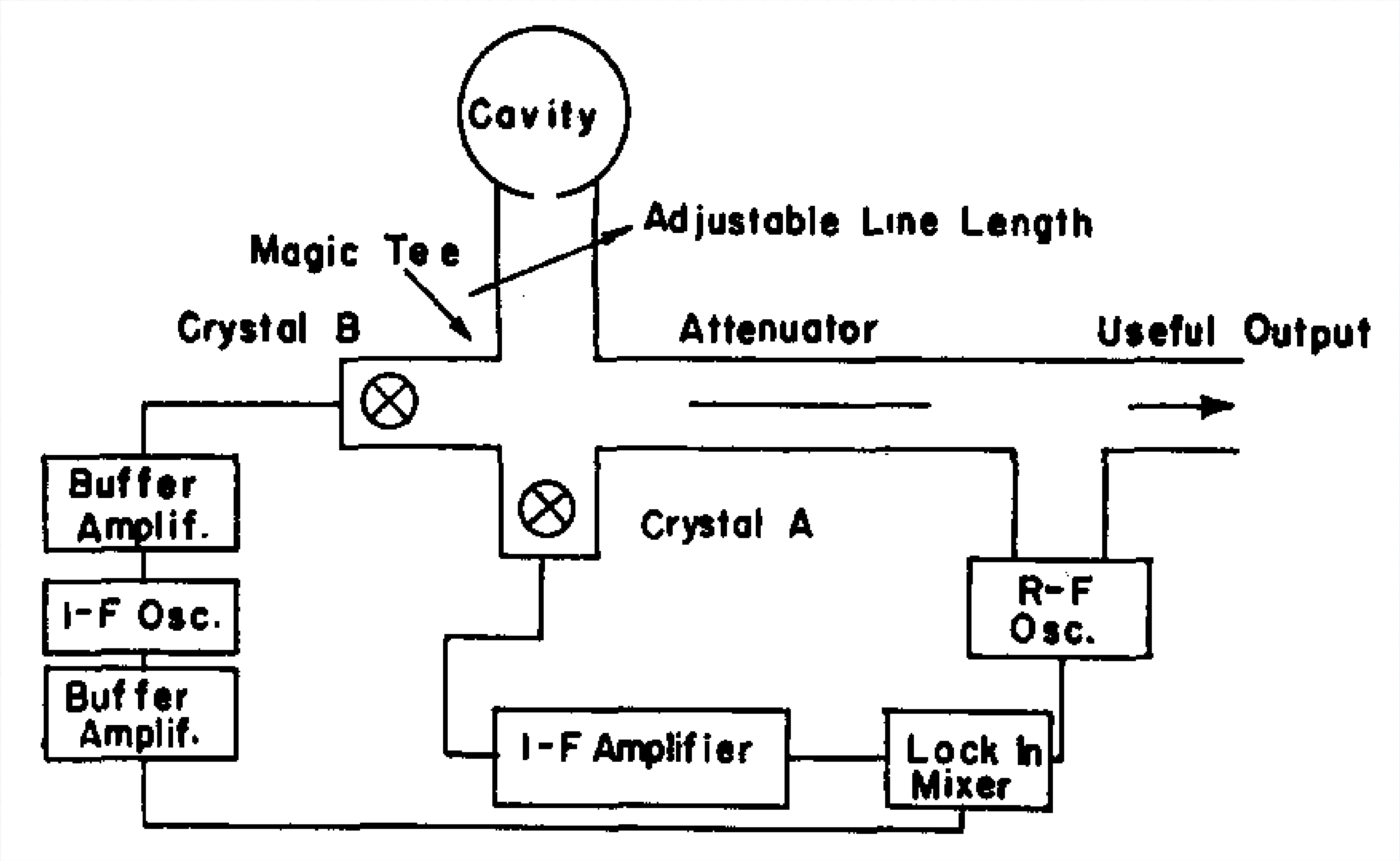

All the key ideas are here

However technology, electrical symbols, and writing style are quite different

R. V. Pound, Rev. Sci. Instrum. 17(11) p. 490–505, Nov. 1946

The Pound-Drever-Hall scheme

The Pound scheme ported to optics

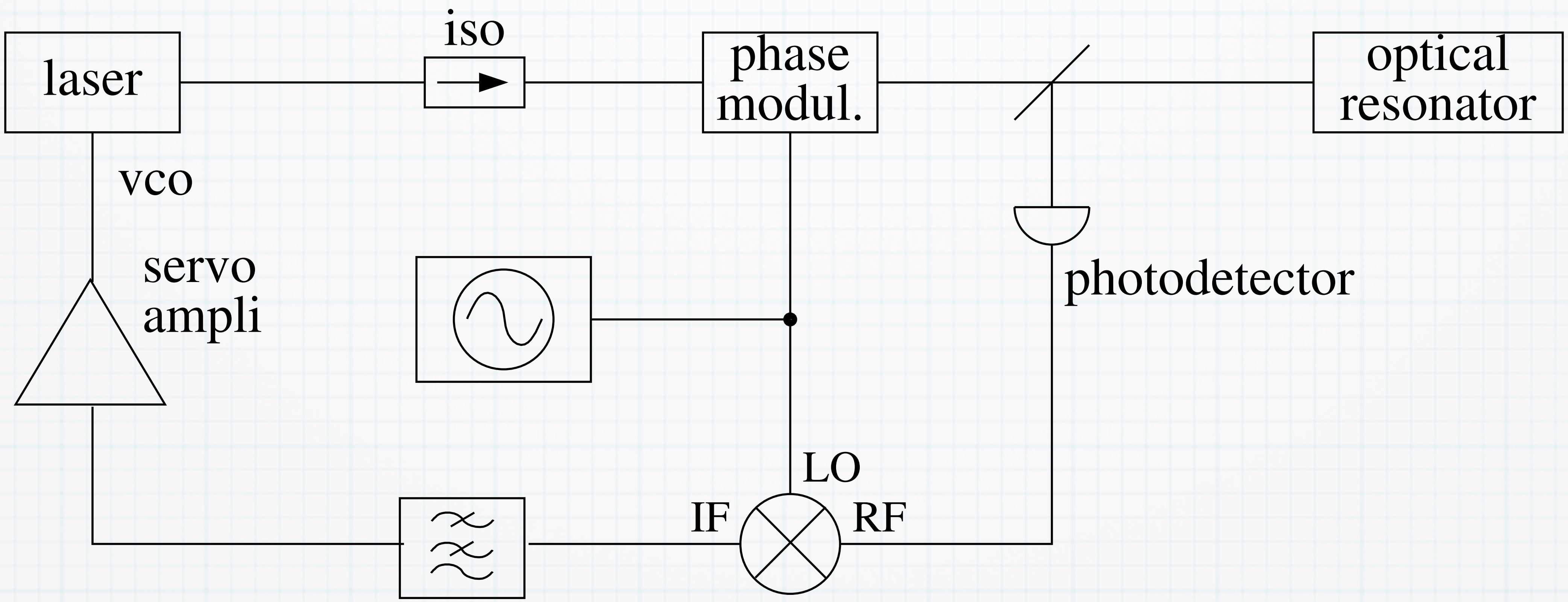

Figure from E. Rubiola, Phase noise and frequency stability in oscillators, © Cambridge University Press

R.P.V. Drever, J.L. Hall & al., Appl. Phys. Lett. 31(2) p.97–105, June 1983

The Pound-Galani oscillator

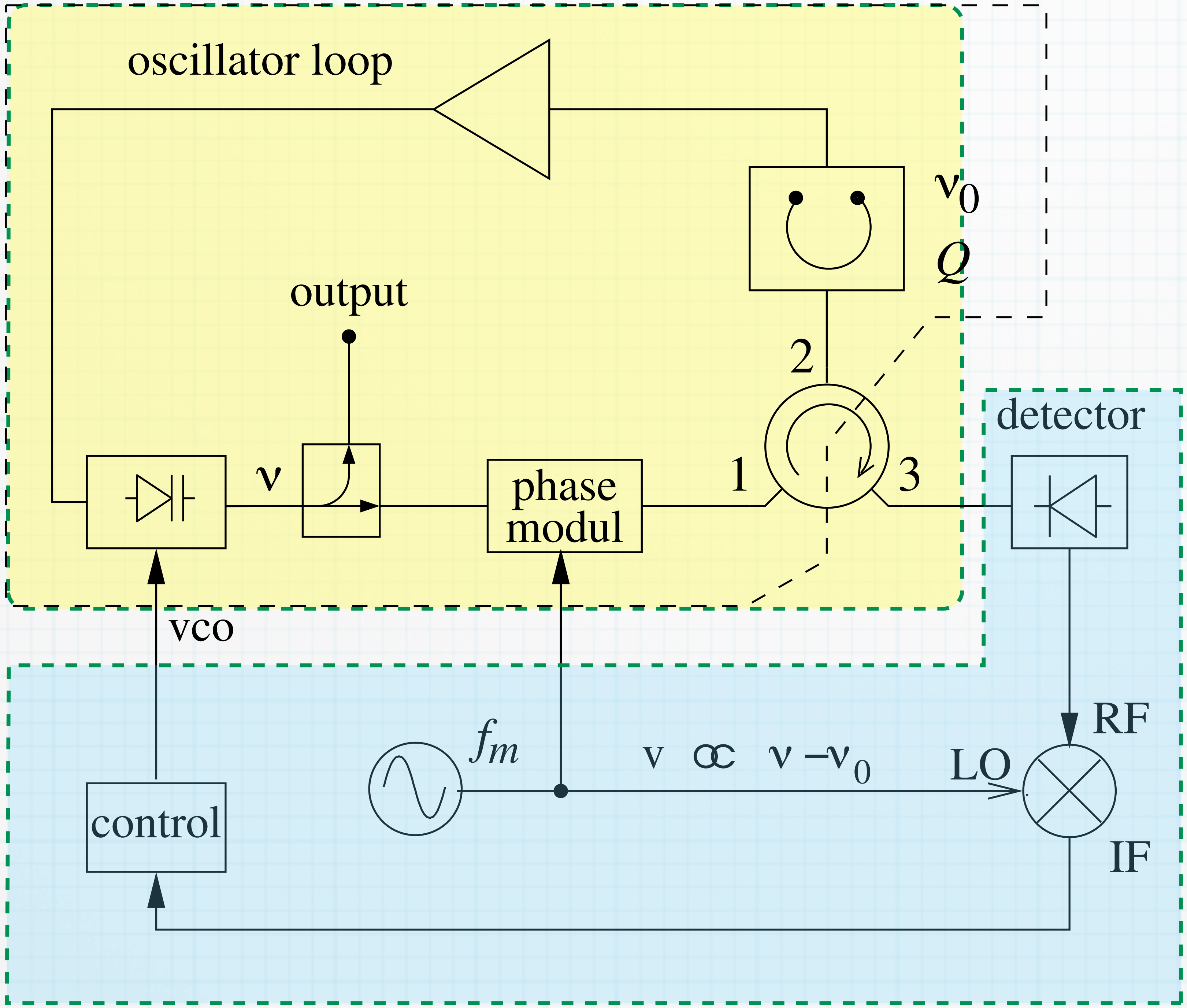

Figure from E. Rubiola, Phase noise and frequency stability in oscillators, © Cambridge University Press

- Great VCO for cheap
- Easier to control

- Two-port resonator
  - More complex
  - Lower Q

Z. Galani & al, Analysis and design of a single-resonator GaAs FET oscillator with noise degeneration, IEEE-T-MTT 39(5), May 1991

Pound-Galani transfer function

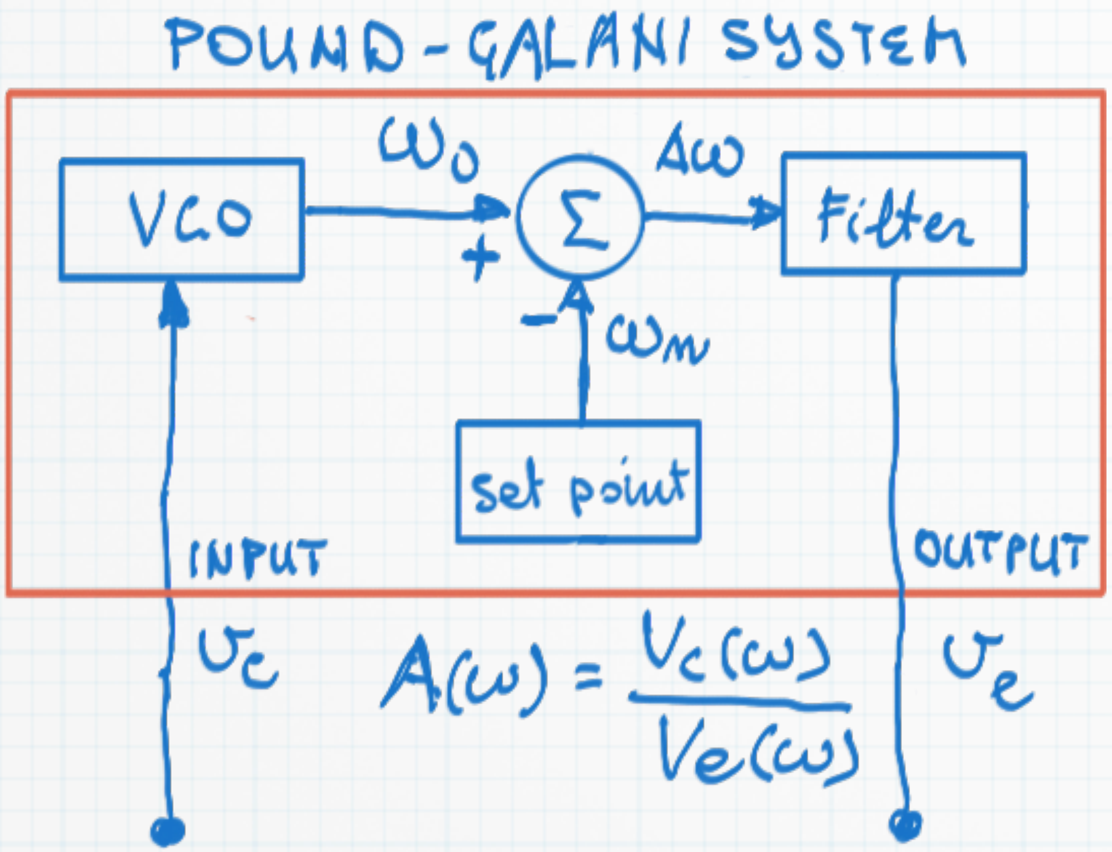

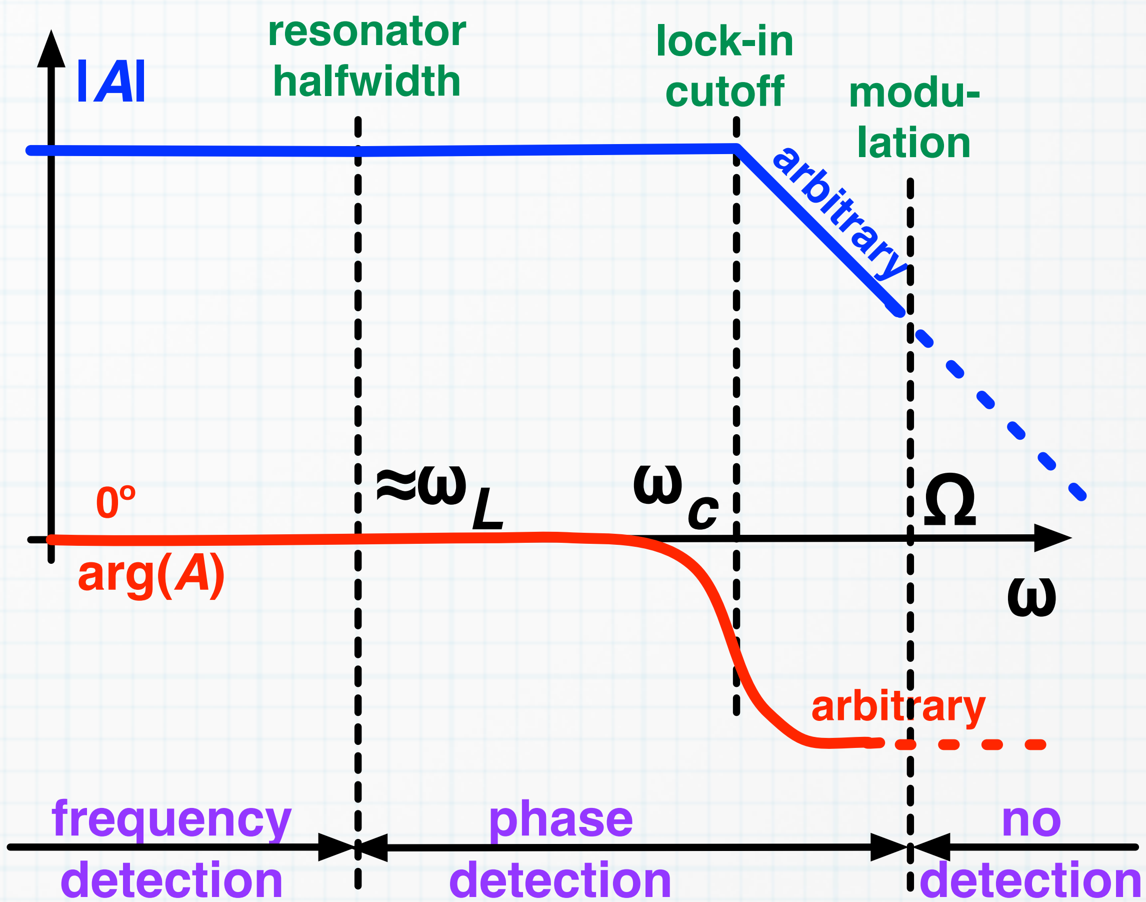

- FD region –> full performance
- PD region
  - Flat frequency response, not for free
  - Poor response of the frequency-error detection
  - Higher noise

The Pound-Sulzer oscillator

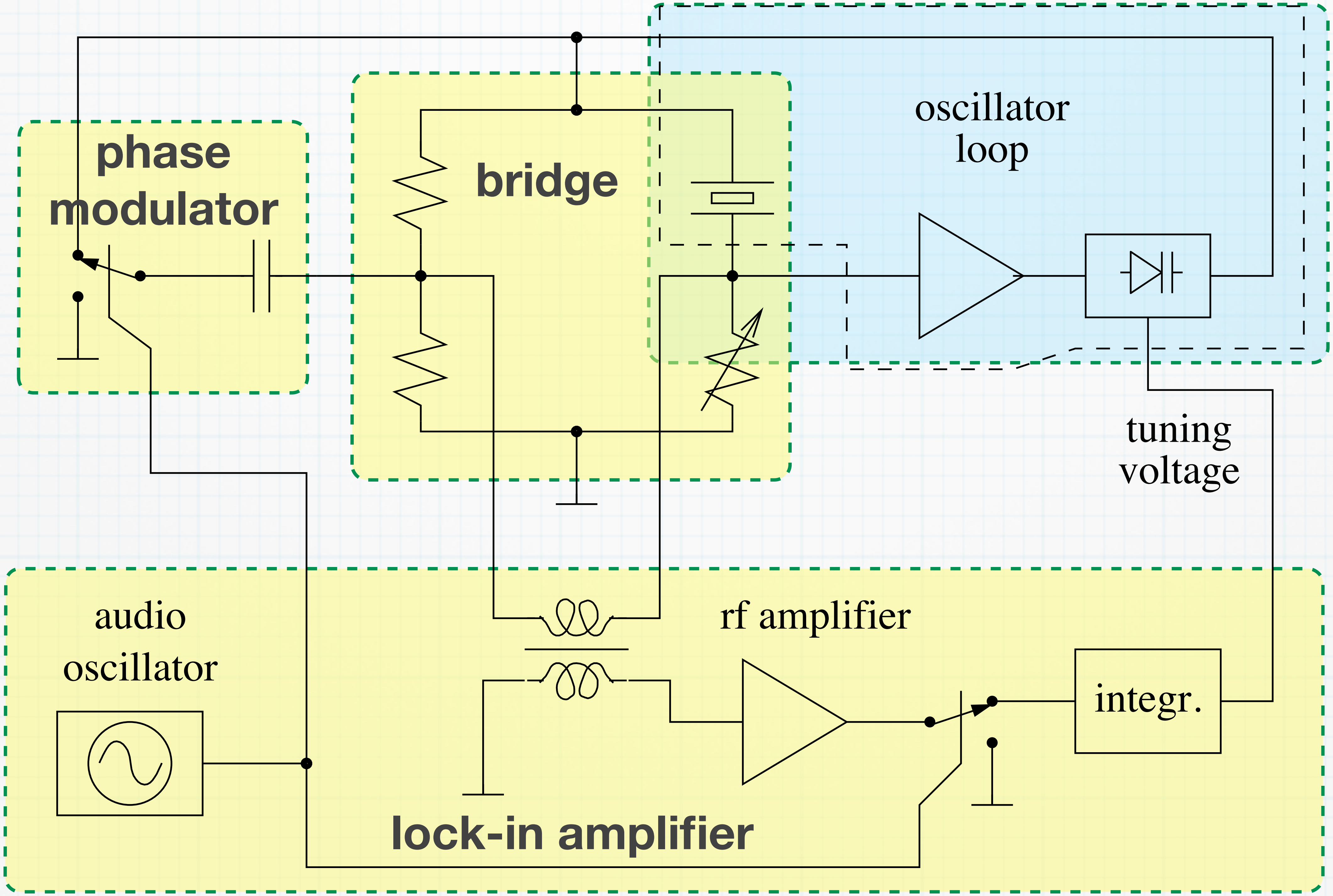

P. Sulzer, Proc. IRE 43(6) p.701-707, June 1955

References

- Black ED, An introduction to Pound–Drever–Hall laser frequency stabilization, Am J Phys 69(1) January 2001
- R.P.V. Drever, J.L. Hall & al., Appl. Phys. Lett. 31(2) p.97–105, June 1983
- Hall JL & al, Laser stabilization, Chapter 27 of Bass et al, Handbook of optics, McGraw Hill 2001
- Mor O, Arie A, JQE 33(4), April 1997
- R.V. Pound, Rev. Sci. Instrum. 17(11) p. 490–505, Nov. 1946
- Z. Galani & al, IEEE-T-MTT 39(5), May 1991
- P. Sulzer, Proc. IRE 43(6) p.701-707, June 1955